Institutionen för skoglig genetic och växtfysiologi
Department of Forest Genetics and Plant Physiology
Umeå Plant Science Centre

Transcriptomes of Populus Lines Modified in Pectin Methylesterase Expression Reveal Activation of Oxidative Stress Signaling Pathways

David Öhman

Supervisor: Ewa Mellerowicz
Examiner: Björn Sundberg
Examensarbete i Biologi/Degree project in Biology Mars 2006

Department of Forest Genetics and Plant Physiology
Umeå Plant Science Centre
Swedish University of Agricultural Sciences, S-90183 Umeå, Sweden

Abstract Pectin methylesterases (PMEs) catalyze the demethylesterification of cell wall polygalacturonans, and this is thought to play important roles in cell wall extensibility and intercellular adhesion. In addition, PMEs influence many physiological processes, such as stem elongation, root development, fertilization, fruit softening, and xylogenesis. This study focuses on establishing gene expression profiles for transgenic poplar (*Populus tremula* L. x *P. tremuloides* Michx.) lines, over-expressed (PME 2B and PME 7) and suppressed (PME 5 and PME 6N), in the expression of *PME1*. Employment of a transcriptomic approach; spotted poplar cDNA 25 K microarrays, allowed for a simultaneous analysis of about 17,000 genes, gaining insight into effects on plant cell metabolism. A concluding remark of the outcome of the microarray experiment was rejection of the hypothesis that lignin biosynthesis is regulated on a transcriptional level, even though the lignin content was altered, as demonstrated by previous molecular characterizations. Thus, to connect lignification with pectin modification machinery, alternative hypothesis were tested and revealed a higher abundance of H_2O_2 and peroxidases in the PME over-expressing lines, compared to wild-type line, confirming a positive correlation between the lignin content, H_2O_2, and peroxidase activity. Furthermore, the up-regulation of a callose synthase gene in the xylem of one suppressed line; in addition to formation of tyloses, as a reaction of PME suppression, indicated a putative defense response. Many other genes involved in oxidative stress responses were observed significantly affected in transgenic lines. This unexpected result implicated activation of signaling cascades and signal transduction through critical stress pathways such as the salicylic acid, jasmonate and ethylene pathways. It might be speculated that the stress signaling was triggered by the elicitor oligogalacturonic acid (OGA), derived from the cell wall, as a result of its altered chemical composition, and that the lines may exhibit an increased pathogen/stress resistance.

Sammanfattning Pektinmetylesteras (PME) catalyserar demetylesterifieringen av cellväggspolygalakturons, vilket anses spela viktiga roller i bl. a. cellväggens utsträckningsmöjligheter och intercellulär vidhäftning. Dessutom påverkar PME åtskilliga fysiologiska processer, såsom stamförlängning, rotutveckling, befruktning, fruktuppmjukning och xylogenes. Denna studie fokuser på att etablera genuttrycksprofiler for transgena poppellinjer (*Populus tremula* L. x *P. tremuloides* Michx.), överuttryckta (PME 2B och PME 7) och underuttryckta (PME 5 och PME 6N), i uttrycket av *PME1*. Användandet av ett transkriptomiskt tillvägagångssätt; 25 K cDNA mikromatriser, tillät en samtidig analys av ca 17 000 gener, vilket gav en inblick i inverkan på växtcellmetabolismen. En slutsats av mikromatrisexperimentet var förkastandet av hypotesen att ligninbiosyntesen är reglerad på en transkriptionell nivå, trots det faktum att lignininnehållet faktiskt förändrats, vilket kunnat påvisas av tidigare molekylär karaktärisering. Följaktligen, för att anknyta lignifiering med pektinmodifieringsmaskineriet, alternativa hypoteser testades vilka påvisade en högre förekomst av H_2O_2 och peroxidaser i PME-överuttryckta linjer kontra vildtypslinje, vilket bekräftade en positiv korrelering av lignininnehåll, H_2O_2 och peroxidasaktivitet. Vidare, överuttrycket av en kallossyntasgene i xylemet hos en underuttryckt linje, samt uppkomst av tyloser som en reaktion på PME-underuttryck, indikerade på en trolig försvarsreaktion. Slutligen, flera andra gener involverade i oxidativ stress respons observerades som signifikant påverkade i transgena linjer. Detta oväntade resultat antydde aktivering av signaleringskaskader och signalförmedlingar via kritiska stressvägar, såsom salicylsyra-, jasmonat- och etylenvägar. Man kan spekulera i huruvuda stresssignalleringen var framkallad av stresssignalmolekylen oligogalakturonsyra (OGA), vars ursprung förmodlingen finns beläget i cellväggen, vilket återspeglar dess förändrade kemiska sammansätting; samt om dessa transgena linjer eventuellt uppvisar en ökad resistens mot patogen och stress.

Keywords: Populus spp., tyloses, wood formation, callose, oligogalacturonic acid, oxidative stress signaling pathways, pectin methylesterase, microarray, peroxidase activity, H_2O_2

Contents

Introduction

Wood (secondary xylem), the fifth most important world trade product and also an endlessly renewable source of energy (reviewed by Plomion et al., 2001), consists of a complex chemical mixture of some major components: cellulose (40-50%), hemicelluloses (25%), and lignins (25-35%); in addition to some minor components: cell wall proteins and pectins. Poplar, a woody perennial species, has emerged as a model tree to unravel the complex processes and molecular events that underlie xylogenesis, and, in particular, wood formation (reviewed by Mellerowicz et al., 2001). In trees, the xylogenesis is controlled by exogenous factors, such as light, temperature, water supply, photoperiod, mineral nutrition; as well as endogenous factors, including phytohormones, sucrose, and nutrients; and by interaction among them. These factors induce a coordinated expression of key regulatory genes and their target genes to synthesize enzymes, ultimately responsible for cellular metabolism (Sterky et al., 1998). Despite the great impact wood has on daily life, knowledge about metabolic and regulatory pathways required in wood formation is still incomplete, for several aspects of wood formation (e.g. cell division, cell expansion, cell wall thickening, programmed cell death, and heartwood formation), and remains to be elucidated by further research.

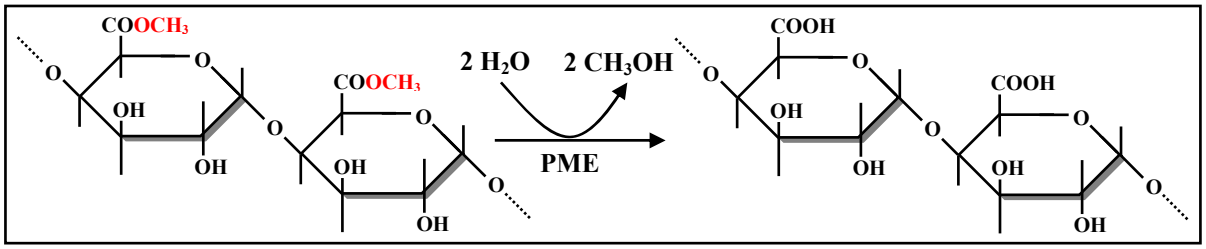

Figure 1. Demonstration of the chemical reaction behind the demethylesterification of pectins by pectin methylesterases, PMEs (modified from: Micheli, 2001).

Pectin methylesterases (PME, EC 3.1.1.11), subsequently referred to as PMEs, belonging to a CAZyme (carbohydrate-active enzyme)-family of carbohydrate esterases (CE) 8 (http://www.cazy.org/CAZY/index.html), are abundantly expressed in wood forming tissues (Micheli et al., 2000; Geisler-Lee et al., 2006). They catalyze the demethylesterification (*in muro*) of cell wall polygalacturonans, releasing acidic pectins and methanol [Fig. 1, reviewed by Micheli (2001)]. Polygalacturonan esterification is thought to play an important role in cell wall extensibility and intercellular adhesion. PMEs have been found in all higher plant species, phytopathogenic fungi, and bacteria. Plant PMEs are usually encoded as pre-pro-proteins having neutral or alkaline isoelectric points (*p*Is), and are subjected to posttranslational modifications. The pre-region is the signal peptide motif required for protein targeting to the endoplasmic reticulum, where it is cleaved off. The remaining pro-protein is targeted to the apoplasm via the *cis*, medial and *trans* Golgi cisternae, and at the *trans* Golgi network, and at some unknown yet step, the pro-region is cleaved, resulting in a mature part that is situated in and bound to the cell wall via electrostatic interactions. The function of the pro-region has been a matter of debate and still remains an unresolved issue. However, one possible function is a regulation of delivery of PME to cell wall and prevention of premature demethylesterification of pectins on their way to the cell wall (Bosch et al., 2005). The pro-region of PME resembles PME inhibitors (PMEIs). PMEIs, together with invertase inhibitors, constitute a family of extracellular proteins that exert silencing on specific targets, rendering them inactive. To date, proteinaceous PMEIs have only been detected in and purified from kiwi fruit (Camardella et al., 2000); nonetheless, at least two similar sequences have been discovered in the *Arabidopsis* genome (Giovane et al., 2004). Since PMEIs impede the

activity of plant PMEs, through the formation of a reversible 1:1 complex with a stability that is strongly influenced by pH (but neither fungal nor microbial PMEs), physiological roles of these inhibitors has been proposed (Hothorn et al., 2004; Di Matteo et al., 2005). A genome rearrangement that might have occurred sometime during evolution could account for reshuffling of the PMEI inhibitory domain and the PME catalytic domain.

In plant cells, PMEs can act on homogalacturonans (HGs) either randomly, thus releasing protons that promote the action of endopolygalacturonases, expansins, and other wall-loosening agents, contributing to overall cell wall loosening; or linearly, exposing blocks of free carboxyl groups that interacts with Ca^{2+}, giving rise to a pectate gel and contributing to cell wall rigification (Micheli, 2001). Recent studies demonstrate that PME activity is highly dependent upon pH: some isoforms act randomly at acidic pH, but switch to act linearly at alkaline pH; and some isoforms are more effective than others at a given pH (Catoire et al., 1998). Finally, PME activity is apparently enhanced by cations, where trivalent cations are the most effective; and, depending on the concentration, the affinity of PMEs for their substrate might also be modified due to cations prevalence (Schmohl et al., 2000). PMEs form a very large multigene family, whose members may differ in enzymatic properties and expression patterns. To date, 58 PME related genes have been identified in *Arabidopsis* (Henrissat et al., 2001) and 87 gene models corresponding to PMEs were found in *Populus* genome (Geisler-Lee et al., 2006).

Studies, where the PME activity in plants was modified by various means, uncovered several aspects of plant development regulated by PMEs. Tomato plants (Tieman and Handa, 1994), which exhibited a 10 times lowered PME activity after the insertion of antisense cDNA encoding a fruit-specific PME, displayed relatively subtle changes in phenotype with apparently no adverse effects on plant growth and development. However, almost complete loss of tissue integrity was observed during fruit senescence. In addition, low PME activity was correlated with a decrease in bound Ca^{2+}, but an increase in soluble Ca^{2+}, in the transgenic fruit pericarp during the ripening process. In transgenic pea hairy roots (induced by wild-type *A. rhizogenes* R1000), where the expression of a PME gene had been partially inhibited by antisense mRNA, root cap border cell separation was inhibited (Wen et al., 1999). The authors draw the conclusion that demethylation of pectin by PME plays a fundamental role in cell wall metabolism of the root cap. Bosch et al. (2005) provided some new insights into regulation of the cell wall dynamics of growing pollen tubes, and they found that application of an exogenous PME induces thickening of the apical cell wall and retards pollen tube growth. On the other hand, Jiang et al. (2005) found that a gene, *VGD1*, encoding a PME homologous protein, plays an important role in growth of pollen tubes in female floral tissues. Null mutation in this gene altered the mechanical characteristics of the pollen tube wall by retarding the growth of the pollen tube in the style and transmitting tract, resulting in significant reduction of male fertility. Apparently, VGD1 is required for the interaction between the pollen tube and female floral tissues. In seeds of yellow cedar, induction of PME activity has been implicated in dormancy breakage (Ren and Kermode, 2000). Hasunuma et al. (2004) investigated the effects of over-expressing a fungal PME in transgenic tobacco plants. In addition to observing a higher degree of demethylated pectins (as expected), they reported changes such as short internodes, small leaves, short length of stem epidermal cells, and, overall, a dwarf phenotype. At the molecular level, the plants exhibited down-regulation of several cell wall-related genes, suggesting affects on cell wall-metabolism in an inversely regulated way. In sum, PME activity influences many physiological processes, such as stem elongation, root development, fertilization, and fruit softening.

PME genes function in the wood-forming tissues is not very well established, despite their high expression levels (Geisler-Lee et al., 2006). At least 8 different PME isoforms have been

found in the cambial region of hybrid aspen that show a remarkable distribution pattern across the cambial region of hybrid aspen at activity and dormancy (Guglielmino et al., 1997; Micheli et al., 2000). The basic isoform, B4, was positioned in meristematic tissues; i.e. vascular cambium and external cortex (including cork cambium), during the active period, while the neutral isoform, N3, could be located throughout all stem tissues without any significant variation between active and dormant stages, suggesting that this is a housekeeping isoform involved in the maintenance of the intercellular spaces through the stem. Further, an acidic isoform, A2, was found to be distributed within the cambial meristem at an active stage, and the function of this isoform has been postulated to be involved in the immediate expansion of the cambial daughter cells; i.e. the differentiation giving rise to xylem and phloem derivatives. Transgenic poplar lines with modified *PttPME1* expression exhibited the expected changes in the PME activity and the corresponding changes in methylesterification patterns (Mellerowicz et al., 2004). These changes resulted in the modification of cell intrusive growth and radial expansion, and also affected the wood chemical composition. The lignin and xylan content was increased while the cellulose and galactan content was decreased in the PME overproducing lines, whereas the opposite trends were observed when the PME activity was reduced. It is not clear how PME affected wood cell chemical composition.

The objective of this thesis, therefore, is to establish the gene expression profiles for two opposite conditions: two poplar lines suppressing (subsequently called PME 5 and PME 6N); and two poplar lines over-expressing (subsequently called PME 2B and PME 7) *PttPME1*, with the employment of a transcriptomic approach (closed architectural system). Spotted poplar cDNAs on 25 K microarrays, based on a collection of over 100,000 ESTs from 19 different poplar tissues and conditions (cDNA libraries), allow for a simultaneous analysis of about 17 000 genes (Segerman et al., submitted). Poplar arrays offer a unique possibility to investigate which, and, in what way, metabolic pathways are affected in poplar transgenic lines exhibiting an altered expression of *PttPME1*. The microarray data, subsequently referred to as MA-data, revealed interesting patterns of gene expression, which, in many instances, can be regarded as novel information. Most importantly, the MA-data allowed the rejection of the hypothesis of transcriptional regulation of lignin biosynthesis in transgenic plants. The alternative hypotheses were put forward and pilot experiments, using histological staining for peroxidases, peroxides, and polyamines, were implemented in order to reveal the mechanism connecting pectin metabolism with lignification. An unexpected result from the microarray experiment was the activation of stress signaling in these plants. It would be interesting to investigate if this leads to increased pathogen/stress resistance. Finally, the pattern of gene expression was correlated with the formation of tyloses observed as a reaction to PME down-regulation, in addition to the up-regulation of a callose synthase gene in the xylem, which expression could be confirmed by means of histological staining of callose. The implications of the findings on cell wall biosynthesis, plant cell metabolism, and, ultimately, wood formation, are discussed.

Materials and Methods

Plant Material and Preparation of Powder from Wood Forming Tissues

Transgenic hybrid aspen (*Populus tremula* L. x *P. tremuloides* Michx.) with modified expression of *PttPME1* gene (Genbank accession number AJ277547) were described in Mellerowicz et al. (2004). Five lines were utilized in this study: two transgenic suppressed lines (PME 5 and PME 6N), two transgenic over-expressing lines (PME 2B and PME 7), and a wild-type line (T89 WT). Lines 5, 2B, and 7 had a *PttPME1* cDNA inserted behind the 35S promoter in sense orientation, while the 6N line had a 3' *PttPME1*-specific fragment inserted in antisense orientation behind the 35S promoter. Transgenic lines, and the T89 WT, were grown in the greenhouse under natural light condition, supplemented with metal halogen lamps with an 18 h light/6 h dark photoperiod at a temperature of 22°C/15°C (day/night). They were watered daily and fertilized once a week with a SuperbraS nutrient solution (Supra Hydro AB, Landskrona, Sweden). When the plants reached about 2 m of height, stem segments of internodes 20-39 were harvested, frozen in liquid nitrogen, and stored at -80°C until they were used in this study. In order to isolate cambial region tissues, stems were partially thawed; the bark was longitudinally cut with a scalpel and then peeled off (debarked). The exposed inner side of the bark was lightly scraped and the tissues, subsequently referred to as 'phloem' fraction, contained xylem elements in the early stage of radial expansion, vascular cambium cells, and possibly some secondary phloem (Gray-Mitsumune et al., 2004). In addition, the exposed wood surface was scraped hard until the wood surface was visibly white, due to lignification. These tissues, subsequently referred to as 'xylem' fraction, contained differentiating xylem elements primarily at the stage of secondary cell wall formation. Collected phloem and xylem fractions (eight trees per line) were immediately frozen in liquid nitrogen and ground to a fine powder with a mortar and pestle. Equal volumes of frozen powder from four trees of the same line were combined to create an epigenetic pool. Thus, two pools for each line were created. The pools of frozen powder were stored in 50 mL tubes in -80°C. This powder was used for all downstream applications described below.

RNA Extraction, Purification, and Integrity Check

Total RNA was isolated from the frozen tissue powder and purified with the RNeasy Plant Mini Kit (Qiagen, Stockholm, Sweden), according to manufacturer's recommendations or, in case of the xylem, with some modifications (Appendix I). The modifications were needed to increase the yield of total RNA, extracted from the xylem samples, before its purification, to account for a low abundance of total RNA per gram of xylem powder. The lysate was obtained with either RLT or RLC buffer (both buffers gave similar results). Severe problems were encountered concerning pipetting the lysate (high viscosity due to wood fibers); hence, it had to be poured instead, under sterile conditions.

The integrity of the total RNA was checked by electrophoresis on a denaturing agarose gel stained with Ethidium bromide, which gave rise to 2 sharp bands (corresponding to 18S and 26S rRNA, respectively) when visualized under UV light. Moreover, quantity of the total RNA was estimated with the NanoDrop ND-1000 Spectrophotometer (NanoDrop Technologies, Wilmington, DE, USA), by measuring the absorbance at 260 nm (nucleic acids) and 280 nm (proteins).

RT-PCR

Removal of Contaminating DNA

Total RNA was treated with DNase with the DNA-*free* kit (Ambion, Huntingdon, Cambridgeshire, UK), which removed any contaminating DNA from the total RNA preparations (Appendix II). This step was necessary to avoid a false-positive signal from contaminating DNA in the subsequent applications, especially the quantitative RT-PCR.

RT-PCR

Total RNA was reverse transcribed using the RETROscript kit (Ambion, Huntingdon, Cambridgeshire, UK) and random decamer primers. The first strand cDNA served as a template during the PCR-reaction, utilizing the *PttPME1*-specific primer set (forward: 5' -ATT TCA TTT TCG GCA ATG CT- 3' and reverse: 5' -GCG CCA CGA AGA GAA TAC AT- 3'), or the 18S rRNA PCR primer and competimer pairs, supplied with the QuantumRNA 18S Internal Standards kit (Ambion, Huntingdon, Cambridgeshire, UK), which served as an internal control. PCR reactions yielded a 516 bp product specific for the sense mRNA of *PttPME1* and a 315 bp product specific for 18S rRNA. The thermocycling conditions were: 94°C for 5 min; then cycles of 94°C – 30 sec, 62°C – 30 sec, 72°C – 30 sec, and finally 72°C for 5 min. The number of cycles and the amount of template were optimized as recommended by manufacturer and explained in more details in Appendix II. First, the linear range of reaction was determined using the samples with the expected lowest (PME 5 Phloem) and highest (PME 7 Xylem) expression levels, based on previous characterizations of the lines (Mellerowicz et al., 2004). This was followed by establishing the optimal ratio of the 18S rRNA PCR primers to competimers. The reaction was linear between 29 and 33 cycles. 31 cycles and a ratio of 2 to 8, of primers to competimers, were subsequently used in the optimized protocol.

Amplified products were subjected to electrophoresis on a native agarose gel, stained with ethidium bromide, and visualized using the 488nm direct blue-excited fluorescence light on the Typhoon 9400 Scanner (GE Healthcare, Uppsala, Sweden). The captured image was further analyzed with the quantification software program ImageQuant TL(GE Healthcare, Uppsala, Sweden), to compare relative yields of the product among the samples.

Microarray Experiment

Microarrays

25 K poplar cDNA microarrays (http://www.populus.db.umu.se/index.html) was used, containing approx. a set of 25,000 poplar unigene clones (PUs), selected to cover basically all ESTs that grouped together into clusters (contigs and singlets) and singletons from the Swedish *Populus* EST collection (Sterky et al., 2004). The array contained approx. 17 000 genes as estimated by matching of PUs to the *Populus trichocarpa* gene models (Segerman et al., submitted).

Experimental Design

A closed architectural system was implemented, which involved hybridization of targets with probes onto 25 K poplar cDNA microarrays in a direct comparison fashion (Fig. 2); i.e. each tissue of each transgenic line was hybridized against a common reference (wild-type tissue). Each transgenic line and tissue consisted of two epigenetic pools of four trees each, representing two biological replicates. For each pool, four technical replicates, including a

dye-swap, were applied. Two different fluorophores, Cy5 and Cy3 (GE Healthcare, Uppsala, Sweden), were used to label a transgenic pool and a wild-type sample.

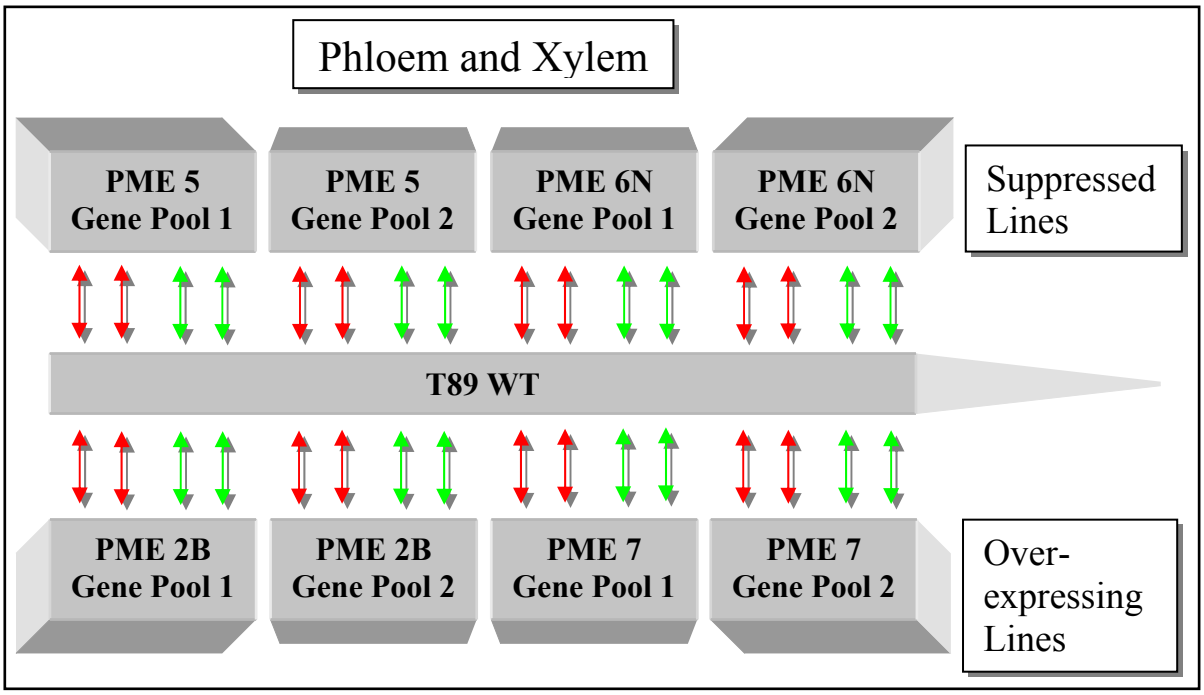

Figure 2. Schematic drawing of the experimental design. Each double-headed arrow represents two hybridizations (one per tissue). Red- and green-colored arrows symbolize dye-swaps. NB: for 'Gene Pool', read: 'Epigenetic Pool'.

Processing Samples

All the procedures and steps concerning target preparation (cDNA synthesis, CyDye-coupling, and purification) were performed according to modified protocols from the *Populus* cDNA microarray database, [UPSC-BASE (http://www.upscbase.db.umu.se)], outlined in Appendix III. Briefly, cDNA was synthesized from mRNA with oligo(dT)-anchor (MWG-Biotech AG, Ebersberg, Germany) and Superscript II (Invitrogen Life Technologies, Carlsbad, CA, USA). cDNA was purified and desalted by using Microcon 30 Concentrator (Millipore Corporation, Bedford, MA, USA), followed by indirect CyDye-coupling (post-labeling) and purification with CyScribe Purification Kit (GE Healthcare, Uppsala, Sweden). Microarray glass slides were prehybridized for 50 min with Calf Thymus DNA (Sigma-Aldrich Sweden AB, Stockholm, Sweden), prior to subjecting purified CyDye-labeled cDNA to hybridization with blockers t-RNA (Invitrogen life technologies, Carlsbad, CA, USA) and olido-dA(80mer) (Cybergene AB, Huddinge, Sweden). A total of 64 slides were hybridized manually inside tightly sealed hybridization chambers and placed in 42°C water bath for 18 hours. Finally, hybridized slides were washed manually in isopropanol and dried with $N_{2(g)}$.

Image Acquisition and Image Analysis

Microarray slides were scanned with ScanArray Lite (PerkinElmer Life and Analytical Sciences, Wellesley, MA, USA) and laser excitation wavelengths were: 633 nm for Cy5 and 543 nm for Cy3 (red channel and green channel, respectively), and the emission filter wavelengths were: 670nm (Cy5) and 570 nm (Cy3), respectively. The slides were scanned at 10 µm resolution with four different settings (Table 1) in order to gather information on high- and low intensity spots.

Table 1. Scanning settings and the order in which they were executed.

Scanning Order	Laser Power (%)	PMT Gain (%)
1	100	70
2	50	70
3	80	70
4	100	80

The images (TIFF- and JPEG-files) obtained were analyzed by GenePix Pro 5.1 (Molecular Devices, Sunnyvale, CA, USA), which generated GenePix Results Files (GPR-Files), containing information on each cDNA spot identity and background/foreground intensities, gathered by the GenePix Array List (GAL file) that fixed a grid to the spots on the merged images from the red and green channels. A spot was considered as bad if the minimum and maximum diameter size was outside the range of 70-140%, and as missing if the composite pixel intensity (CPI) did not reach the threshold level set to 300. Bad and/or missing spots were automatically flagged, but not removed from the analysis. Up-regulated genes were colored red, while down-regulated genes were colored green (for the dye-swapped slides, these conditions were opposite), and in those cases where expression of both channels was approximately similar, the spots were colored yellow.

Data Treatment and Statistical Analysis

GPR-files and images were subsequently uploaded to the UPSC-BASE (http://www.upscbase.db.umu.se) and were subjected to various treatments (Fig. 3) according to the UPSC-BASE standardized procedures. First, the median foreground (FG) intensity of the four data sets, each scanned with different settings, underwent 'Restricted Linear Scaling' (RLS) to correct the problem of saturated signals. RLS generated a new raw data set (combined) containing the extrapolated values for saturated signals. Second, this raw data set was subjected to 'Step-wise normalization', which implemented three different normalization methods, tested them, and then finally applied the method giving the most satisfying results, based on default mathematical algorithms/criteria (BIC). Finally, 'B-statistics' (B-STAT) was used, a moderated version (programmed in the R statistical language) of the Student's t-test, that returned a hierarchy of significant genes, based on calculated P-values (from the t-test) and B-values (log-odds). A gene was considered differentially regulated in a significant way when $B \geq 0$ (50-50% chance) and $P \leq 0.05$ (false discovery rate of five genes out of one hundred) when a transgenic line was compared against a common reference (WT); i.e. a parametric two-sample t-test. Spots flagged as bad/missed were assigned a much lower weight, set to a default value (0.1 that of non-flagged spots) by the software. Furthermore, these statistical outputs, together with PU numbers (PUs), M-values ($\log_2$ fold changes for PUs), A-values (average expression level for PUs across all arrays and channels), and t-values (moderated t-statistics) were exported to a spreadsheet, which was supplemented with *Populus* gene models; model mapping qualities; closest *Arabidopsis* homolog hits, scores, and annotations; functional classes (MIPS); gene ontologies (GO); gene ontology descriptions; enzyme classes (EC); and enzyme class descriptions.

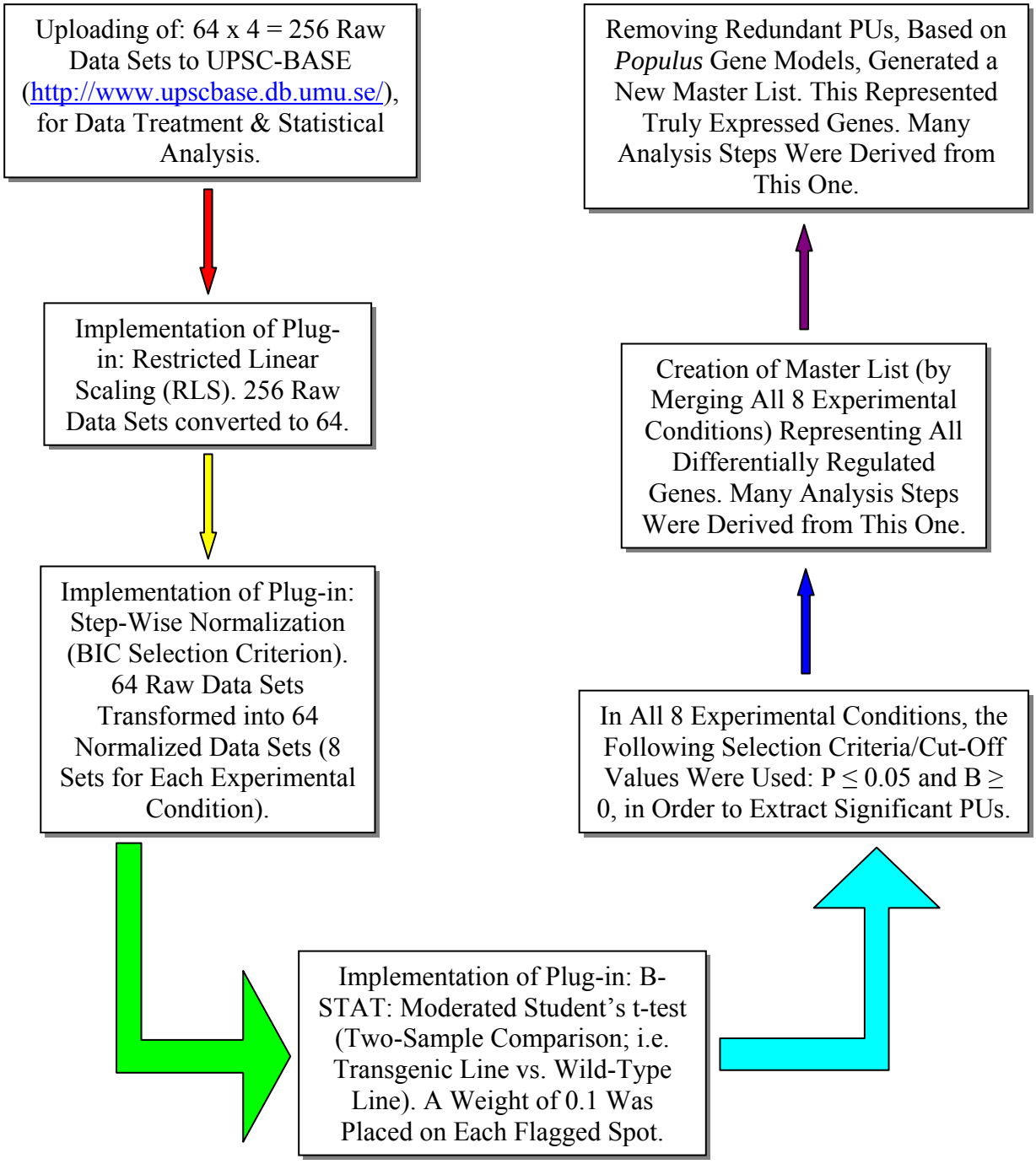

Figure 5. Schematic drawing illustrating the work flow, concerning processing of microarray data.

Cyto and Histochemistry; and Microscopy

Staining for Tyloses and Callose

Three lines: PME 5 (nine trees), PME 6N (10 trees), and T89 WT (10 trees), were analyzed for the presence of tyloses and callose. Frozen stem segments were dissected from internode 41, mounted on a holder, and cryosectioned at -20°C, using the Microtome Cryostat HM 505 E (MICROM Laborgeräte GmbH, Walldorf, Germany) to obtain 60 µm thick, radial, longitudinal, and transverse sections. For detection of tyloses, the sections were stained with saffranin/alcian blue solution [0.33%/0.67% (w/v)], which stains lignified cell walls red and non-lignified tyloses blue. Callose was detected by staining with a solution of 0.05% aniline

blue in 0.01 M phosphate buffer (pH 8.5), which specifically detected callose under UV light (Krishnamurthy, 1999). Excessive dye was removed with tissue paper, followed by mounting the sections on glass slides with 50% glycerol and a cover slip.

Staining for H_2O_2 and Peroxidases

Occurrence of hydrogen peroxide, H_2O_2, and peroxidases was examined with DAB (3,3'-diaminobenzidine, Sigma) reagent prepared by dissolving DAB in acidified water at 1 mg/1 mL according to Thordal-Christensen et al. (1997). Freshly collected leaves, from young plants grown *in vitro* (NB: the suppressed line 6N was substituted with another PME suppressed line; PME 10), were incubated in DAB reagent for 24 hours at RT then DAB was replaced by ethanol and boiled at 60-70°C for about 1 hour, in order to remove chlorophyll. Whole mounts were observed under a light microscope.

Staining for Peroxidases and Polyamine Oxidases

The 'Syringaldazine mehod' was used to detect peroxidase (Krishnamurthy, 1999) in transverse free-hand sections of young plants grown *in vitro* (NB: the suppressed line 6N was substituted with another PME suppressed line; PME 10). One to two droplets of each, 0.1% syringealdazine in ethanol and aqueous 0.03% H_2O_2, were added after one another onto the sections, cover slip was added and the sections were observed under a light microscope. Intense purple color indicated sites of peroxidase activity. The 'Starch Reagent Method' (Krishnamurthy, 1999) was applied to detect polyamine oxidases. Transverse tissue sections as above were prepared and incubated for one hour at room temperature in a medium containing: 1.3% starch, 20 mM potassium iodide, 10 mM spermidine, and 1 mM phosphate buffer (pH 5.8). Sites of the active enzyme turned blue.

Microscopy

Zeiss Axioplan 2 (Göttingen, Germany) microscope with a UV attachment was used. Images were captured with a Carl Zeiss AxioCam HR (Hallbergmoos, Germany), using Zeiss AxioVision (Hallbergmoos, Germany) software.

Short Metabolomic Study

Metabolite Extraction, Analysis and Derivatization

10-12 mg of sample powder, from two technical replicates of each line, tissue, and epigenetic pool, were processed through a GC/TOF-MS, which enabled the identification of several metabolic compounds. Further, this allowed for a global metabolic comparison between the transgenic lines and the wild-type line, in an open architectural system.

Data Treatment and Statistical Analysis of GC/TOF-MS-data

All data treatment procedures, such as normalization of the data, based on sample weights and internal standards, were performed prior to multivariate analysis. The multivariate analysis, *per se*, was performed with SIMCA-P+ software (Umetrics AB, Umeå, Sweden). Moreover, a unique quantification mass for the metabolite salicylic acid was obtained from each sample, which allowed for a comparison of relative amounts between transgenic lines and wild-type line.

Results and Discussion

In order to identify differentially regulated genes, a microarray experiment was conducted, implementing a direct comparison strategy design. On a global gene expression scale, there are no records in the literature of previously characterized PME modified poplar. The generated microarray data in this study, therefore, should be interpreted with great caution, bearing in mind that any affected biochemical pathway(s) might, in fact, be due to false positives/negatives, resulting from uncontrolled abiotic and/or biotic factors. Nevertheless, obtained data of significant genes proved to be relevant for drawing main conclusions on key aspects of plant cell wall biochemistry and determining which cellular processes that was disrupted or compromised in some way.

Previously Characterized Phenotypes of Transgenic PME Poplar Lines Served as Valid References, When Cross-Compared with Results from the Present Study

Mellerowicz and co-workers (2004) generated transgenic poplar lines exhibiting down- or up-regulation of *PttPME1* expression. The lines exhibited changes in PME enzyme activity and pectin methylesterification quantity, as expected. Furthermore, noteworthy significant effects on the growth phenotype were detected. Down-regulated lines showed elongated internodes, though the formation of internodes was less abundant compared to wild-type line. Up-regulated lines, however, displayed opposite effects; i.e. had a reduced internode length, but the formation of internodes was not affected. Significant effects on wood cell growth in the primary cell wall stage could also be observed. The length and width of fibers were increased in the down-regulated lines but were found to be decreased in the up-regulated lines, in comparison with the wild-type. In addition, effects on the chemical composition of the secondary cell wall in wood tissue were observed. *PttPME1* expression was positively correlated with lignin and xylan content, and negatively correlated with cellulose and galactan content. These results, *per se*, proved to be a valuable source of reference material, when compared with results acquired from all down-stream experiments carried out below.

RT-PCR Verified Expected Levels of PttPME1 in All Transgenic Lines and Tissues

A critical prerequisite for conducting the microarray experiment entails utilization of the wood-forming tissues, in which the levels of *PttPME1* fulfilled the correct criteria; i.e. suppression or over-expression. This was confirmed by quantitative RT-PCR on both phloem and xylem fractions using *PttPME1*-specific primers that recognize transcripts from the sense construct and the native gene, but not the ones from the antisense construct (the forward primer was outside the 3' fragment of the coding sequence used for antisense construct). The experiment was carried out once. Fig. 4 displays the signals from *PttPME1* transcript in relation to the 18S rRNA (internal standard) signals, while Fig. 5 quantifies these signals. Two pools were used for each line to provide some insight to the intra-line (epigenetic) variability. In general, the expression of *PttPME1* in transgenic lines was similar to that observed in the previous experiments (Mellerowicz et al. 2004). In the phloem fraction, where the native *PttPME1* gene is mostly expressed, lines 5 and 6N were down-regulated to 36% and 48%, respectively, while the lines 2B and 7 were over-expressed to 121% and 135%, respectively. In the xylem, where the native *PttPME1* gene is low expressed, no suppression was detected, while the line 2B and 7 showed strong over-expression to 374% and 476%, respectively (Fig. 4-5). Some discrepancies were observed between the two epigenetic pools. For example, both suppressed lines (PME 5 and PME 6N) in the xylem

fractions showed one pool suppressed; with transcription values of 81% and 76%, respectively, and the other pool over-expressed (169% and 152%, respectively). If this was due to real differences between these pools or a noise in the dataset remains to be established, preferably by additional experimental repetitions.

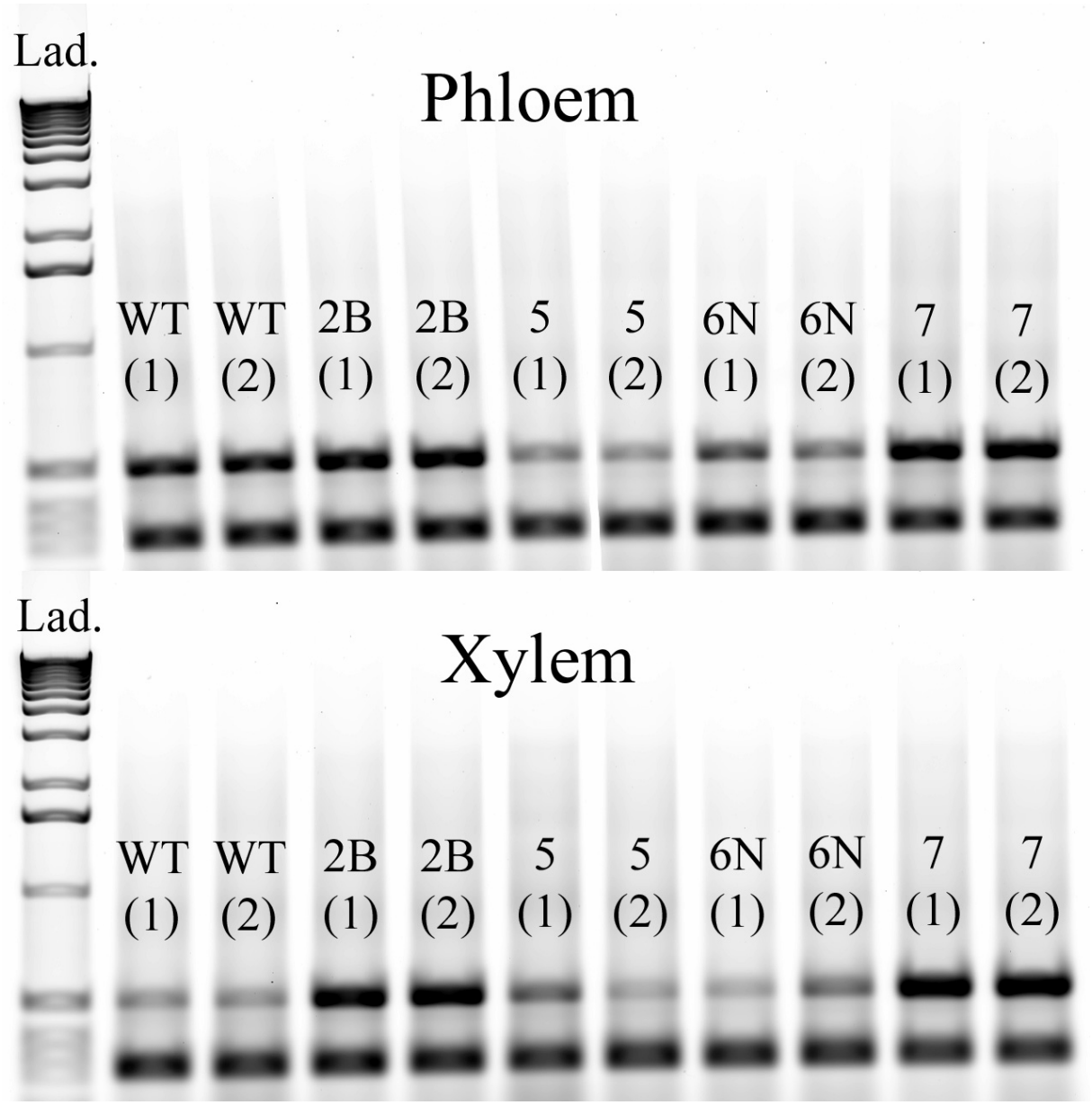

Figure 4. RT-PCR analysis of *PttPME1* expression in transgenic lines and wild-type line of both tissues, phloem (upper image) and xylem (lower image). The larger amplified fragment (upper band) corresponds to *PttPME1*, while the smaller one (lower band) accounts for the amplified 18S rRNA control fragment. Lad, DNA size marker (1 kbp ladder); WT, T89 WT; 2B, PME 2B; 5, PME 5; 6N, PME 6N; 7, PME 7; (1), epigenetic pool 1; (2), epigenetic pool 2.

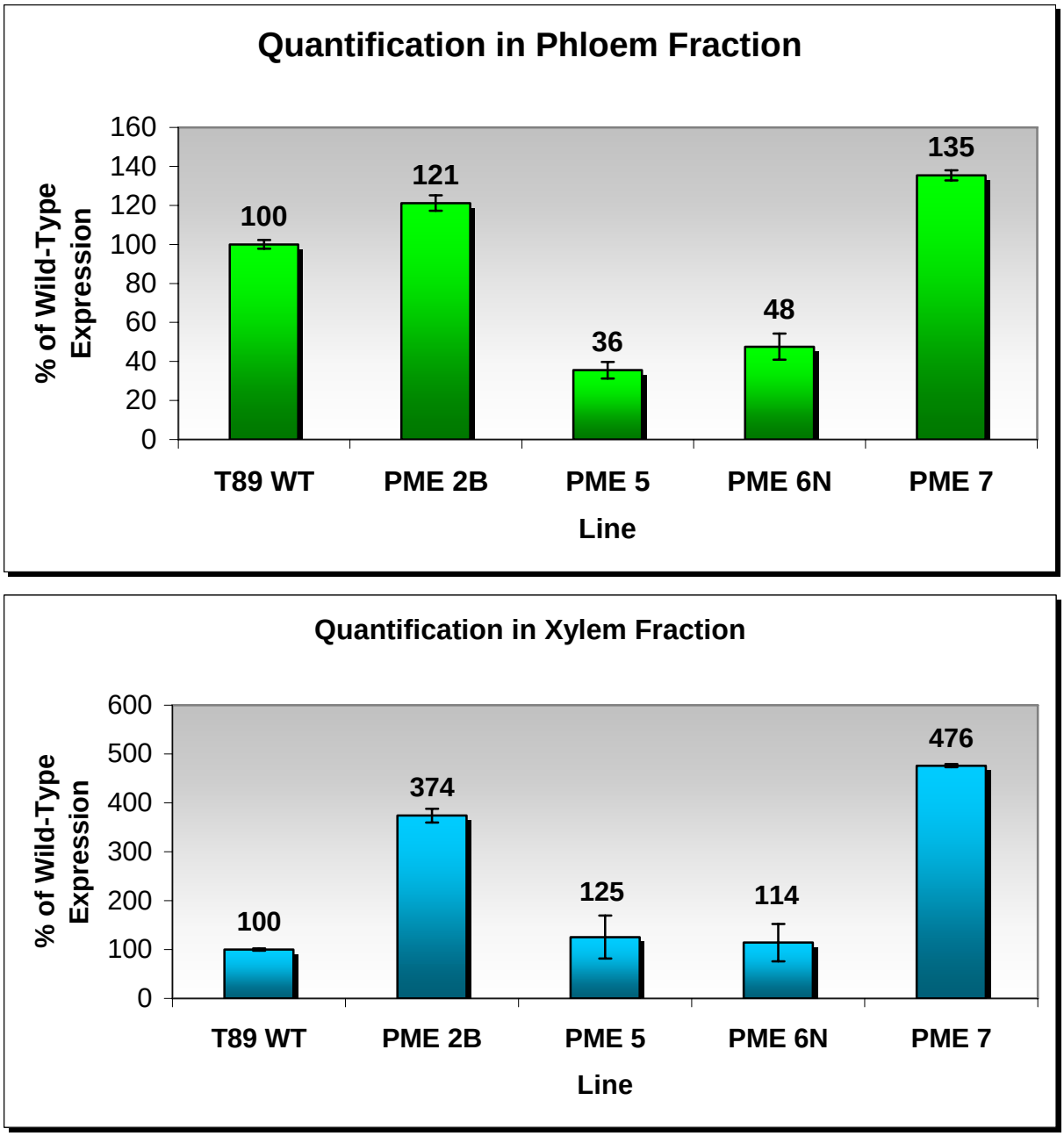

Figure 5. Quantification of the relative amounts of *PttPME1* expression in all lines, in relation to the internal standard, 18S rRNA, of both tissues, phloem (upper graph) and xylem (lower graph). Average of the two pools in % of WT and a range (standard deviation from mean value) are shown.

Microarray Design and Data Validation

To explain the phenotypes of lines with modified PME expression (Mellerowicz et al., 2004) at the genetic level, the transcriptome of lines 5, 6N, 2B, and 7 was compared to WT in two tissues, phloem and xylem, and two epigenetic pools, characterized by RT-PCR. Target cDNA was post-labeled with either red or green fluorophore (CyDye), and hybridized with probes spotted on 25 K microarrays, containing approx. 25,000 clones (PUs). The clones were selected from a collection of over 100,000 ESTs from 19 different poplar tissues and conditions (cDNA libraries), which represent about 17 000 genes (Segerman et al., submitted). In this two-color experiment, a pool of each transgenic line was labeled with one color and the WT was labeled with another color for a direct comparison (Fig. 2). This was

repeated four times. Different validation procedures (Fig. 3) were used to verify the signals obtained from microarrays, following detection of differentially expressed genes.

Microarray Data for *PME1* Correlated with RT-PCR Data, and Failed to Support a Hypothesis of Epigenetic Variability Between Pools

Correlation between microarray data of the relative intensities of *PME1* (PU01960) and the data obtained from quantitative RT-PCR is visualized in Fig. 5. The results from two different methods correlated well for all lines except line 6N. This odd line has an antisense construct of *PttPME1* and therefore would have abundance of antisense transcripts interfering with quantification of the sense transcripts on the microarray. When disregarding the data for line 6N, the correlation coefficient (R^2) between RT-PCR and microarray data was 0.80, which added confidence to the microarray data. Contrary to what was observed in RT-PCR in the epigenetic pools of xylem of lines 5 and 6N, there was no variability between the two pools in the microarray data (four repetitions for each pool), thus strengthening the hypothesis that the variation seen is probably due to experimental factors, not biological.

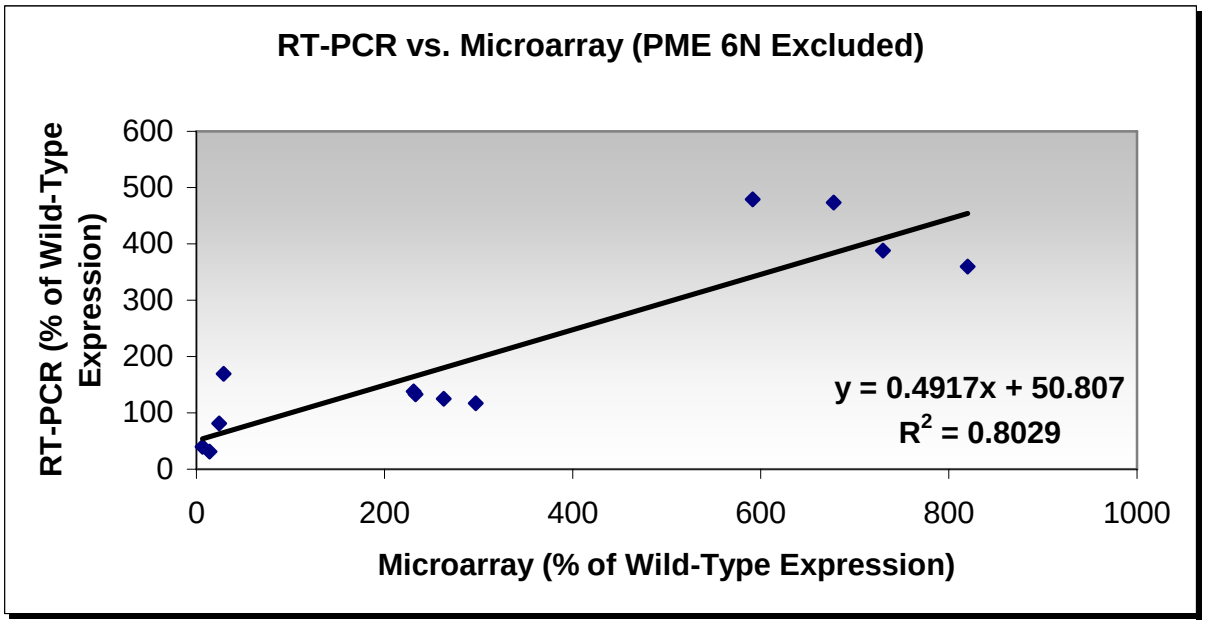

Figure 5. Correlation between MA-data of relative signal intensities from PU01960 and *PttPME1* expression from RT-PCR for all epigenetic pools of transgenic lines, except for PME 6N, relative wild-type line. The equation of a straight line and its correlation coefficient are shown, as well.

Employment of Different Selection Criteria for Retrieval of Significantly Affected Genes, Allowed for the Creation of a Master List

Employing the cut-off values of $P \leq 0.05$ and $B \geq 0$ for selection of significantly affected genes generated a master list (not presented here) displaying relative signals, M-values ($\log_2$ ratios), from each transgenic line and tissue, respectively, which is subsequently referred to as an 'experimental condition', that belong to a unique PU. In the MA-data, however, many PUs match to the same *Populus* gene model, hence, there are redundant PUs, representing the same gene. Transition from PU to gene was achieved by manually, in alphabetical order with respect to PU, removing all but one PU matching to the same gene model, resulting in one gene model, subsequently referred to as 'gene', corresponding to only one PU. Moreover, each single gene model is most likely to represent a truly expressed gene from the *Populus* genome, which was the main reason to base the filtering of redundant PUs on. This allowed for the creation of a master list (not presented here) showing genes affected in at least one

experimental condition, entailing 3834 genes, all matching to a complete or incomplete gene model (genes matching to no gene model were filtered out). When a choice had to be made between two or more PUs, the PU affected in a highest number of experimental conditions was kept or, as a second criterion, the PU affected in the first experimental conditions listed in alphabetical order. This should correspond to a random selection of PUs for each gene.

In the phloem of the over-expressing lines PME 2B and PME 7, 510 genes were affected (156 down- and 354 up-regulated) in total, and 52 of them (46 down- and 6 up-regulated) were modified in both lines in common. In the xylem of the same lines, 456 genes were affected (331 down- and 125 up-regulated) in total, and 35 of them (31 down- and 4 up-regulated) were modified in both lines in common. In the suppressed lines PME 5 and PME 6N, however, 2524 genes were affected in the phloem (1142 down- and 1382 up-regulated), and 1733 genes in the xylem (833 down- and 900 up-regulated). Of these, 29 down- and 53 up-regulated genes in the phloem were modified in both lines in common, for a total of 82 genes. In the xylem, 49 down- and 24 up-regulated genes were affected in both lines in common, yielding a total of 73 genes. It was evident that the suppressed line 6N contains several folds the number of differentially expressed genes selected as significant, compared to other transgenic lines. Considering the fact that the microarray hybridization was performed in a consistent manner throughout all arrays, biological factors; i.e. genetic, biotic stress in the greenhouse, etc., are likely to have a more profound impact on the outcome, than experimental variation.

Application of Principal Component Analysis Led to Rejection of PME 6N and Displayed a Clear Separation of PME 5 from the Suppressed Lines

In order to generally characterize the different sets of transcriptome data of all lines and tissues, a principal component analysis (PCA) was performed. This analysis tried to decompose the MA-data into sets of expression patterns that represented the behavior of all significant genes. Fig. 6 shows the separation of PME 6N Phloem and Xylem, with respect of principal component (PC) 1 that explained 51.84% of variance in the dataset. Other lines were not separated based on PC1. It is evident that line 6N differs considerably from other lines, which was also reflected in the very large number of genes differentially expressed in this line compared to all other transgenic lines. This may result from the fact that this line was growing more slowly than other lines, and was allowed to grow longer to achieve the same physiological age as other lines. Separation of line 6N from other lines, and lack of separation among other lines on PC1, suggested that line 6N was significantly affected in some other ways, in addition to being affected in PME expression. This line also showed a separation of the two pools in both xylem and phloem. Therefore, the line was excluded and a new PCA was performed on the remaining lines (Fig. 7). A clear separation of the suppressed line PME 5 and the over-expressing lines 2B and 7 could be observed with respect of PC 2 that explained 14.36% of variance in the dataset. Interestingly, no separation of xylem and phloem tissues was evident when analyzing first three PCs that, in sum, explained 65.91% of total variance. This indicated that overall genes in transgenic lines were similarly affected in both tissues. Finally, exclusion of PME 6N necessitated the creation of a second master list, which contained 1854 significant genes affected in at least one experimental condition over a total of six experimental conditions. This master list was used and interpreted for all the analysis steps described below.

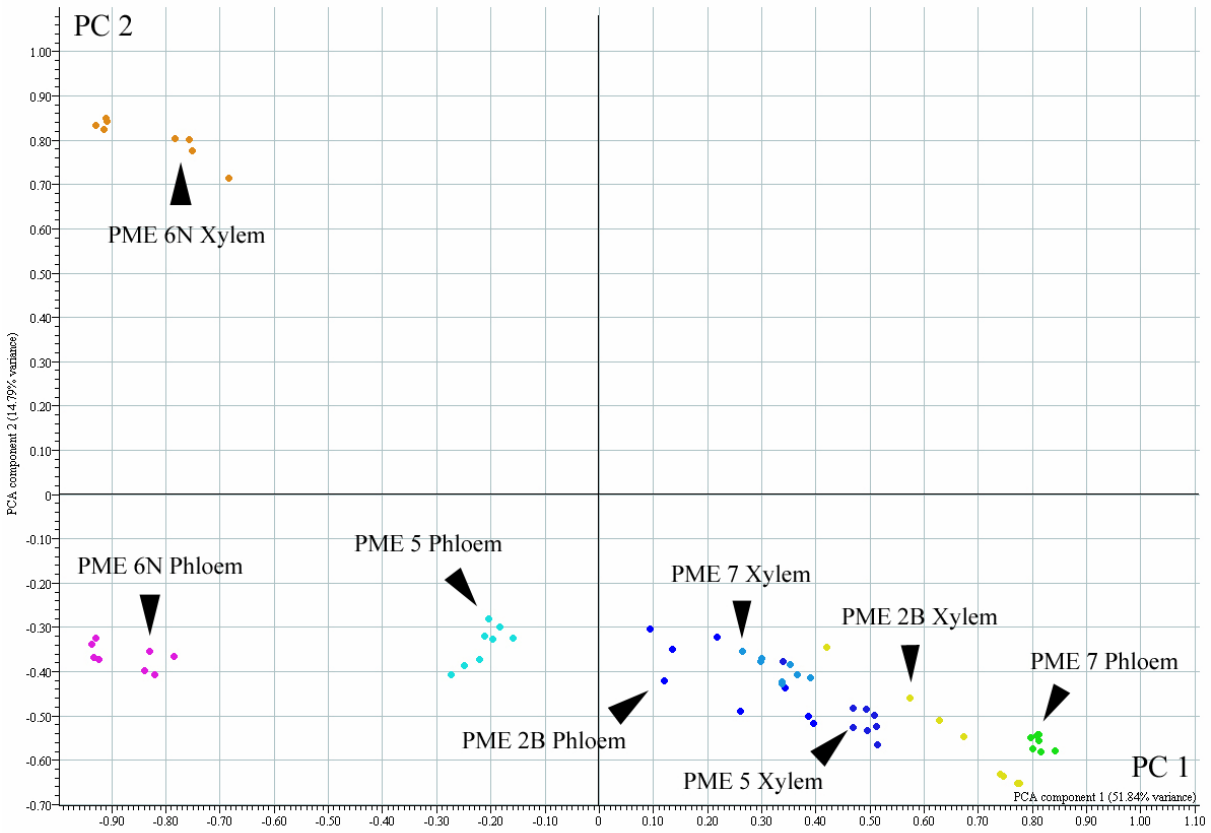

Figure 6. PCA scatter plot showing an evident separation of PME 6N Phloem and Xylem, with respect to PC 2. Each line and tissue is color-coded for clarity and each dot represents one hybridized array.

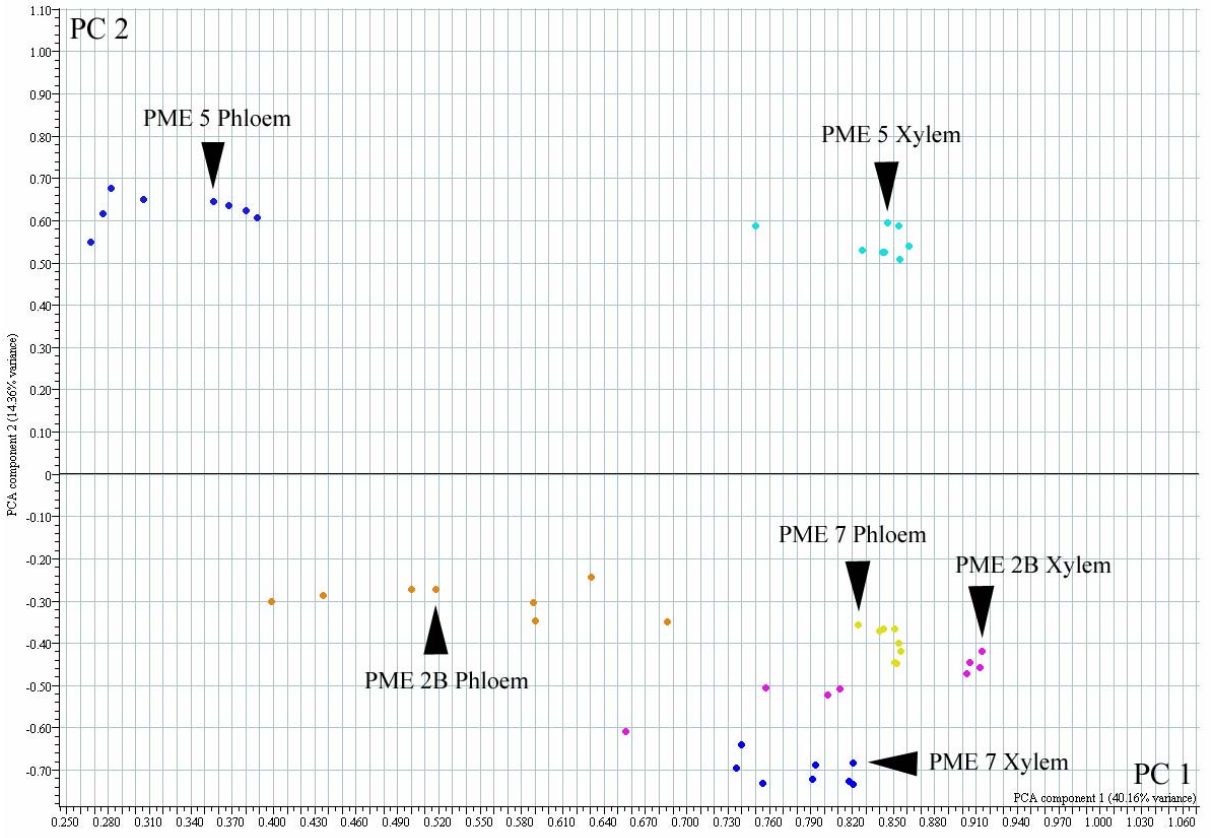

Figure 7. PCA scatter plot displaying a clear separation of the down-regulated line PME 5 and the up-regulated lines 2B and 7, with respect to PC 2. Each line and tissue is color-coded for clarity and each dot represents one hybridized array.

Venn Diagrams Revealed an Abundant Number of Genes Affected in Common in the Over-Expressing Lines 2B and 7, and a Low Number of Genes Affected also in the Suppressed Line 5

The reason for having at least two lines similarly affected in the *PME1* expression is that each line could exhibit changes unrelated to *PME1* modification, due to gene disruption by the transgene insertion. The two over-expressing lines 2B and 7 showed a close resemblance in their gene expression profiles, in contrast with the suppressed lines 5 and 6N, exhibiting a less close resemblance. This ultimately led to the exclusion of PME 6N, since it failed to be validated as a comparable suppressed line. Nevertheless, when PME 5 Phloem and Xylem transcriptomes were compared with these of the over-expressing lines in Venn diagrams (Fig. 9), some genes with key functions in the plant cell appeared to be in common, which are presented in Table 2, together with genes only in common between the over-expressing lines. In addition, fold change ($\log_2$ ratio) values of wild-type expression for genes in common between the over-expressing lines showed a good agreement (Fig. 8) and no gene was correlated in a conflicted way (e.g. up-regulated in PME 2B and down-regulated in PME 7) between the two lines.

A logical expectation when comparing the over-expressing lines against the suppressed line would be to find genes that have the same correlation, either positive or negative, in both conditions (i.e. if a gene is up-regulated in one condition, it should be down-regulated in the opposite). Surprisingly, no genes showing a consistent correlation with *PME1* expression for up- and down-regulated lines could be identified, except for the target gene *PME1* (PU01960) and a closely related *CE8_78* (PU21606), which might cross-hybridize with *PME1*. This adds further complexity in the analysis of the MA-data and also the ultimate unraveling of affected metabolic pathways. Fig. 9 contains Venn diagrams displaying relevant combinations and comparisons. A gene (*PttGT47A*), similar to a pectin beta-glucuronyltransferase (PU00356, CAZy: *GT47_73*), was found up-regulated in PME 5 Phloem, but down-regulated in PME 7 Phloem, while another gene coding for a light responsive protein was up-regulated in PME 5 Phloem, but down-regulated in PME 2B Phloem. Furthermore, in PME 5 Xylem, a gene coding for a disease resistance- responsive-protein appeared to be down-regulated, but, at the same time, showed to be up-regulated in PME 7 Xylem. Among genes similarly affected in all three lines, 12 down-regulated and two up-regulated genes were found in the phloem, in addition to 23 down-regulated genes and one up-regulated gene in the xylem.

A majority of differentially regulated genes in over-expressing lines were down regulated (Fig. 9). This was not the case for the PME suppressed line 5. Interesting to note is that affected genes showed no direct relationship with xylogenesis (wood formation), except for the target gene *PME1*, which was clearly positively correlated in all three lines. However, numerous genes showed a direct relationship with genes that are involved in oxidative stress signaling, and this was more prominent in the over-expressing lines.

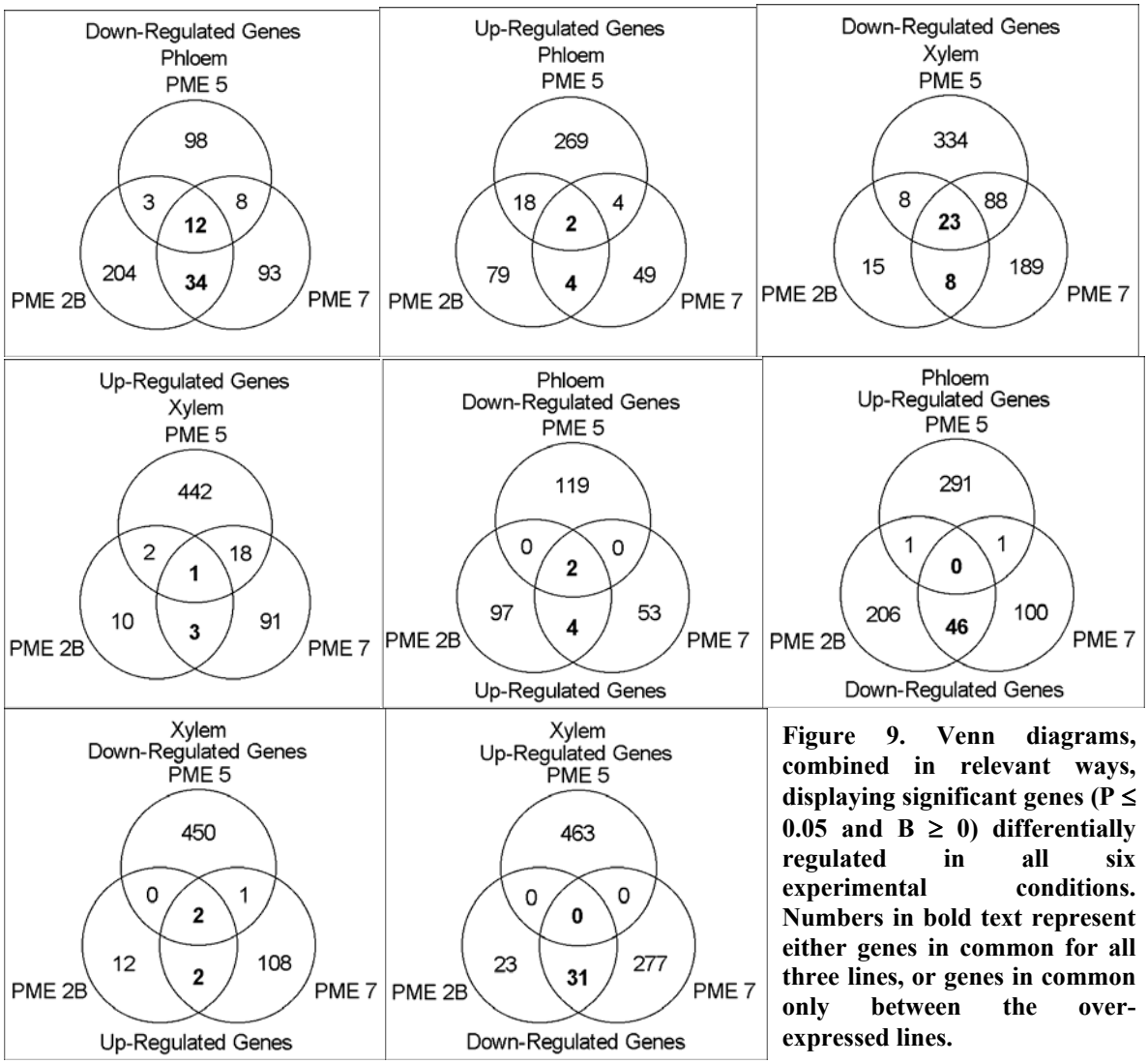

Figure 9. Venn diagrams, combined in relevant ways, displaying significant genes ($P \leq 0.05$ and $B \geq 0$) differentially regulated in all six experimental conditions. Numbers in bold text represent either genes in common for all three lines, or genes in common only between the over-expressed lines.

Table 2. Presented in the columns: all differentially expressed ($P \leq 0.05$ and $B \geq 0$) genes (PU ID and description of gene function) in common between over-expressing lines PME 2B and PME 7 in the phloem and xylem tissue fractions, and genes affected in PME 5 Phloem and Xylem in common with any of over-expressing lines. log_2 ratios (given only for the significantly affected genes) show change relative to WT.

PU ID	Description	PME 2B Phloem	PME 7 Phloem	PME 5 Phloem	PME 2B Xylem	PME 7 Xylem	PME 5 Xylem
PU00045	calcium-binding EF hand family protein	1.60	0.57	1.00			
PU00149	expressed protein	0.61	0.37				
PU01604	1-aminocyclopropane-1-carboxylate oxidase (ACC oxidase)	-0.93	-0.69	-0.57			-0.66
PU01948	Bet v I allergen family protein			-0.39	-1.87	-1.56	-2.18
PU01960	pectin methylesterase (*PttPME1*) (*CE8_79*)	1.47	1.18	-3.44	2.93	2.65	-1.97
PU02523	WD-40 repeat family protein	0.52	0.56		0.66	0.74	0.49
PU02686	expressed protein				-0.67	-0.61	-0.75

PU03099 CCAAT-binding transcription factor (CBF-B/NF-YA)	-0.42	-1.09				
PU03117 phosphorylase family protein	-1.01	-1.88				-2.23
PU03138 expressed protein	-0.64	-1.20				
PU03140 expressed protein	-0.73	-1.90		-2.03	-1.71	-2.02
PU03184 14-3-3 protein GF14 kappa (GRF8)	-0.43	-0.68				
PU03233 expressed protein	-0.89	-1.55		-1.14	-0.79	-1.29
PU03243 beta-glycanase (*GH5_17*)	-0.93	-1.82		-1.60	-1.70	-1.88
PU03283 microtubule-associated EB1 family protein	-0.89	-1.88		-1.70	-1.77	-2.07
PU03333 expressed protein	-0.78	-1.53		-0.95	-0.88	-1.23
PU03355 RNA-binding protein	-0.54	-0.81				
PU03357 9-cis-epoxycarotenoid dioxygenase	-1.14	-1.32	-1.32			
PU03380 isocitrate lyase	-0.77	-1.67		-1.02	-1.26	-1.41
PU03393 aspartate aminotransferase	-0.90	-1.76		-1.41	-1.65	-1.80
PU03398 type I phosphodiesterase/nucleotide pyrophosphatase family protein	-0.49	-1.05				
PU03435 expressed protein	-0.70	-1.10				0.65
PU03467 invertase (*GH32_2*)	-0.63	-1.21				1.15
PU03509 phosphorylase family protein	-1.00	-1.73				-2.28
PU03543 expressed protein	-0.79	-1.31				
PU03548 phosphorylase family protein				-1.87	-1.74	-2.04
PU03636 heterogeneous nuclear ribonucleoprotein (hnRNP)	-0.37	-0.46				
PU03640 gibberellin response modulator (GAI) (RGA2)	-0.55	-1.18				-0.67
PU03647 dehydrin (RAB18)	-0.68	-0.84	-1.02			-0.70
PU03667 hydrophobic protein/low temperature and salt responsive protein	-0.58	-0.81	-0.95			
PU03669 GDSL-motif lipase/hydrolase family protein	-0.75	-1.42				
PU03696 fertilization-independent endosperm protein	-0.78	-1.48				-0.70
PU03741 ubiquitin fusion degradation UFD1 family protein	-0.60	-0.96				-0.33
PU03772 rRNA processing protein-related	-0.51	-0.65	-0.63			
PU03891 Bet v I allergen family protein/Pathogenesis-related protein	-1.25	-0.62	-0.53	-1.67	-0.75	
PU04714 AP2 domain-containing transcription factor				-1.19	-0.85	
PU04831 18.1 kDa class I heat shock protein (HSP18.1-CI)	-1.15	-0.84	-0.58			
PU04936 expressed protein				-0.98	-0.84	-0.83
PU04982 hypothetical protein				-1.27	-1.03	-1.33
PU05004 protease inhibitor/seed storage/lipid transfer protein (LTP)			0.43	-1.39	-1.23	-1.50
PU05250 expressed protein				-0.81	-0.63	-0.70
PU05262 DNA polymerase delta small subunit-related				-0.72	-0.57	-0.82
PU05437 expressed protein				-1.03	-0.65	
PU05477 histone H2B				-0.92	-0.51	-1.16
PU05525 expressed protein				-1.23	-0.70	-0.68
PU05694 drought-responsive protein/drought-induced protein (Di21)			-0.50	-0.67	-1.38	-0.75
PU06991 F-box family protein (FBL6)				-0.48	-0.69	
PU07035 VQ motif-containing protein				-0.56	-0.75	
PU07483 fasciclin-like arabinogalactan-protein (FLA1)				0.50	0.66	
PU08800 no description				-0.43	-0.66	-0.85
PU09347 homeobox-leucine zipper protein 12 (HB-12)/HD-ZIP transcription factor 12	-1.52	-1.58	-1.89			
PU12175 double-stranded RNA binding protein-related (DsRBD)	-0.59	-1.17				
PU12569 dehydrin family protein	-0.71	-0.77	-0.97			-0.68
PU21379 no description				-0.99	-0.96	-1.25
PU21590 expressed protein	-0.89	-0.46				
PU21606 Pectin methylesterase (*CE8_78*)	1.52	1.30	-2.60	2.91	1.67	-0.69
PU21994 glutaredoxin family protein				-0.63	-0.54	

PU23062	late embryogenesis abundant group 1 domain-containing protein (LEA)	-1.39	-1.43	-1.49			
PU23318	hypothetical protein				-1.46	-3.57	-1.47
PU23841	zinc finger (C2H2 type) family protein (ZAT12)			-1.14	-0.87	-0.79	-1.36
PU23843	stress protein-related				-0.79	-0.51	
PU25136	phosphorylase family protein				-2.01	-1.81	-2.24
PU25138	homocysteine S-methyltransferase 2 (HMT-2)	-0.87	-1.74				
PU25158	hypothetical protein	-0.73	-1.44				
PU25160	calcium-transporting ATPase, plasma membrane-type	-0.62	-1.13				
PU25168	protein kinase family protein	-0.70	-0.93				
PU25180	acylphosphatase family	-0.71	-1.52				
PU25184	AAA-type ATPase family protein	-0.82	-1.61				
PU25440	protein phosphatase 2C family protein/PP2C family protein				-0.70	-0.66	-0.62
PU27338	pathogenesis-related thaumatin family protein	1.30	0.66	0.88			
PU28865	zinc finger (C3HC4-type RING finger) family protein	-0.71	-0.70				-0.84
PU29302	dehydrin (RAB18)	-0.66	-0.73	-0.84			-0.54
PU29304	hypothetical protein	-0.39	-0.47				
PU29410	expressed protein	-0.43	-0.71				
PU29541	AP2 domain-containing protein RAP2.2 (RAP2.2)	-0.72	-0.65	-0.60			
PU29973	expressed protein and genefinder				-0.63	-0.63	
PU30946	calcium-binding protein				-0.91	-0.67	
PU31220	structural maintenance of chromosomes (SMC) family protein	-0.51	-0.42				
PU31262	ABC transporter family protein	-0.45	-0.43				

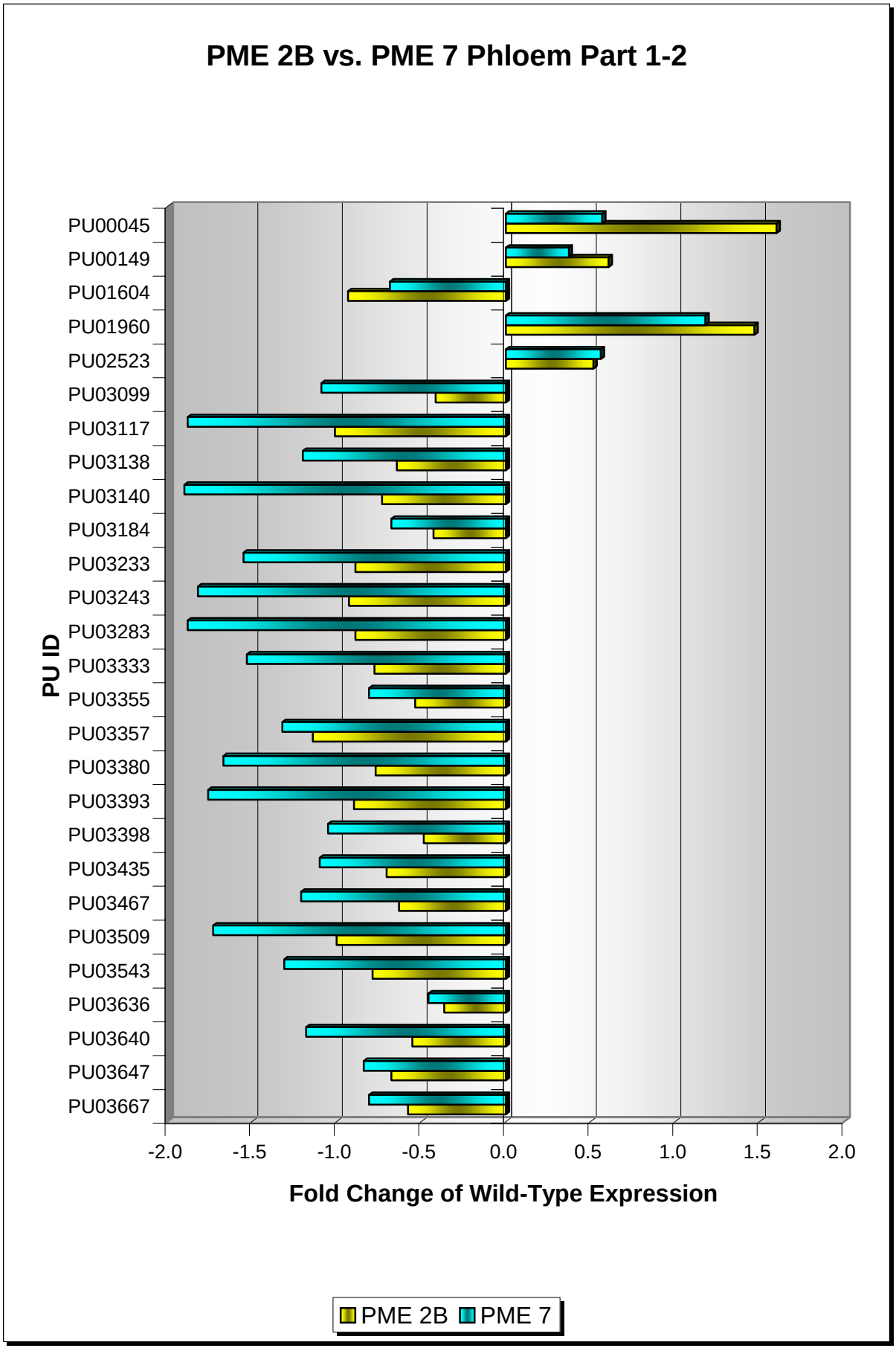
PME 2B vs. PME 7 Phloem Part 1-2
PU ID
PU00045
PU00149
PU01604
PU01960
PU02523
PU03099
PU03117
PU03138
PU03140
PU03184
PU03233
PU03243
PU03283
PU03333
PU03355
PU03357
PU03380
PU03393
PU03398
PU03435
PU03467
PU03509
PU03543
PU03636
PU03640
PU03647
PU03667
-2.0
-1.5
-1.0
-0.5
0.0
0.5
1.0
1.5
2.0
Fold Change of Wild-Type Expression
PME 2B
PME 7

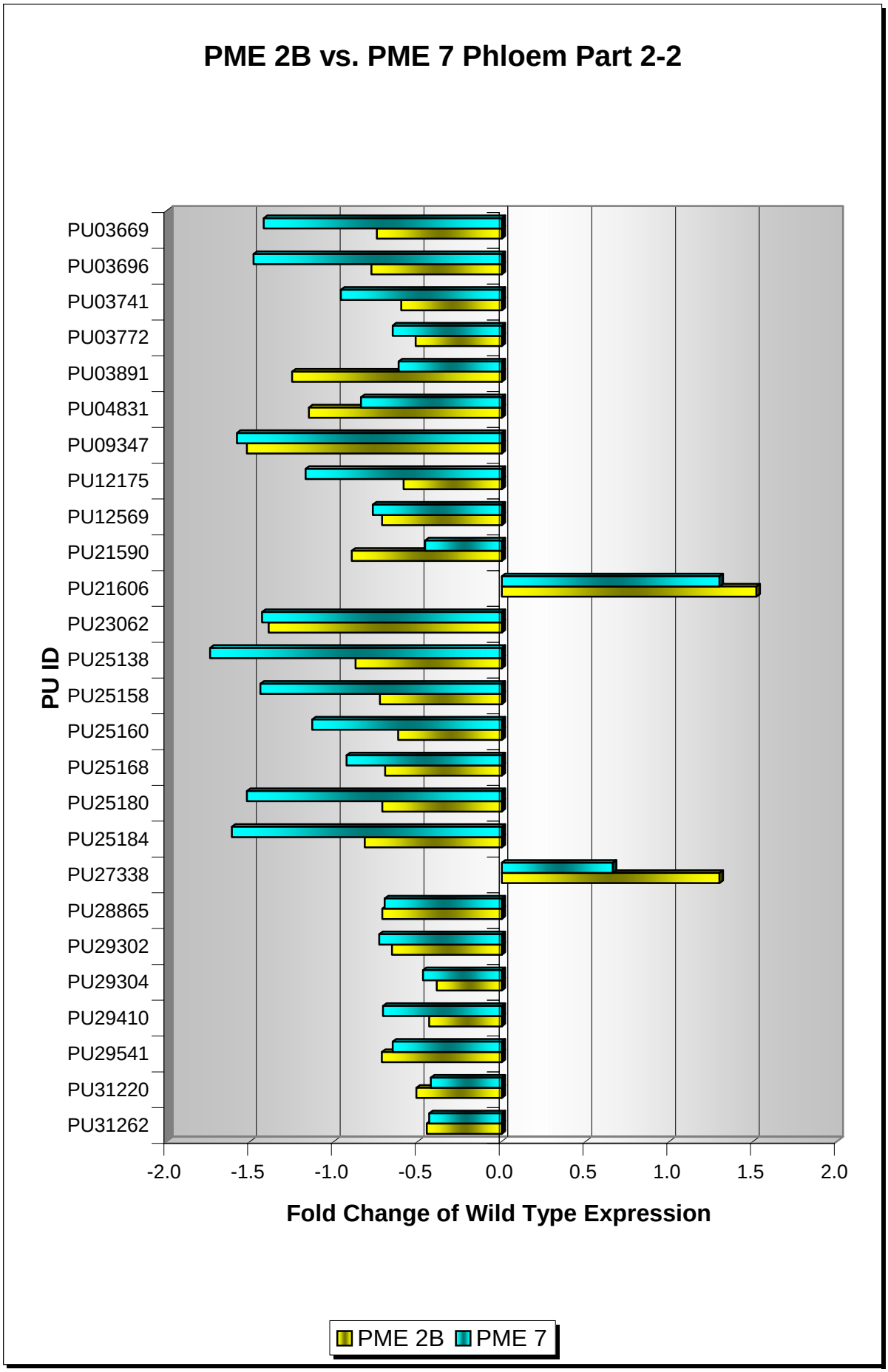
PME 2B vs. PME 7 Phloem Part 2-2
PU ID
PU03669
PU03696
PU03741
PU03772
PU03891
PU04831
PU09347
PU12175
PU12569
PU21590
PU21606
PU23062
PU25138
PU25158
PU25160
PU25168
PU25180
PU25184
PU27338
PU28865
PU29302
PU29304
PU29410
PU29541
PU31220
PU31262
-2.0
-1.5
-1.0
-0.5
0.0
0.5
1.0
1.5
2.0
Fold Change of Wild Type Expression
PME 2B
PME 7

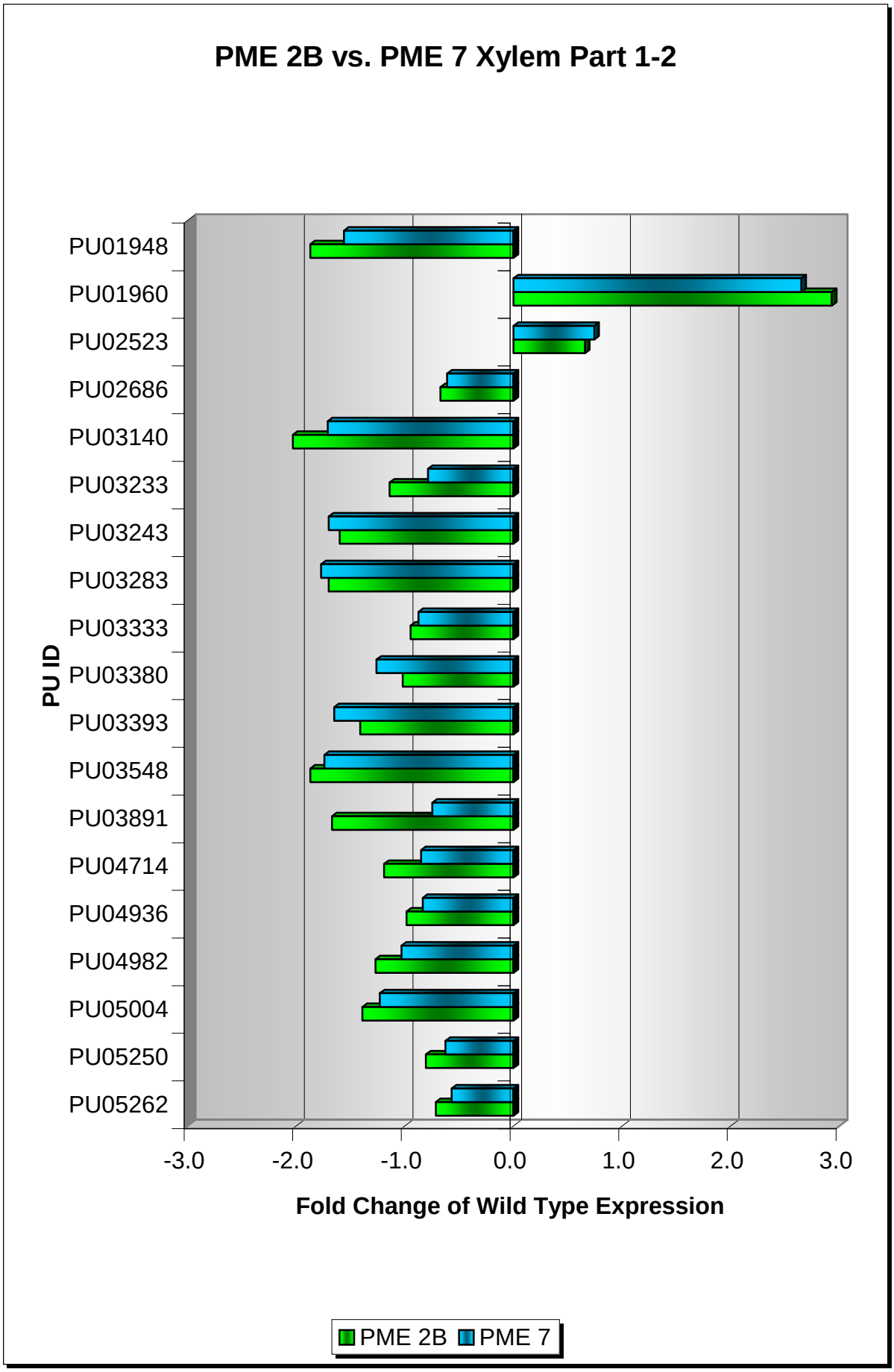
PME 2B vs. PME 7 Xylem Part 1-2
PU01948
PU01960
PU02523
PU02686
PU03140
PU03233
PU03243
PU03283
PU03333
PU03380
PU03393
PU03548
PU03891
PU04714
PU04936
PU04982
PU05004
PU05250
PU05262
PU ID
-3.0
-2.0
-1.0
0.0
1.0
2.0
3.0
Fold Change of Wild Type Expression
PME 2B
PME 7

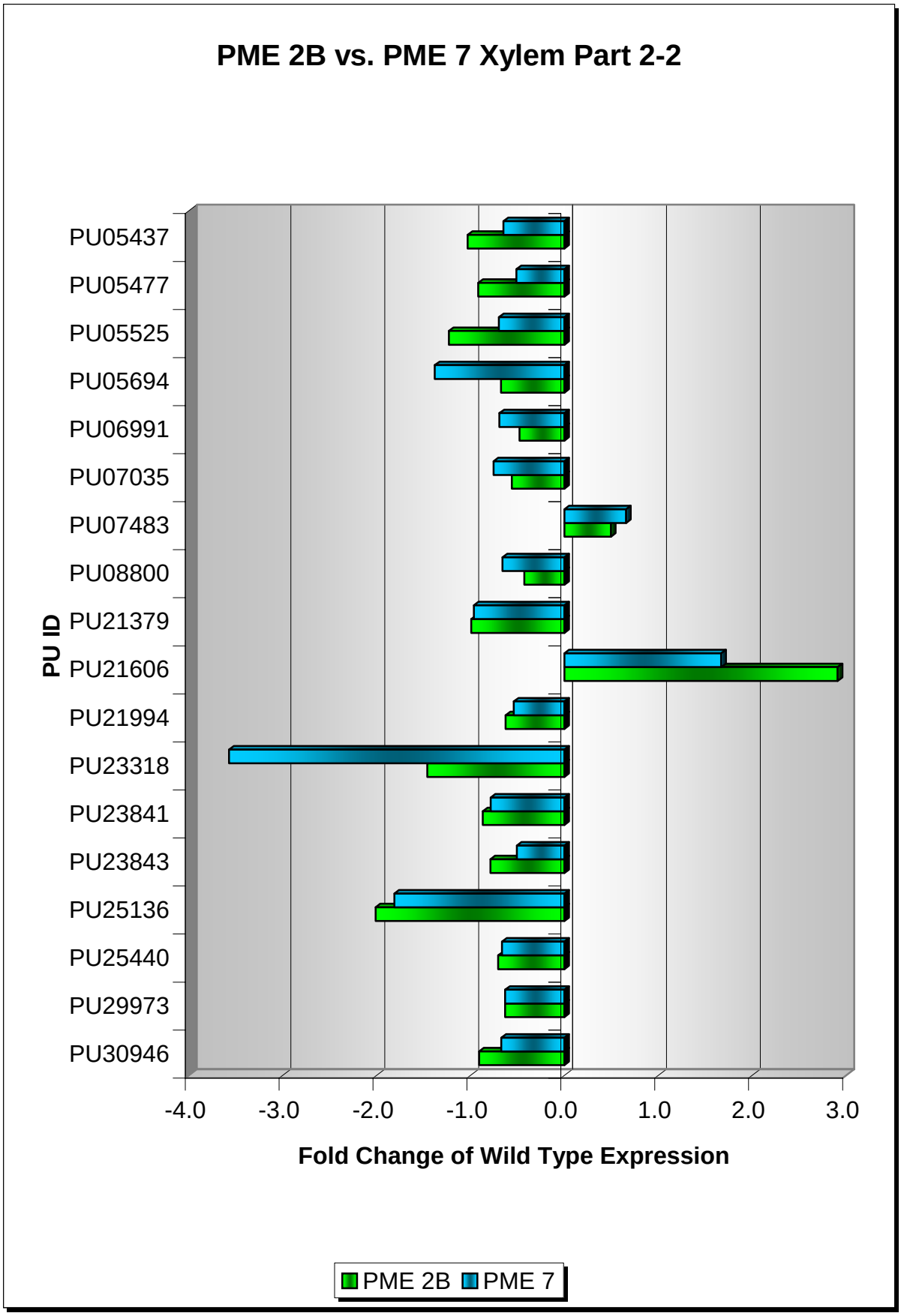

Figure 8. Graphic presentation of significantly affected genes ($P \leq 0.05$ and $B \geq 0$) in common in over-expressing lines PME 2B and PME 7 in the phloem (two parts) and xylem (two parts) fractions. Y-axis displays the PU id, while X-axis displays the $\log_2$ ratios (fold change of WT expression).

Lacking an additional suppressed line to compare with PME 5, necessitated the search for other published array data that could aid in the fundamental comparison. Here, a study made by Eriksson et al. (2004) on the effect of the *Cnr* (*Colorless non-ripening*) mutation on cell wall biochemistry and gene expression during tomato fruit development and ripening, suited well for a comparison, mainly due to the fact that expression of a gene coding for PME was found to be down-regulated in their MA-data, as well. In essence, the MA-data of the tomato *Cnr* mutant revealed a transcriptome profile where many genes related to stress signaling and pathogenesis defense responses were significantly up-regulated, concomitant with PME 5, and some of these key genes in common are presented in Table 3. Interestingly, this coincides with the similarities observed between the over-expressing lines, which, in contrast, constituted a majority of down-regulated genes. It is likely that PME 5 resides in an active defense and rescue mode, over-expressing central genes encoding proteins like ACC oxidase, basic chitinase (GH19_7), disease resistance response protein, glutaredoxin family protein, lipoxygenase (LOX2), and monooxygenase family protein. Important to point out is that even in the MA-data of the *Cnr* mutant, when scrolling and comparing, significantly affected genes related to cell wall metabolism are in a great minority, in accordance with MA-data of PME 5. Evidently, many of the genes between these two suppressed lines are regulated in the same way, and it would be interesting to confirm whether this observation is due to affected levels of PME or not.

Table 3. Genes affected in common between *Cnr* mutant and the suppressed line PME 5 Phloem and Xylem. Shown in the columns are descriptions of gene functions, regulation in *Cnr* mutant (up/down), corresponding PU ID, and relative signal intensities (log_2 ratios) in PME 5 Phloem and Xylem.

Description	*Cnr* Mutant	PU ID	PME 5 Phloem	PME 5 Xylem
1-aminocyclopropane-1-carboxylate oxidase (ACC oxidase)	up	PU30620	0.92	
ADP-ribosylation factor	down	PU06607		-0.51
amino acid transporter family protein	up	PU03852		0.30
invertase (*GH32_2*)	up	PU03467		1.15
basic chitinase (*GH19_7*)	up	PU28920	1.30	
cytochrome P450 family protein	up	PU26151	0.52	
disease resistance response protein-related/dirigent protein-related	up	PU21440	1.21	0.33
DNA-binding family protein/remorin family protein	up	PU00542		0.32
elongation factor Tu family protein	up	PU13346		0.38
expansin family protein (EXPR3)	up	PU09130	0.77	
F-actin capping protein beta subunit family protein	up	PU08060	0.49	0.36
glutaredoxin family protein	up	PU04875	0.42	0.96
immunophilin/FKBP-type peptidyl-prolyl cis-trans isomerase family protein	up	PU23867	0.84	
late embryogenesis abundant group 1 domain-containing protein (LEA)	down	PU03305	-0.93	
lipoxygenase (LOX2)	up	PU02955	1.23	0.66
monooxygenase family protein	up	PU08682		0.40
NADH-ubiquinone oxidoreductase B8 subunit	up	PU07349	0.70	0.58
oxidoreductase/2OG-Fe(II) oxygenase family protein	up	PU09288		0.45
pectin methylesterase (*CE8_79*)	down	PU01960	-3.44	-1.97
ubiquitin-conjugating enzyme	up	PU02483	0.44	0.37

Implementation of Different Clustering Techniques Allowed for the Discovery of Sets of Genes, Potentially Coordinately Regulated

To discover groups of genes co-regulated in different lines and tissues, GeneSpring clustering software, including Gene and Condition Tree clustering, K-Means clustering, and Self-Organizing Maps (SOMs), was used. In general, Gene and Condition Tree clustering reduces the complexity of the MA-data and allows for identification of co-expressed genes that are primarily responsible for the variation. This two-way cluster tree displays relationships between genes on the Y-axis, while relationships among the expression levels of experimental conditions are shown on the X-axis. In contrast, K-Means clustering yields a total of five groups showing a high degree of similarity of expression within each group but a low degree of similarity between groups. The advantage with K-Means, overall, is that the average behavior in each group is distinct from any of the other groups. For both clustering methods, a standard correlation algorithm was implemented, and a list of all redundant PUs affected in at least one experimental condition was selected (PME 6N excluded). SOM, though similar to K-Means, is a clustering technique that, on the whole, tries to illustrate the relationship between groups, by assigning them one coordinate out of 12, in addition to dividing genes into groups based on expression patterns. SOMs are useful for visualizing the number of distinct expression patterns in the data and determining which of these patterns are variants of one another. In addition, PUs lacking significant ($P \leq 0.05$ and $B \geq 0$) effects in four or more experimental conditions were discarded, prior to the analysis, in order to concentrate on most consistently affected co-regulated genes.

A two-way cluster tree is presented in Fig. 10. The distance between two nodes on the Y-axis illustrates the interrelationship between expression patterns of two different PUs, while the distance along the X-axis demonstrates the relationships between experimental conditions. According to X-clustering, PME 5 Phloem forms a separate cluster, while the over-expressing lines and PME 5 Xylem form another cluster. Further, the xylem fractions of both PME 2B and PME 7 cluster together, suggesting a very similar regulation of gene expression in the xylem of these two lines. These patterns reflect the *PttPME1* expression, very low in PME 5 Phloem, and very high in PME 2B and PME 7 Xylem, and intermediate in the remaining experimental conditions. The classification suggests that PME 5 Xylem was closer to over-expressing lines than to PME 5 Phloem in gene expression. A closer look at the Y-clustering revealed two nodes, a minor one containing 14 PUs and a major one containing 124 PUs, which were further split into a total of 138 nodes of PUs. K-Means analysis yielded a total of 5 groups showing a high degree of similarity of expression within each group and a low degree of similarity between groups (Fig. 11). Table 4 lists all the PUs clustered according to these two methods and results from the SOM clustering, as well. Obviously, many PUs derived from the same gene were clustered together, not only in the tree, but also in K-Means and SOMs, as well, suggesting a tight relationship among these PUs. For instance, several PUs, belonging to the same phosphorylase gene, were clustered together, mainly by the gene tree clustering method, and their gene expression pattern might, in fact, be linked to that of the mitogen-activated protein kinase (MAPK), described below. Other examples include F-box family proteins, dehydrin (RAB18), and fasciclin-like arabinogalactan-protein (FLA12), most prominent in the gene tree clustering, as well. When comparing the five groups of K-Means with the 12 groups (map coordinates) of SOMs clustering, it is evident that SOMs attempted to divide the K-Means clusters further into smaller clusters of more or less close relationships. Interestingly, K-Means cluster one, which contained a variety of expressed genes, failed to be split up further into more clusters by SOMs, when considering the small upper part of the tree only (i.e. first 13 clustered PUs belonging to K-Means cluster one). All PUs in this cluster, therefore, were taken into consideration and processed further for interpretation and analysis.

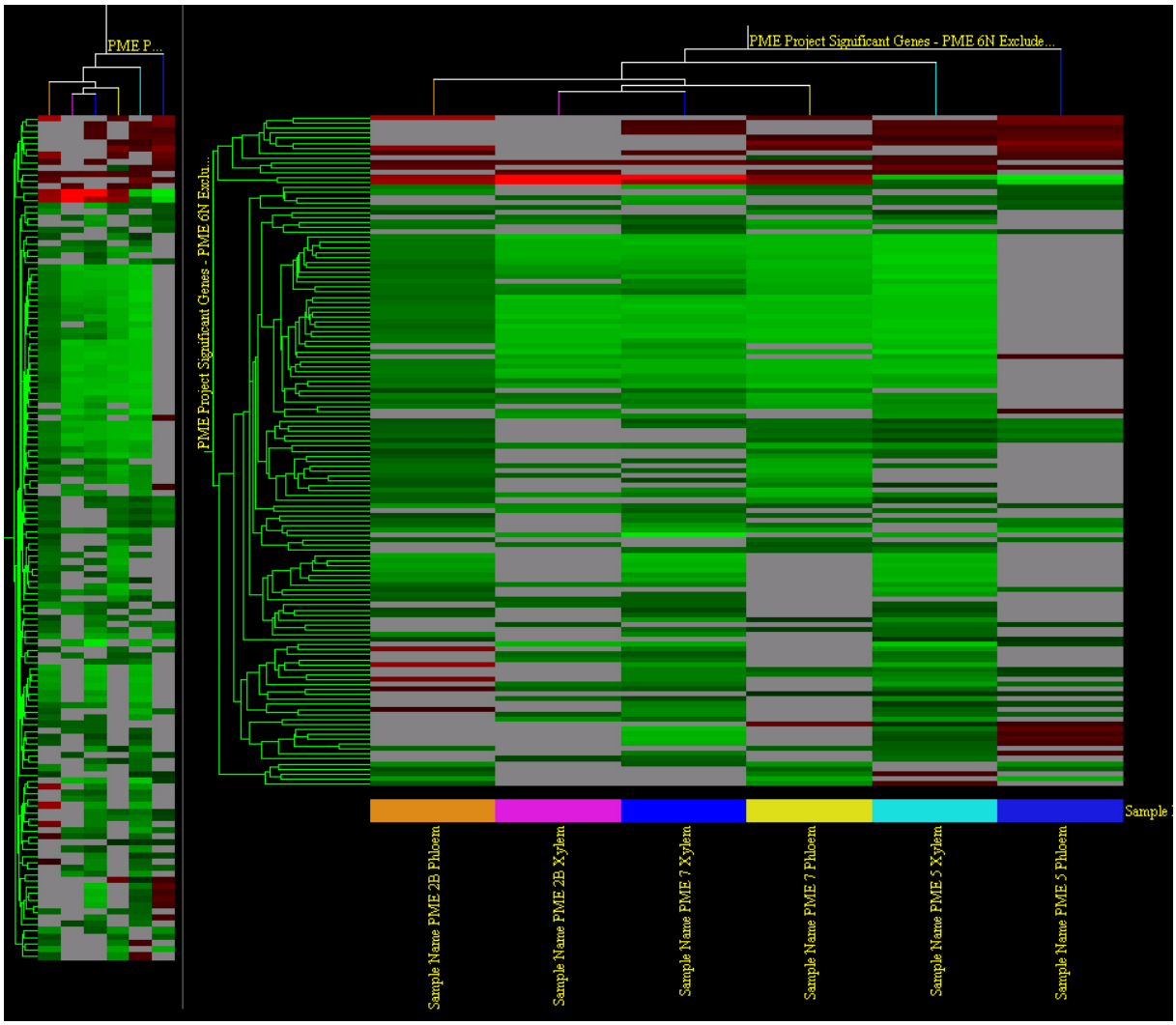

Figure 10. Gene and Condition Trees of significant genes (derived from master list, PME 6N excluded). Displayed on the Y-axis: nodes showing the relationships between redundant PUs. On the X-axis: nodes showing the relationships between all six experimental conditions. Green color indicates down-regulation, red color up-regulation, and grey color not significant change.

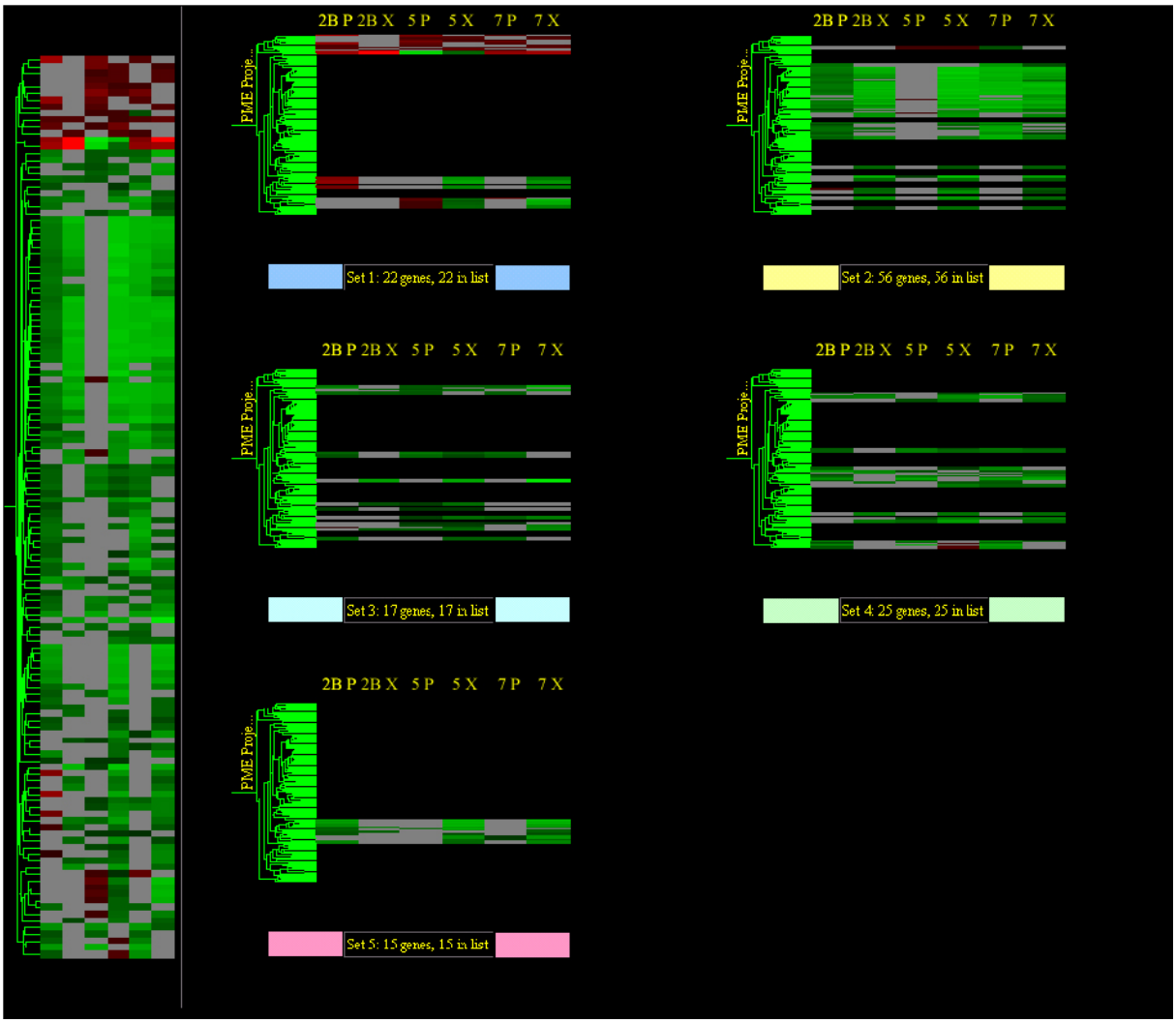

Figure 11. Overview of K-Means clustering. Shown are the five different groups (color-coded), and the number of redundant PUs belonging to each group, in addition to their position in the Gene Tree from Figure 10.

Table 4. Clusters of co-regulated significantly affected genes outlined in the Gene Tree (Figue 10). In the columns: PU ID (redundant PUs), *Populus* gene model, gene description, relative signal intensities (log_2 ratios), K-Means group, and SOMs coordinates. The two main clusters of the Gene Tree are separated by a thicker header for clarity, and K-Means and SOMs clustering groups/coordinates are color coded. The log_2 ratio values are displayed only for the significantly affected genes ($P \leq 0.05$ and $B \geq 0$).

PU ID	*Populus* Gene Model	Description	PME 5 Phloem	PME 2B Phloem	PME 7 Phloem	PME 5 Xylem	PME 2B Xylem	PME 7 Xylem	K-Means	SOM (4x3)
PU00045	estExt_fgenesh4_pg.C_1800002	calcium-binding EF hand family protein	1.00	1.60	0.57				1	3,4
PU27262	estExt_fgenesh4_pm.C_LG_I0233	DREPP plasma membrane polypeptide family protein	0.90			0.64		0.43	1	3,4
PU03161	gw1.VIII.2.1	oxygenase-related	0.45			0.50		0.55	1	3,4
PU03143	gw1.I.3775.1	expressed protein	0.64			0.60		0.52	1	3,4

PU04890	eugene3.00011709	serine carboxypeptidase	0.72		0.32	0.37			1	3,4
PU11967	eugene3.01780010	tRNA synthetase-related/tRNA ligase-related	1.18		1.08	0.60			1	3,4
PU27338	estExt_fgenesh4_pm.C_LG_I0604	pathogenesis-related thaumatin family protein	0.88	1.30	0.66				1	3,4
PU02759	eugene3.00410190	cytochrome c	0.65	0.52				0.51	1	3,4
PU00356	grail3.0008017001	pectin beta-glucuronyltransferase (GT47_73)	0.46		-0.50	0.49			2	3,4
PU02523	estExt_fgenesh4_pm.C_LG_XII0164	WD-40 repeat family protein		0.52	0.56	0.49	0.66	0.74	1	3,4
PU04875	gw1.VI.81.1	glutaredoxin family protein	0.42	0.69		0.96			1	3,4
PU11450	gw1.V.5250.1	nodulin MtN21 family protein			0.48	0.83	0.58		1	3,4
PU01960	estExt_fgenesh4_pm.C_290002	pectin methylesterase (*PttPME1*) (*CE8_79*)	-3.44	1.47	1.18	-1.97	2.93	2.65	1	3,4
PU21606	eugene3.00030462	pectin methylesterase (*CE8_78*)	-2.60	1.52	1.30	-0.69	2.91	1.67	1	3,4
PU01604	grail3.0003067001	1-aminocyclopropane-1-carboxylate oxidase (ACC oxidase)	-0.57	-0.93	-0.69	-0.66		-1.70	3	3,2
PU04831	eugene3.101950001	18.1 kDa class I heat shock protein (HSP18.1-CI)	-0.58	-1.15	-0.84				3	1,3
PU05694	estExt_fgenesh4_pg.C_LG_X0149	drought-responsive protein/drought-induced protein (Di21)	-0.50			-0.75	-0.67	-1.38	3	3,2
PU27587	estExt_fgenesh4_pg.C_LG_X0149	drought-responsive protein/drought-induced protein (Di21)	-0.64			-0.78		-1.23	3	3,2
PU29541	estExt_Genewise1_v1.C_LG_X3745	AP2 domain-containing protein RAP2.2	-0.60	-0.72	-0.65		-0.69		3	1,4
PU03068	estExt_Genewise1_v1.C_410611	phosphorylase family protein		-0.50	-1.10	-0.35			4	1,4
PU05250	grail3.0054013701	expressed protein				-0.70	-0.81	-0.63	4	1,4
PU03233	estExt_fgenesh4_pm.C_LG_VIII0544	expressed protein		-0.89	-1.55	-1.29	-1.14	-0.79	4	1,3
PU03543	estExt_Genewise1_v1.C_LG_IV0651	expressed protein		-0.79	-1.31			-0.50	2	1,3
PU28819	eugene3.00111024	structural maintenance of chromosomes (SMC) family protein	-0.52			-0.88		-0.65	4	1,4
PU03117	estExt_Genewise1_v1.C_410611	phosphorylase family protein		-1.01	-1.88	-2.23	-1.91	-1.63	2	1,1
PU03283	grail3.0015004101	microtubule-associated EB1 family protein		-0.89	-1.88	-2.07	-1.70	-1.77	2	1,1
PU03743	estExt_Genewise1_v1.C_410611	phosphorylase family protein		-0.87	-1.88	-2.08	-1.66	-1.70	2	1,1
PU03784	estExt_Genewise1_v1.C_410611	phosphorylase family protein		-0.85	-1.82	-2.16	-1.66	-1.71	2	1,1
PU25145	estExt_Genewise1_v1.C_410611	phosphorylase family protein		-0.92	-1.69	-2.30	-1.70	-1.52	2	1,1
PU25166	estExt_Genewise1_v1.C_410611	phosphorylase family protein		-0.83	-1.73	-2.37	-1.49	-1.38	2	1,1
PU25167	estExt_Genewise1_v1.C_410611	phosphorylase family protein		-0.75	-1.82	-2.01	-1.31	-1.44	2	1,1
PU25132	estExt_Genewise1_v1.C_410611	phosphorylase family protein		-0.83	-1.69	-2.15	-1.30	-1.17	2	1,1
PU29406	estExt_Genewise1_v1.C_410611	phosphorylase family protein		-0.84	-1.68	-2.31	-1.09	-1.46	2	1,1
PU25183	estExt_Genewise1_v1.C_410611	phosphorylase family protein		-0.88	-1.68	-1.82		-0.94	2	1,2
PU25155	estExt_Genewise1_v1.C_410611	phosphorylase family protein		-0.78	-1.56	-2.25	-1.11	-1.08	2	1,2
PU25156	estExt_Genewise1_v1.C_410611	phosphorylase family protein		-0.84	-1.45	-2.10	-0.99	-0.77	2	1,2
PU03140	eugene3.00150430	expressed protein		-0.73	-1.90	-2.02	-2.03	-1.71	2	1,1
PU03510	estExt_Genewise1_v1.C_410611	phosphorylase family protein		-0.80	-1.85	-2.00	-1.80	-1.76	2	1,1
PU03352	estExt_Genewise1_v1.C_410611	phosphorylase family protein		-0.87	-1.87	-1.99	-1.79	-1.93	2	1,1
PU03548	estExt_fgenesh4_pg.C_410195	phosphorylase family protein		-0.85	-1.79	-2.04	-1.87	-1.74	2	1,1
PU03708	estExt_Genewise1_v1.C_410611	phosphorylase family protein		-0.89	-1.90	-2.02	-1.91	-1.82	2	1,1
PU25134	estExt_Genewise1_v1.C_410611	phosphorylase family protein		-0.82	-1.78	-2.21	-1.64	-1.66	2	1,1
PU25136	estExt_Genewise1_v1.C_410	phosphorylase family protein		-0.75	-1.86	-2.24	-2.01	-1.81	2	1,1

	611									
PU03508	estExt_Genewise1_v1.C_410611	phosphorylase family protein		-0.83	-1.91	-2.03	-1.80	-1.79	2	1,1
PU03824	estExt_Genewise1_v1.C_410611	phosphorylase family protein		-0.89	-1.91	-2.08	-1.78	-2.01	2	1,1
PU03698	estExt_Genewise1_v1.C_410611	phosphorylase family protein		-0.85	-1.75	-1.94	-1.88	-1.45	2	1,1
PU05856	estExt_fgenesh4_pg.C_LG_IV0455	Bet v I allergen family protein (Pathogenesis-related protein)				-1.74	-1.59	-1.22	2	1,2
PU03509	estExt_fgenesh4_pg.C_410195	phosphorylase family protein		-1.00	-1.73	-2.28	-1.93	-1.58	2	1,1
PU05004	grail3.0010043801	protease inhibitor/seed storage/lipid transfer protein (LTP) family protein	0.43			-1.50	-1.39	-1.23	2	3,1
PU03243	gw1.VIII.377.1	beta-glycanase (*GH5_17*)		-0.93	-1.82	-1.88	-1.60	-1.70	2	1,1
PU03393	estExt_fgenesh4_pm.C_LG_XVIII0241	aspartate aminotransferase, cytoplasmic isozyme 1/transaminase A (ASP2)		-0.90	-1.76	-1.80	-1.41	-1.65	2	1,1
PU29403	estExt_Genewise1_v1.C_410611	phosphorylase family protein		-0.98	-1.78	-2.03	-1.84	-1.62	2	1,1
PU25143	estExt_Genewise1_v1.C_410611	phosphorylase family protein		-0.89	-1.62	-1.56	-1.62	-1.29	2	2,1
PU03380	estExt_Genewise1_v1.C_640140	isocitrate lyase		-0.77	-1.67	-1.41	-1.02	-1.26	2	2,2
PU03820	estExt_Genewise1_v1.C_410611	phosphorylase family protein		-0.91	-1.95	-1.60	-1.33	-1.47	2	2,1
PU03398	estExt_fgenesh4_pg.C_1450022	type I phosphodiesterase/nucleotide pyrophosphatase family protein		-0.49	-1.05			-0.71	2	1,4
PU03474	estExt_Genewise1_v1.C_410611	phosphorylase family protein		-0.96	-1.71	-1.21	-0.83	-1.04	2	1,3
PU23277	estExt_Genewise1_v1.C_410611	phosphorylase family protein		-0.76	-1.46	-1.04	-1.02	-0.93	2	1,3
PU04029	estExt_Genewise1_v1.C_410611	phosphorylase family protein		-0.88	-1.38	-1.18		-1.07	2	1,3
PU04787	grail3.0006039501	histone H2B	0.36			-1.13	-1.30		2	3,1
PU04982	estExt_fgenesh4_pg.C_LG_X1194	hypothetical protein				-1.33	-1.27	-1.03	2	2,2
PU03167	eugene3.00130614	dehydrin family protein	-0.87	-0.59	-0.78	-0.52		-0.58	4	1,4
PU03647	eugene3.00130613	dehydrin (RAB18)	-1.02	-0.68	-0.84	-0.70		-0.70	4	1,4
PU29302	grail3.0016050401	dehydrin (RAB18)	-0.84	-0.66	-0.73	-0.54			3	1,4
PU12569	eugene3.00130614	dehydrin family protein	-0.97	-0.71	-0.77	-0.68			3	1,4
PU26465	grail3.0016050401	dehydrin (RAB18)	-0.76	-0.55	-0.63	-0.42			3	1,4
PU03333	eugene3.00010981	expressed protein		-0.78	-1.53	-1.23	-0.95	-0.88	2	1,3
PU25175	estExt_Genewise1_v1.C_410611	phosphorylase family protein		-0.46	-0.79	-0.87			2	2,3
PU03640	fgenesh4_pm.C_LG_VIII000571	gibberellin response modulator (GAI) (RGA2)		-0.55	-1.18	-0.67			2	1,4
PU25180	eugene3.00280205	acylphosphatase family		-0.71	-1.52			-0.60	2	1,3
PU03696	estExt_fgenesh4_pm.C_LG_XIII0359	fertilization-independent endosperm protein (FIE)		-0.78	-1.48	-0.70	-0.84		2	1,3
PU25184	eugene3.42360001	AAA-type ATPase family protein		-0.82	-1.61			-0.68	2	1,3
PU25158	eugene3.00020653	hypothetical protein		-0.73	-1.44		-0.63		2	1,3
PU25160	gw1.XVIII.392.1	calcium-transporting ATPase, plasma membrane-type/Ca2+-ATPase (ACA10)		-0.62	-1.13			-0.47	2	1,4
PU03741	grail3.0045011701	ubiquitin fusion degradation UFD1 family protein		-0.60	-0.96	-0.33			4	1,4
PU25138	estExt_fgenesh4_pg.C_LG_II0463	homocysteine S-methyltransferase 2 (HMT-2)		-0.87	-1.74			-1.04	2	1,2
PU25182	estExt_Genewise1_v1.C_410611	phosphorylase family protein		-0.68	-1.63	-0.91	-1.15	-0.90	2	1,3
PU04085	estExt_Genewise1_v1.C_410611	phosphorylase family protein		-0.65	-1.15	-0.79			4	1,4
PU03891	estExt_Genewise1_v1.C_LG_XVII0327	Bet v I allergen family protein (Pathogenesis-related protein)	-0.53	-1.25	-0.62		-1.67	-0.75	4	1,3
PU05525	grail3.0054013301	expressed protein				-0.68	-1.23	-0.70	4	1,3
PU03184	estExt_fgenesh4_pg.C_LG_V0735	14-3-3 protein GF14 kappa (GRF8)		-0.43	-0.68			-0.92	4	2,3
PU21068	grail3.1504000201	armadillo/beta-catenin repeat family	-0.94	-0.62		-0.81		-0.88	4	1,4

		protein/U-box domain-containing protein								
PU03305	grail3.0004009401	late embryogenesis abundant group 1 domain-containing protein (LEA)	-0.93	-0.83	-0.81			-1.31	4	1,3
PU23062	grail3.0004009401	late embryogenesis abundant group 1 domain-containing protein (LEA)	-1.49	-1.39	-1.43			-1.65	4	1,2
PU23318	LG_IX: 3531235-3531658	hypothetical protein				-1.47	-1.46	-3.57	3	2,1
PU03667	eugene3.00080380	hydrophobic protein/low temperature and salt responsive protein	-0.95	-0.58	-0.81				4	1,4
PU26170	fgenesh4_pg.C_scaffold_137000005	glycine-rich protein			-0.55	-0.56	-0.94		4	3,3
PU23492	gw1.II.1765.1	phosphate-responsive protein (EXO)			-0.66	-0.90		-0.75	4	1,4
PU07307	eugene3.01340013	F-box family protein-related similar to F-box protein family		-1.51		-1.75		-2.02	5	1,1
PU21092	eugene3.01340013	F-box family protein-related similar to F-box protein family		-1.33		-1.68		-1.74	5	1,1
PU27911	eugene3.01340013	F-box family protein-related similar to F-box protein family		-1.43		-1.74		-1.71	5	1,1
PU22659	eugene3.01340013	F-box family protein-related similar to F-box protein family		-1.27		-1.44		-1.85	5	1,1
PU22422	eugene3.01340013	F-box family protein-related similar to F-box protein family		-1.02		-1.68		-1.25	5	1,2
PU22428	eugene3.01340013	F-box family protein-related similar to F-box protein family		-1.18		-1.77		-1.47	5	1,1
PU21379	LG_XII: 9909476-9909763	no description		-0.70		-1.25	-0.99	-0.96	5	1,3
PU26673	grail3.0013032202	zinc finger (C3HC4-type RING finger)	-0.70	-0.57		-1.66			5	1,2
PU28015	eugene3.15590001	ribosomal protein L16 family protein		-0.76		-1.27		-0.67	5	1,3
PU29973	estExt_Genewise1_v1.C_LG_IX2012	expressed protein and genefinder		-0.61			-0.63	-0.63	5	1,4
PU25440	gw1.I.4026.1	protein phosphatase 2C family protein (PP2C)				-0.62	-0.70	-0.66	2	1,4
PU28240	LG_XIX: 3939714-3940205	secretory carrier membrane protein (SCAMP) family protein		-0.53		-0.47		-0.44	5	2,4
PU28382	fgenesh4_pg.C_LG_XVI001214	expressed protein		-0.60		-0.65		-0.64	5	1,4
PU29967	fgenesh4_pg.C_scaffold_375000004	hypothetical protein			-0.32	-1.13		-1.32	5	3,2
PU26575	estExt_fgenesh4_pg.C_LG_V1038	F-box family protein	-0.38			-0.82	-0.53		3	2,4
PU27979	LG_I: 32115515-32115953	hypothetical protein			-0.38	-0.72		-0.72	5	2,4
PU28379	scaffold_127 889504: 239527-239730	no description		-1.07		-0.73		-0.95	5	1,3
PU29772	eugene3.00130614	dehydrin family protein	-0.60	-0.40		-0.56			3	2,4
PU01948	estExt_fgenesh4_pg.C_LG_IV0455	Bet v I allergen family protein (Pathogenesis-related protein)	-0.39			-2.18	-1.87	-1.56	2	1,1
PU21143	eugene3.01210029	GDSL-motif lipase/hydrolase family protein		1.24		-1.26		-0.86	1	3,3
PU05262	eugene3.00061214	DNA polymerase delta small subunit-related				-0.82	-0.72	-0.57	2	1,4
PU04936	eugene3.25610001	expressed protein				-0.83	-0.98	-0.84	4	1,3
PU20764	eugene3.01210029	GDSL-motif lipase/hydrolase family protein		1.42		-1.48		-1.33	1	3,3
PU10193	estExt_fgenesh4_pm.C_LG_X0729	zinc finger (CCCH-type) family protein	-0.37		-0.63	-0.79		-1.01	3	2,3
PU09430	estExt_fgenesh4_pm.C_LG_XIV0172	WRKY family transcription factor	-0.72		-0.93	-1.03		-1.00	4	1,3
PU12468	eugene3.01210029	GDSL-motif lipase/hydrolase family protein		1.06		-1.12		-0.96	1	3,3
PU23841	estExt_Genewise1_v1.C_LG_I1393	zinc finger (C2H2 type) family protein (ZAT12)	-1.14			-1.36	-0.87	-0.79	4	1,3
PU02686	grail3.0001018301	expressed protein		0.47		-0.75	-0.67	-0.61	2	3,3
PU06214	grail3.0001042602	bifunctional dihydrofolate reductase-thymidylate synthase 1/DHFR-TS (THY-1)	-0.35		-0.29	-0.31			3	3,4
PU05477	grail3.0006039501	histone H2B				-1.16	-0.92	-0.51	2	1,4
PU05580	gw1.IV.2305.1	leucine-rich repeat transmembrane protein kinase	-0.45			-0.42		-0.95	3	3,3
PU07241	gw1.II.1879.1	pfkB-type carbohydrate kinase family protein		0.31		-0.66		-1.04	3	3,3

PU29457	estExt_fgenesh4_pg.C_LG_X 0149	drought-responsive protein/drought-induced protein (Di21)	-0.63			-0.77	-0.61	-1.06	3	2,3
PU03311	estExt_fgenesh4_pg.C_LG_X 1194	hypothetical protein				-1.28	-1.17	-0.82	2	1,3
PU28351	gw1.XI.2013.1	serine carboxypeptidase S10 family protein	0.43		0.83	-0.27			1	3,4
PU07213	eugene3.00131210	fasciclin-like arabinogalactan-protein (FLA12)	0.74			-0.89		-2.01	1	3,1
PU07326	grail3.0094006801	fasciclin-like arabinogalactan-protein (FLA12)	0.49			-0.61		-1.72	1	3,2
PU30269	eugene3.00131210	fasciclin-like arabinogalactan-protein (FLA12)	0.65			-0.53		-1.87	1	3,2
PU08307	grail3.0096005001	leucine-rich repeat transmembrane protein kinase	0.46			-0.63		-1.71	1	3,2
PU28865	grail3.0013032202	zinc finger (C3HC4-type RING finger) family protein		-0.71	-0.70	-0.84			3	1,4
PU08336	estExt_Genewise1_v1.C_261 0036	expressed protein	0.42			-0.75		-1.00	1	3,2
PU08800	eugene3.00030563	no description				-0.85	-0.43	-0.66	2	3,3
PU03357	eugene3.00110845	9-cis-epoxycarotenoid dioxygenase	-1.32	-1.14	-1.32			-0.55	4	1,3
PU03772	estExt_fgenesh4_pg.C_LG_II 1111	rRNA processing protein-related	-0.63	-0.51	-0.65				4	1,4
PU03435	gw1.XIV.2046.1	expressed protein		-0.70	-1.10	0.65			4	2,4
PU09347	eugene3.00140486	homeobox-leucine zipper protein 12 (HB-12)/HD-ZIP transcription factor 12	-1.89	-1.52	-1.58				4	1,2
PU03467	gw1.XVI.2454.1	invertase (*GH32_2*)		-0.63	-1.21	1.15			4	2,4

Many Differentially Regulated Genes Were Related to Oxidative Stress Responses

K-Means cluster 1, (Table 4) constituted the most interesting group, since it contained genes potentially coordinately regulated with the target gene *PME1*. The corresponding SOM coordinates (mainly coordinate: 3,4) in this cluster reinforced this argument. Functional classification of these genes revealed that most of them were highly related to stress signaling, induced by reactive oxygen species (ROS), including H_2O_2. H_2O_2 is now widely recognized as a key stress-signaling molecule, mediating adaptability and cross-tolerance towards other stresses (Desikan et al., 2001). *Arabidopsis* MA-data on genes induced and regulated by H_2O_2 reveals a close resemblance with genes expressed in the present analysis, such as heat shock proteins, calcium-binding EF hand family proteins, zinc finger proteins, and WRKYs. Nanjo et al. (2004) subjected *Populus* trees to diverse environmental stresses and investigated the transcriptome changes by generating a full-length enriched cDNA library from leaves of the axenically grown trees, followed by EST sequencing. Indeed, there was a striking resemblance between the differentially expressed genes in their study and the significant genes in the present analysis. Both studies identified many regulatory proteins, like protein phosphatase 2C (PP2C), drought-induced proteins, and some transcription factors including ERF domain transcription factors, implicated to play important roles in stress responses. These transcription factors mediate signal transduction via critical signaling pathways, ultimately leading to activation or inactivation of key stress-related genes and their products. In general, mechanisms and molecules involved in stress responses appear to be conserved between plant species, aiding in a relative straightforward comparison between *Arabidopsis* and *Populus* gene model systems.

Stress responses in plants (perception of stress, synthesis of chief signaling molecules and perception of these, and the final response) is currently considered to involve generation of ROS and further signaling via three main pathways (Devoto and Turner, 2005). These signaling pathways, which also interact with each other, can be distinguished on the basis of their regulating signaling molecules, namely jasmonates (JA), salicylic acid (SA), and ethylene (ET). These key elements are integrated in a network that involves signaling 'cross-talk' between the down-stream response pathways, as well as regulatory steps, characterized

by transcription, protein-protein interaction, and targeted protein destruction. Many of these regulatory steps are currently not well understood. The down-stream oxidative signaling events, outlined in Fig. 11, are dependent on a flux of the ubiquitous second messenger Ca^{2+} to facilitate protein phosphorylation, which is regulated by MAPK cascades, further increasing the rapid and transient phosphorylation of specific nuclear, cytosolic, and membrane-bound proteins (Baier et al., 2005).

Pathogens have been shown (Hu et al., 2004) to trigger stress responses in plants via generation of oligogalacturonates (OGAs). OGAs can elicit an oxidative burst that induces the transcription and expression of stress signaling and defense genes. The requirements for this are, firstly, increases in cytosolic calcium; and, secondly, generation of H_2O_2, which accumulation is mediated by the activation of a membrane-bound NADPH oxidase complex. OGA fragments are derived from plant cell walls as a result from the action of wound-inducible enzyme polygalacturonase (PG). PG is, apparently, indirectly regulated by the polypeptide signal systemin, which is released into the vascular system after wounding (Stennis et al., 1998; Orozco-Cárdenas et al., 2001). It is likely that stress-related genes, significantly affected in the present study, are regulated by complicated signaling events, linked to the oxidative burst and generation of H_2O_2 accumulation, which might originate from cell wall-derived OGAs. These OGAs, together with the triggered stress response, are probably an involuntarily outcome unique for the transgenic poplar lines, due to the fact that they exhibits an altered transcription and expression of *PME1* and, hence, altered properties of the cell wall. Although far from complete, the defense pathways that plants tend to rely on when exposed to stress, have been reviewed thoroughly by Anderson et al. (2005) and Thatcher et al. (2005). The authors suggested that the SA and JA pathways often seem to work antagonistically, while the ET and JA pathways often appear to work synergistically.

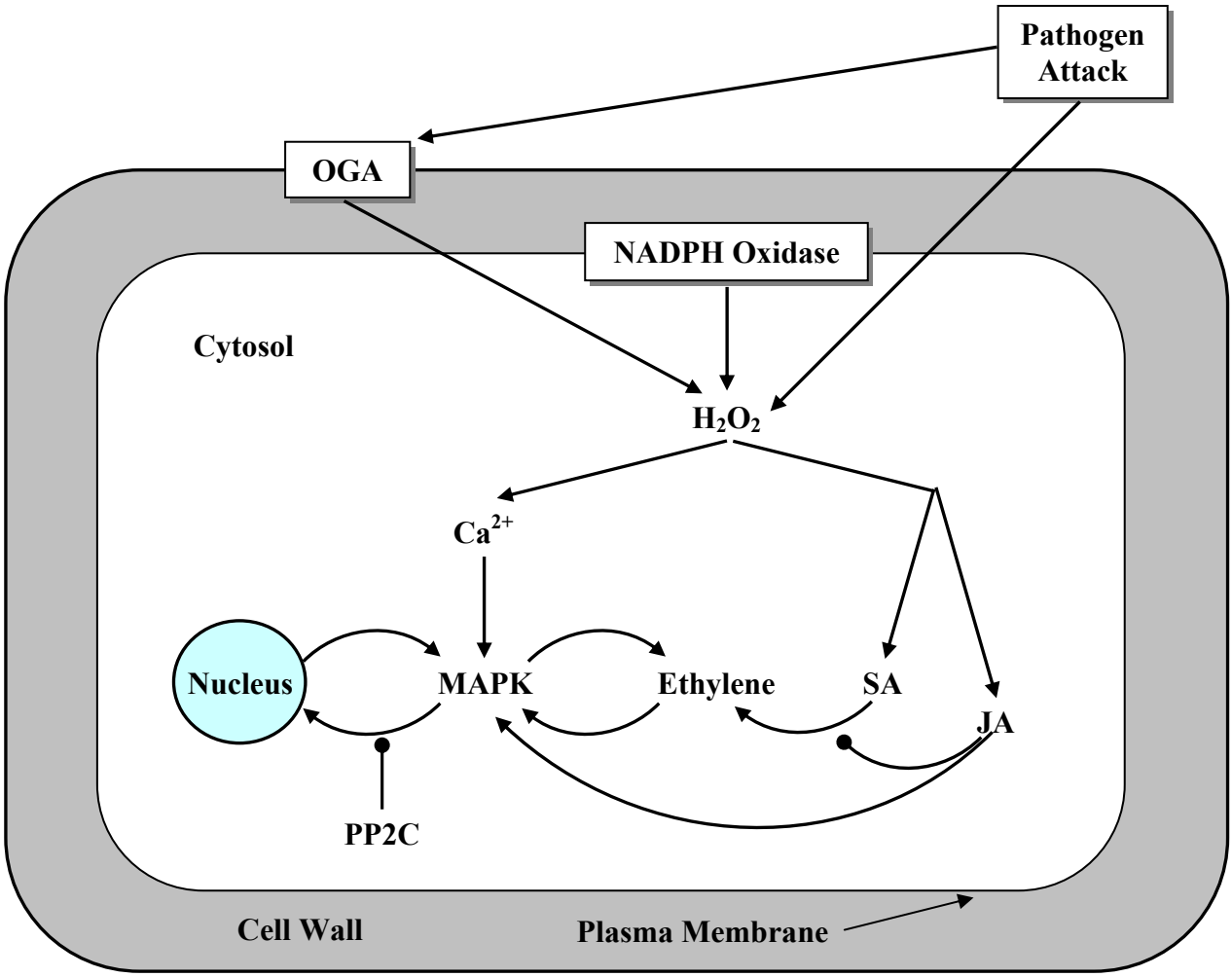

Figure 11. Stress signal transduction cascade. The stress signal could be elicited by OGA and pathogen attack and, in addition, also be mediated through NADPH oxidase complex. The oxidative burst (accumulation of H_2O_2) induces increase of cytosolic Ca^{2+}, which activates protein phosphorylation cascades, regulated by MAPKs. These induce ethylene production, in a positive feedback loop, thus further stimulating MAPK-signaling. Furthermore, SA promotes ethylene biosynthesis, while JA inhibits this SA-induced pathway. Nevertheless, JA induces MAPK-signaling. MAPK-signaling involves feed-forward loops, where signaling kinases are expressed, thus further increasing the phosphorylation activity. Phosphatases, like PP2C, function as negative regulators, inhibiting loop-signaling, and these enzymes can be redox-regulated themselves (modified from: Baier et al., 2005).

Fig. 12 illustrates the reaction of stress pathway genes in two over-expressing lines, PME 2B and PME 7, and in the suppressed line, PME 5. These pathways might be triggered by OGAs. RPM1-interacting protein RIN4 is one of several pathogen perception proteins initiating a defense response by the SA-mediated pathway (Dangl and Jones, 2001). It is likely acting as a negative regulator of defense signaling. A homologous gene was found down-regulated in PME 5 Xylem, suggesting that SA-pathway is affected in this tissue. Decreased levels of this protein are sensed by RPM1 (an *R*-protein). This is a component of indirect system of pathogen recognition, switching on defense pathway genes (Dangl and Jones, 2001). MA-data indicated that transcripts of two different *R*-proteins were down-regulated in PME over-expressing lines, while a different *R*-protein transcript was down-regulated in the suppressed line (Fig 12). These *R*-genes encode nucleotide-binding site leucine rich repeat proteins, containing N-terminal homology to the Toll and Interleukin-1 receptors (TIR-NBS-LRR), reviewed by Martin et al. (2003). Regulation of these *R*-proteins, though, reflects signaling through SA, which is a secondary signaling molecule, essential for systemic acquired resistance (SAR). In the SA-dependent signaling pathway, however, a gene encoding putative SON1 (an F-box protein), which is thought to act as a component of an SCF ubiquitin ligase complex that targets NPR1 for destruction (Kim and Delaney, 2002), was down-regulated in PME 2B Phloem. *NPR1* is a positive regulator that encodes an ankyrin-repeat protein (Cao et al., 1997). bZIP transcription factors, known as TGAs, specifically interact with the ankyrin domain of NPR1 (Zhou et al., 2000), and stimulate the transcription of *PR*-genes involved in the SA-dependent SAR. In PME suppressed line and PME up-regulated lines, many TGAs were down-regulated but a few were up-regulated (Fig.12). WRKYs represent another important family of transcription factors, which recognize and bind to a W-box motif containing an invariant and conserved TGAC core, implicated in mediating pathogen defense responses (Eulgem et al., 2000). W-box is located in the promoter of *NPR1*, thus WRKYs factors induce the expression of this gene. The MA-data revealed that all genes encoding these transcription factors were down-regulated in all experimental conditions, analogous with the expression of many TGAs (Fig. 12). Altogether, TGAs and WRKYs promote the expression of many pathogenesis-related (*PR*) proteins; e.g. beta-1,3-glucanases, chitinases, and thaumatin-like proteins (Thatcher et al., 2005). Interestingly, these *PR*-proteins tend to be up-regulated on the microarray, especially in the PME suppressed line 5, and some *PR*-genes were also upregulated in the suppressed lines 2B and 7 (Fig.12). It is therefore interesting that the transcript levels of *PR*-inducing transcription factors were most frequently down-regulated. It might be that this serves to regulate the pools of these proteins by negative feedback loops.

In the JA biosynthesis pathway, four poplar homologous genes encoding lipoxygenases (LOXs) were apparently affected (Fig. 12). In PME 5 Phloem, two genes were found to be up-regulated, while, on the other hand, one gene in PME 2B Phloem was down-regulated. In the xylem fraction, though, only PME 5 was affected, which accounted for two genes differentially regulated in a highly conflicted way; i.e. up- and down-regulated, respectively. LOXs have been demonstrated to catalyze the oxygenation of fatty acids to their hydroperoxy

derivatives (Devoto and Turner, 2005), and this reaction is an intermediate step in the octadecanoid pathway. This pathway, *per se*, entails many regulatory proteins/enzymes, starting from phospholipase A1/defective anther dehiscence1 (PLA1/DAD1), progressing down-stream through e.g. LOX, allene oxide synthase (AOS), allene oxide cyclase (AOC), 12-oxo-phytodienoic acid reductase3 [OPR3 (*dde1*)], and *S*-adenosyl-$_L$-methionine:jasmonic acid carboxyl methyltransferase (JMT). In the JA-signaling pathways, a gene coding for a mitogen-activated protein kinase kinase 9 (MKK9) and another gene encoding a MAPK (MPK4) were all found to be up-regulated in PME over-producing lines (Fig. 12). Interestingly, MPK4 has been postulated to induce the JA-signaling pathway (Petersen et al., 2000), while impairing the SA-mediated signaling pathway. It is possible that a redirection from SA to JA mediated signaling might have occurred, considering that signal transduction in each pathway results in the transcription of specific defense-associated genes in the PME over-producing lines. MPK3, which has been implicated to act in signaling cascades triggered by H_2O_2 (Dr. Brian Ellis, personal communication), homologue was found up-regulated in the PME suppressed line (Fig. 12). Since MPK3 is involved in the suppression of SA signaling pathway, and many SA-responding *PR*-genes were found up-regulated in the line PME 5, it is tempting to speculate that SA signaling might be triggered by PME deficiency. This is further supported by the up-regulation of a basic chitinase gene in *Cnr* mutant (Table 3). As a final point, signal transduction in JA pathway (Anderson et al., 2004) is mediated by coronatine insensitive1 (COI1) and MYC2 [allelic to jasmonate insentive1 (JIN1)], which leads to expression of vegetative storage proteins (VSP1 and VSP2).

ET stress-signaling is a well-known and thoroughly characterized response pathway, induced by various abiotic and biotic stimuli (Wang et al., 2002). Starting from *S*-adenosylmethionine (SAM), this compound is converted to 1-aminocyclopropane-1-carboxylic acid (ACC) by the action of ACC Synthase (ACS), followed by the production of ET by ACC oxidase (ACO). In the MA-data (Fig. 12), four genes coding for ACO-like proteins were affected, though, mostly contradicting each other in their expression across all six experimental conditions. In PME 5, two were up- and 1 was down-regulated in Phloem, while one was up- and three were down-regulated in Xylem. In the over-expressing lines, however, a slightly different expression pattern was observed; all genes, except for one, were down-regulated. Finally, several affected genes could be linked to the ET-dependent signaling pathway, via ethylene receptor 2 (ETR2). Two putative ETR2 homologues were down-regulated in PME 7 Phloem and Xylem, and an ethylene insensitive 3 (*EIN3*)-like gene was up-regulated in PME 5 Phloem. The ethylene insensitive 2 (*EIN2*)-like gene, which precedes *EIN3*-like gene, was not significantly affected on the array. A protein kinase (CTR1), that inhibits expression of *ETR2* (Wang et al., 2002), was down-regulated in PME 2B Phloem, reflecting a possible promotion of this defense pathway. The second last step in the signaling transduction includes expression of certain transcription factors known as EREBPs (e.g. ERF1). Three EREPBs were found to be down-regulated in both over-expressing and suppressed lines. These transcription factors, *per se*, bind to GCC box promoter elements to activate defense genes, such as defensins, thionins, and basic chitinases (e.g. *PDF1.2*, *Thi2.1*, and *CHI-B*), and one of these, *PDF2.3*, was apparently down-regulated in PME 5 Phloem. Similarly in the *Cnr* mutant, one gene encoding a putative CHI-B was up-regulated, suggesting activation of defense mechanisms to protect the plant from pathogen attack. Taken together, the ET-mediated signaling pathway demonstrated a suppressed gene expression pattern, most prominent in line 5, which perhaps justifies the assumption of negative regulation of protein pools, similarly with that observed in SA-mediated signaling.

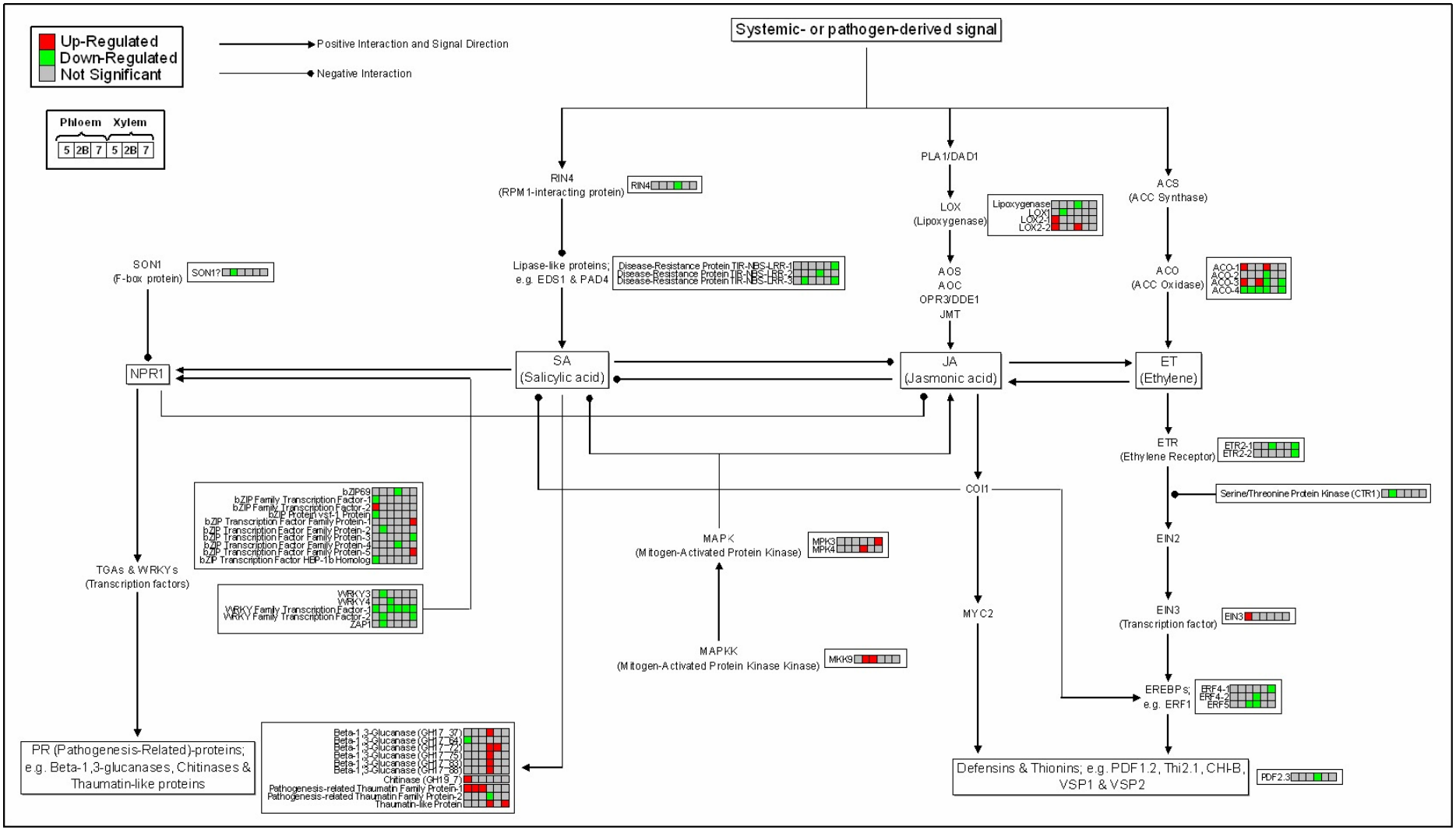

Figur 12. Stress/defense responses in all experimental conditions. Signal transduction occurs mainly through three stress-deduced pathways, comprising three key signaling molecules; SA, JA, and ET, regulating down-stream signaling events. Genes, differentially regulated in a significant way ($P \leq 0.05$ and $B \geq 0$), are assigned a color, depending on which kind of regulation (up-regulated, down-regulated, or not significant). In addition, all experimental conditions are represented in a box-wise fashion, as showed in the schematic drawing (modified from: Anderson et al., 2005 and Thatcher et al., 2005).

As a result of the pathogen attack or wounding, there is a burst of production of active oxygen species (AOS) that is involved in the downstream reactions described above, as well as in the hypersensitive (HR) response (Thatcher et al., 2005). During HR, AOS induce enzymes such as: phenylalanine ammonia-lyase (PAL) and glutathione *S*-transferase (GST). Surprisingly, two homologous genes encoding PAL1-like proteins were up-regulated in PME 2B Phloem, while one gene encoding another homologous PAL1 was, apparently, down-regulated in PME 7 Xylem (data not shown). Similarly, among three genes encoding GSTs, one was down-regulated in PME 2B Phloem, while another was up-regulated (data not shown). The third gene encoding a GST was up-regulated in PME 5 Xylem. Moreover, genes important for the regulation of protein turnover metabolism in the defense pathways were affected on the microarray (data not shown), which involved ubiquitin-mediated proteolysis; i.e. the final degradation by the 26S proteasome of proteins targeted for destruction. The down-regulation of several genes encoding F-box containing proteins (data not shown), which constitutes a part of the SCF (SKP1-CDC53p/CUL1-F-box) complex, in PME 5 Phloem and Xylem and PME 7 Xylem, as well, suggests an impaired turnover rate of key proteins in JA- and ET-signaling pathways. Moreover, a set of F-box-like proteins were down-regulated (Table 4), which could be implicated in negative regulation of signal transduction, thus reducing the pools of regulatory proteins/enzymes.

From a general overview, it is obvious that many genes related to stress-response cascades were down-regulated in both PME over-expressing lines and PME suppressed line. A rationale for this might be the possible incidence of feedback inhibition, a regulation mechanism that prevents unnecessary overproduction of key enzymes; i.e. returning to a 'steady-state' level. The stress-response in this study can be considered as a long-term experiment, spanning over a long period of time, from seedling to harvesting, unlike the short-term studies discussed above (e.g. Nanjo et al., 2004).

Oxidative stress cascades in the PME-modified lines could be triggered by OGAs. Interestingly, the elicitor and signaling molecule OGA has been implicated to induce ethylene production in tomato fruits, to initiate ripening processes (reviewed by Ridley et al., 2001). Considering the fact that demethylesterified pectins are more subjected to cleavage by PGs (i.e. methylated pectins are more resistant to PGs) than methylesterified PGs (Limberg et al., 2000; Van Alebeek et al., 2002), the over-expressing lines are more likely to display a phenotype exhibiting stress responses caused by OGAs. Nonetheless, the defense/stress response observed in the suppressed line could be related to OGAs, as well, but is more likely to be related to another, yet unidentified factor(s), which origin probably reside in the plant primary and/or secondary cell wall, exhibiting an altered chemical composition and morphology.

An Unexpected Outcome of the Microarray Data: Low Abundance of Cell Wall-Related Genes Significantly Affected by PME Modification

MA-data were mined for genes involved in xylem cell-wall formation, such as carbohydrate-active enzymes (CAZymes). CAZyme genes in polar have been recently identified (Geisler-Lee et al., 2006). CAZymes are vital for plant metabolism, growth, and development; and plants rely on them to convert products of photosynthesis into oligo- and polysaccharides, such as cellulose, pectin, and xylan; and to metabolize a variety of glycosylated compounds (glycolipids, glycoproteins, lignin precursors, and secondary metabolites). Fig. 13 shows genes significantly affected in metabolic pathways related to carbohydrate metabolism. Despite the decision to exclude line 6N from the data analysis, it was included in the following discussion, since this line alone accounted for the majority of modifications in transcripts of carbohydrate-related pathways. Taken as a whole, modification of *PME1* did not appear to involve any major redirection of carbon flux from one pathway to another,

suggesting that effects are most likely subtle and/or discrete for all eight experimental conditions. Concerning central metabolism, glycolysis (fructose-bisphosphate aldolase, glyceraldehyde-3-P dehydrogenase, enolase, lactate dehydrogenase) and TCA cycle (isocitrate dehydrogenase, succinyl-CoA ligase, and succinate dehydrogenase) genes were generally down-regulated, while penthose phosphate pathway genes, such as transaldolase, and gluconeogenesis genes; such as PEP caroxylase, PEP carboxylase kinase 2, and PEP carboxykinase, tended to be up-regulated in both over-expressing and suppressed lines. Interestingly, production of ethanol was possibly up-regulated in PME 6N, while in the same instance being down-regulated in PME 7 Xylem. Cell wall carbohydrate biosynthetic pathways rely on utilizing UDP-glucose as a primary substrate, however, considering the apparent down-regulation of *PtSUS* genes (in lines 5 and 7, xylem fractions) and *UGPase* (in line 7 Xylem), the pool of this central molecule must be in shortage. Moreover, the majority of pathways linked to this chief molecule appeared to be suppressed to a more or less extent, possibly as a consequence of the hypothetic shortage. This involved production of hemicellulose and pectin precursors such as GDP-mannose, GDP-fucose, and UDP-xylose (all in line 6N), UDP-GalA (in lines 6N and 7) and UDP-arabinose (in lines 5 and 6N), while biosynthesis of UDP-rhamnose, on the other hand, was found to be up-regulated (in line 6N).

Microarray data displayed potential changes in carbon flux through the cellulose biosynthesis and degradation machinery in lines 6N and 5. Cellulose synthase, *PtCesA1*, a main secondary wall CesA in poplar (Djerbi et al., 2005) and a *KORRIGAN1*-like cellulase gene, *PtCel9A1-2*, were up-regulated in line 5. Interestingly, this line exhibited increased cellulose content in the wood (Mellerowicz et al., 2004). In line 6N, a down-regulation of *PtCesA5* and changes in the abundance of transcripts for three different cellulases (Fig. 13), suggest a down-regulation of cellulose biosynthesis and an increase in cellulose degradation, consistent with its reduced growth phenotype. However, no changes in the expression of either *PtCesA* genes or cellulases were evident in the PME over-expressing lines. In contrast, in tobacco plants over-expressing fungal PME, Hasunuma et al. (2004) reported a down-regulation of these genes. This discrepancy might be explained by a severe dwarf phenotype in transgenic tobacco in contrast with a mild growth inhibition observed in transgenic poplar (Mellerowicz et al., 2004).

It is tempting to hypothesize that breakdown of the polysaccharide polymer cellulose, the main constituent of plant cell wall, might have implications in building up a pool of sucrose for various purposes. Could it be that defense/rescue responses necessitates the mobilization of sucrose to be transported from source to sink tissue in the phloem; i.e. where its utilization is required and where there are high demands for this ultimate and sustainable source of C? One additional observation that supported the hypothesis of stress responses in the lines was the up-regulation of several poplar genes encoding xyloglucan endotransglucosylases (XETs), for example *PtXTH6*, *PtXTH17*, *PtXTH30*, *PtXTH34*, *PtXTH35*, and *PtXTH36*, and this was more prominent in PME 5. Indeed, in *Arabidopsis* plants, various stresses can induce expression of XET genes (Antosiewicz et al., 1997), which function in modifying cell wall xyloglucans and, hence, altering the mechanical and chemical properties of plant cell wall.

Up-regulation of UDP-glucose-4-epimerase and two isoforms of beta-galactosidase in the xylem of line 5 indicated an increased beta-galactan biosynthesis. This is consistent with the increased galactan content in the wood of this line (Mellerowicz et al., 2004). Up-regulation of a xylosidase (*GH3_26*) in line 7 Xylem (Fig. 13) hints changes in the xylan metabolism and is consistent with the increase in xylan content in the wood of PME over-expressing lines (Mellerowicz et al, 2004).

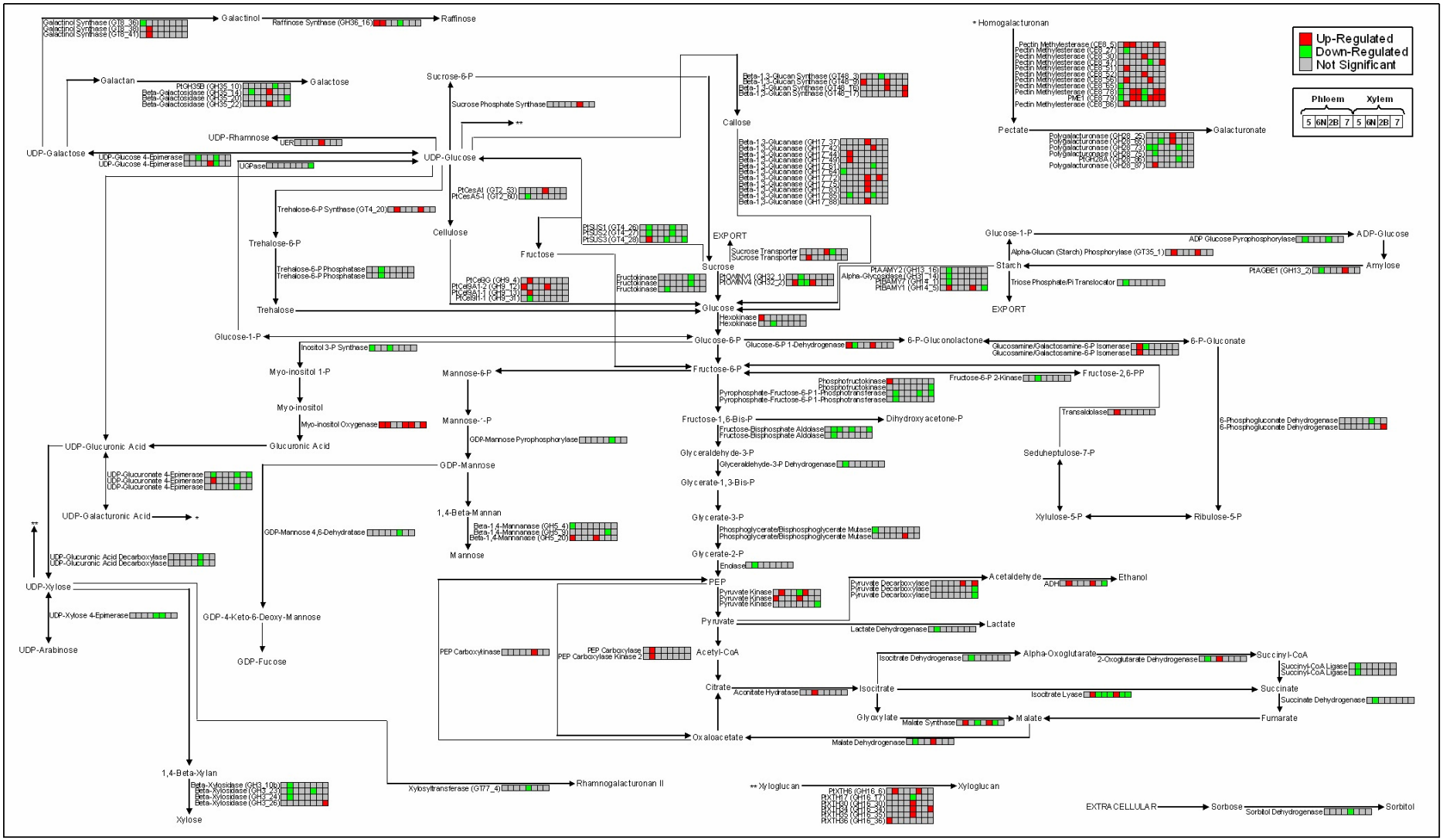

Figure 13. Differentially regulated genes among transgenic poplar lines (eight experimental conditions) involved in carbohydrate metabolism. Genes significantly regulated ($P \leq 0.05$ and $B \geq 0$), are indicated by red (up-regulated) or green (down-regulated); not significant genes are shown in gray.

Finally, a gene encoding a xylosyltransferase (*GT77_4*), involved in biosynthesis of the pectic polysaccharide rhamnogalacturonan (RG) II (Matsunaga, et al., 2004), proved to be down-regulated in PME 5 Xylem (Fig. 13), in accordance with previous findings on pectin content (Mellerowicz et al., 2004). In addition, there were several affected genes involved in pectin modification and degradation machinery. As expected, *PME1* signal was positively correlated with hypothesized degree of methylesterifed HGs in all lines except for PME 6N (Fig. 13). Interestingly, in PME 5 Xylem, at least two other PME genes (*CE8_30* and *CE8_52*) seem to be affected in an opposite way; i.e. negatively correlated with *PME1* expression. This unexpected up-regulation likely reflects a compensation mechanism, employed by other PME isoforms, in order to reestablish a balance. This opposite regulation, however, was not observed in the over-expressing lines. In this case, it cannot be ruled out a possibility of interfering cross-hybridization among the highly expressed and closely related family members of the PME multigene family, thus limiting the validation of the microarray data. Furthermore, retarding of pectin degradation was suggested by several down-regulated PGs, most of them in PME 6N, e.g. *GH28_73*, *GH28_75*, and *PtGH28A*. Up-regulation of two PG genes (*GH28_25* and *GH28_65*) in PME 5 Xylem, however, might account for the increased digestion of pectate to oligogalacturonate (OGA), resulting in the triggering of an oxidative burst, as described previously.

The discovery of at least two significantly up-regulated genes coding for callose synthase (*GT48_9* and *GT48_16*) in PME 5 (Fig. 13), prompted further investigation by expanding the study to incorporate a cytochemical study, as described below. Callose is synthesized by plants as a response to stress, mainly to infections and wounding (Frye and Innes, 1998). *PMR4* encodes a callose synthase, which expression is induced as a response to fungal infection (Vogel and Somerville, 2000). Another gene, also encoding a callose synthase (*GT48_3*), was, in contrast, down-regulated in PME 7 Phloem (Fig. 13), suggesting that expression of callose synthase-related genes is likely to be regulated in opposite ways in the suppressed vs. the over-expressing lines. In addition, several genes coding for beta-1,3-glucanases were evidently up-regulated, especially in PME 5 Xylem, indicating callose degradation. Since expression of callose hydrolases have been implicated in defense/stress responses (Thathcher et al., 2005), this observation could reflect a possible negative feedback regulation; i.e. halt any further deposition of callose.

No Differentially Regulated Genes Involved in Lignin Biosynthesis, Though, Lignin Content was Modified in Transgenic Lines

Previous experiments (Mellerowicz et. al., 2004) have revealed that the lignin content of xylem fraction was decreased in PME suppressed line 5 and increased in the PME overproducing lines 2B and 7. Therefore, the MA-data were searched for lignin biosynthesis genes. However, no genes encoding the enzymes catalyzing lignin monomer biosynthesis were found differentially expressed. This indicated that the regulation of lignin content in PME lines is exerted at other level than gene expression. Since lignification is initiated at the middle lamella and the cell corners, which both are rich in Ca^{2+} pectate, and taking into account the putative role that Ca^{2+} pectate-bound peroxidases might play in the spatial control of lignin deposition (Boerjan et al., 2003), the lowered levels of lignin in PME 5 could be explained by the fact that this line also has more methylesterified pectin, hence, less Ca^{2+} pectate; and the opposite increase in lignin content in lines 2B and 7 could be explained by the more demethylesterified pectin (Mellerowicz et al., 2004). This point was further studied with cytochemical techniques (see below).

Cyto and Histochemistry; and Microscopy

Occurrence of Callose and Tyloses Confirmed the Interpreted Microarray Data and Also Shed Some New Light in Explaining the Phenotypes

Callose is a β-1,3-glucan polymer synthesized and deposited at the outer surface of the plasma membrane by callose synthases that are localized in the membrane. Callose represents a highly dynamic and amorphous component of the plant cell wall, and has recently been shown (Parre and Geitmann, 2005) to serve a fundamental role as a load-bearing structure, by providing mechanical resistance against tension stress in pollen tubes, and against compression stress in general. Plants are known to respond to mechanical injuries (Bretschneider et al., 1989), and callose constitutes a well documented permeability barrier that serves as a leak sealant in plant cells, suffering from pathogen infection and physical- and chemical stresses (Parre and Geitmann, 2005). Investigations made by Ruan et al. (2004) led to yet another putative role for callose; its deposition and degradation (turnover), respectively, appear to regulate plasmodesmata closure and reopening (gating) in cotton fibers, based on genotypic and developmental evidence. In the present investigation, *GT48_9* and *GT48_16* coding for callose synthase were significantly up-regulated in PME 5 Xylem. This interesting discovery led to the hypothesis that the production of callose was greater in this line and perhaps also in the other suppressed line, PME 6N. To test this hypothesis, cross sections of the stem were stained with aniline blue and visualized under UV light. Callose deposits, detected by a yellow fluorescence, were found in the xylem, and their occurrence was more obvious in the two suppressed lines studied compared to the T89 WT (Fig. 14). Callose was detected mostly in the paratracheal fibers and/or parenchyma. It would be useful to confirm this finding using an immunocytochemistry approach; i.e. to raise antibodies against β-1,3-glucans for immunolocalization of callose.

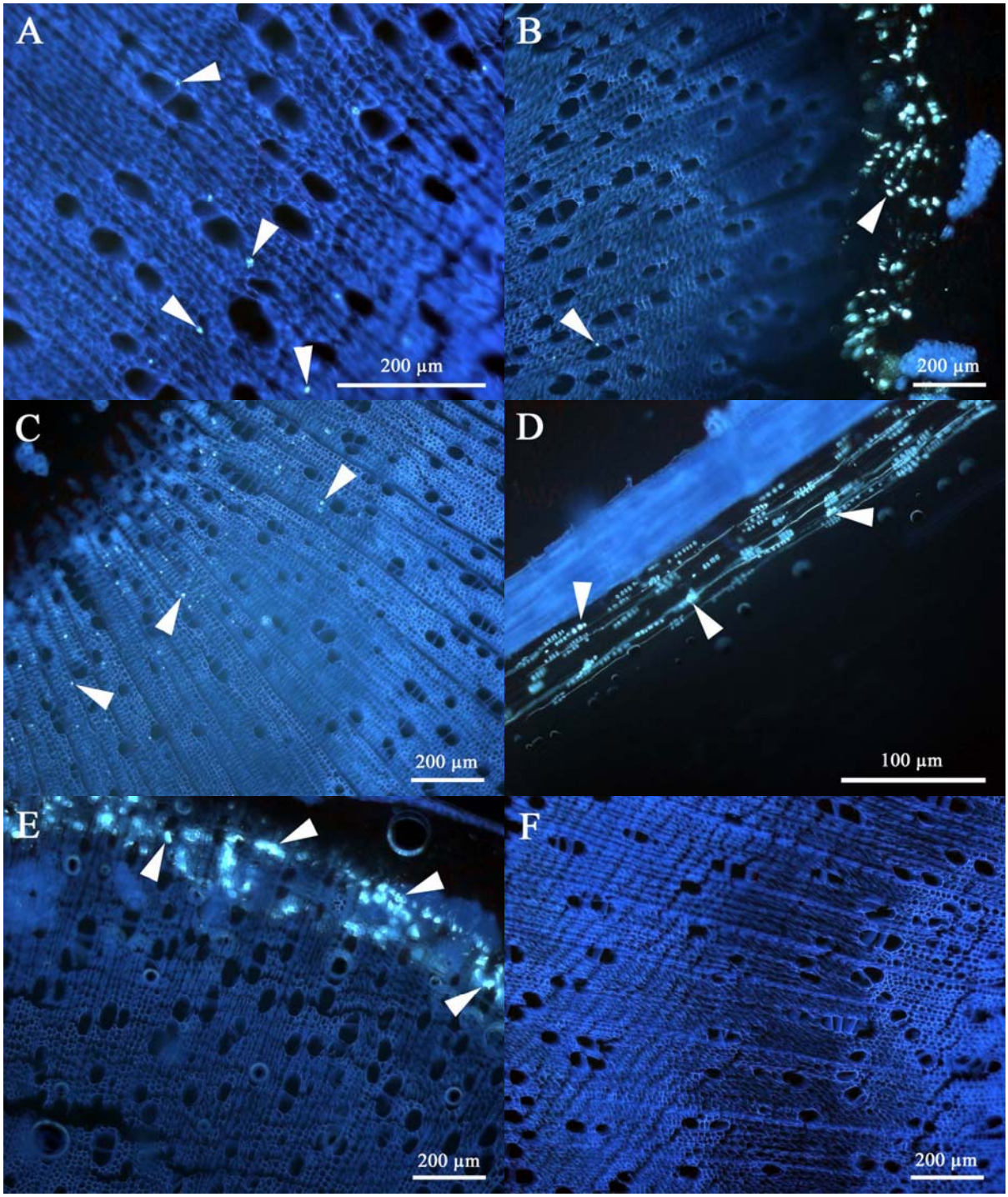

Figure 14. Localization of callose by aniline blue staining in the stems of PME supressed lines 5 and 6N and of WT. A and B, PME 5; C and D, PME 6N; E and F, T89 WT. Arrow-heads indicate callose deposits in xylem and phloem areas. Note that the callose deposits in xylem are abundant in PME-suppressed lines but not in the WT.

Tyloses are globular, balloon like structures that partially or completely occlude the lumens of dead xylem vessels in woody dicots (Scheckler and Galtier, 2003). They result from outgrowth of living ray or axial wood parenchyma contact cells; i.e. expansion of their primary cell walls to protrude through pit cavities into vessel elements. Formation of tyloses has been well correlated with vessel embolism, marking the beginning of the transition from conducting sapwood to non-conducting heartwood in the center of a tree trunk. Canny (1997)

hypothesized that tyloses formation is triggered by the frequent embolization of some vulnerable vessels, which yields an incompressible tissue, thus highlighting the importance of tyloses in mechanically maintaining tissue pressure; a requirement for refilling embolisms in the remaining vessels, in accordance with his compensating pressure theory of transpiration. Infections are also known to induce formation of tyloses, as part of defense mechanism triggered in pathogenesis that prevents or limits further reproduction and spread of the pathogen (Rioux et al., 1998). Mellerowicz and co-workers (unpublished) observed the prevalence of tyloses in one suppressed line, PME 5 (J. Lesniewska and E.J. Mellerowicz, unpublished; Fig. 15), prompting the present investigation. All trees of transgenic PME-suppressed lines 5 and 6N and the T89 WT trees were examined for the presence of tylosis. At least in one tree in PME 6N, tyloses were found in abundance in mature wood very close to the cambium (Fig. 16), and structures resembling tyloses were also seen in other trees on this line, however, these might be derived from cell wall remnants due to sectioning. This suggests that tyloses might develop as a response to the reduced PME level.

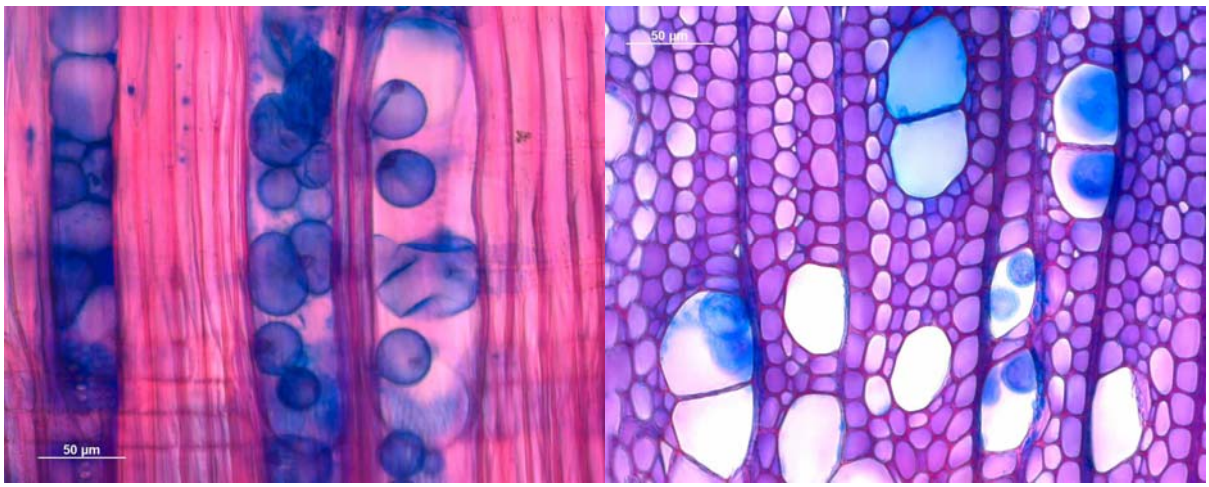

Figure 15. Occurrence of tyloses, plugging the vessels of PME 5, observed in longitudinal section (left image) and transverse section (right image). Figure provided by: Dr. Joanna Leśniewska, Department of Botany, University of Białystok, Świerkowa 20 b, 15-950 Białystok, Poland.

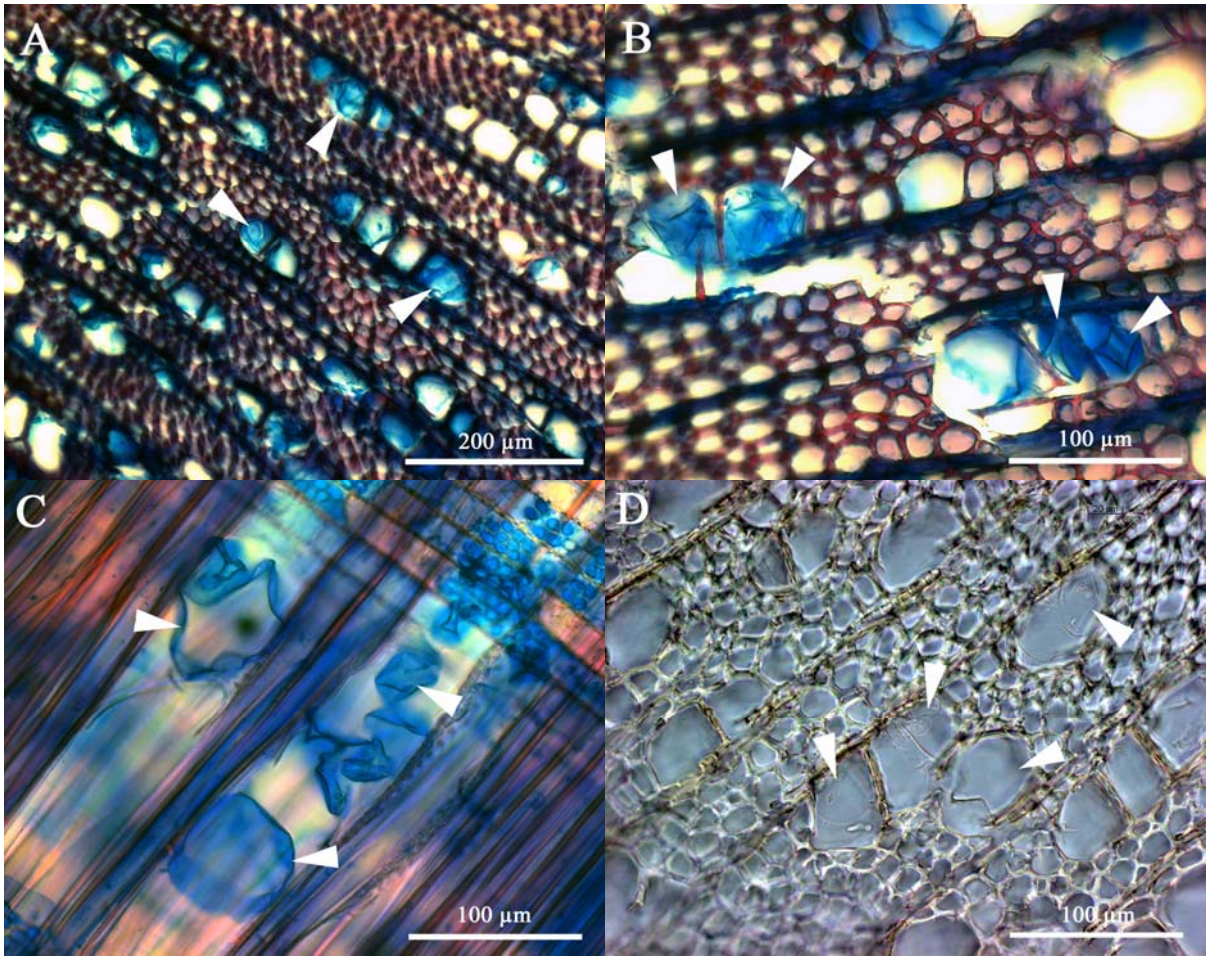

Figure 16. Visualizing tyloses, occluding the vessels of PME 6N. A-C, sections stained with saffranine/alcian blue; D, unstained section viewed in Nomarski optics. A, B, and D, transverse sections; C, longitudinal radial section. Arrow-heads in A-D indicate tyloses primary wall.

An additional hypothesis to be tested was if the tyloses observed in PME 6N Xylem actually contain callose? Kpémoua et al. (1996) observed callose (by utilizing polyclonal antibodies raised against β-1,3-glucans) within the fibrillar material that plugs the vessels, and their hypothesis was that this callose containing material might be excreted by tyloses themselves. In the present study, transverse sections of stained (aniline blue) and unstained material (autofluorescence control) were compared under UV light to detect callose. The outcome, however, was inconclusive, since tyloses in both conditions had a somewhat 'greenish' appearance, with no obvious visual difference between callose-stained and control section (Fig. 17). The use of callose-specific antibodies might bring some clarity into this matter, and perhaps either confirm or refute the hypothesis.

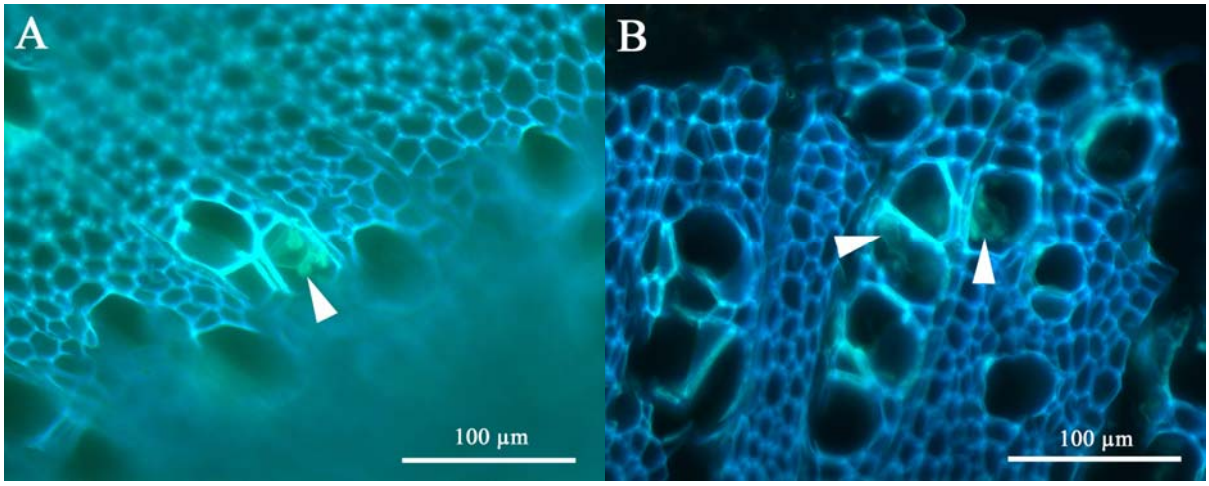

Figure 17. Transverse sections of stained (A) and unstained (B) tyloses. When compared under UV light, no apparent difference between the two different conditions (aniline blue-stained vs. unstained autofluorescence control) was observed, based on the fluorescent green color, derived from tyloses.

Accumulation of H_2O_2 and Peroxidases in Leaf Tissues Supported the Hypothesis of Oxidative Stress Signaling

The generation of reactive oxygen species (ROS), subsequently converted to hydrogen peroxide (H_2O_2), in plant cells originate mainly from organelles with a highly oxidizing metabolic activity or with intense electron transport reactions (e.g. chloroplasts, mitochondria, and peroxisomes), including cell walls (Mittler et al., 2004). Enhancement in ROS production is observed during a biotic (pathogen attack) and abiotic (drought, salt, temperature, and high-light) stress. Though, being a highly reactive, toxic, and hazardous oxidant to cellular membranes and components, recent studies, reviewed by Hung et al. (2005), assign H_2O_2 an important role as a signaling molecule, triggering signaling pathways involved in activating oxidative stress response pathways during stress (biotic and abiotic) and development (programmed cell death, ABA-mediated stomatal closure, auxin-regulated gravitropic responses, and mechanical wounding response). Nevertheless, restoring the redox homeostasis is of outmost importance for the plant cell (to prevent reactions with lipids, proteins, and nucleic acids) and this is achieved by efficient ROS-scavenging enzymes together with non-enzymatic antioxidants, reviewed by Foyer and Noctor (2005). The authors also high-light the existence of a strong correlation between the exposure to ROS and the gene expression of antioxidants; depending on whether the surrounding cells are undergoing death responses due to ROS, which would result in a decreased antioxidant activity. Moreover, nitrogen oxide (NO) has emerged (Neill et al., 2002) as a stress signal molecule exhibiting many common features with H_2O_2; the generation and detection of NO under conditions in which H_2O_2 generation is also stimulated (following pathogen attack and the subsequent activation of similar defense responses), and it is obvious that both H_2O_2 and NO can mediate transcription of specific downstream genes in a signaling cascade. The present study (Fig. 12) showed that oxidative stress responses were triggered in the PME-modified lines. To determine if the H_2O_2 content was indeed affected by PME modification, the leaves of transgenic lines and the WT were subjected to 3,3'-diaminobenzidine (DAB)-test that detects H_2O_2 and peroxidase activity. Fig. 18 demonstrates the occurrence of H_2O_2 and peroxidases in leaf tissues of two suppressed lines, two over-expressing lines, and one wild-type line. When the transgenic lines were compared with the wild-type line, a striking difference could be observed on the basis of the intensities of the stained tissues. H_2O_2 and peroxidases were apparantly least abundant in the PME-suppressed lines, intermediate in the wild-type line and most abundant in the over-expressing lines, which added further

confidence to the interpreted MA-data and confirmed the hypothesis of a modified redox status and activation of signal transduction via oxidative stress responsive pathways. In general, a high abundance of H_2O_2, followed by action of peroxidases, should be expected in green tissues, where photosynthesis takes place and, hence, where plant cells are more subjected to accumulation of ROS. Nevertheless, repetitions of this experiment with more than one clone per line are required for a certain confirmation of obtained results.

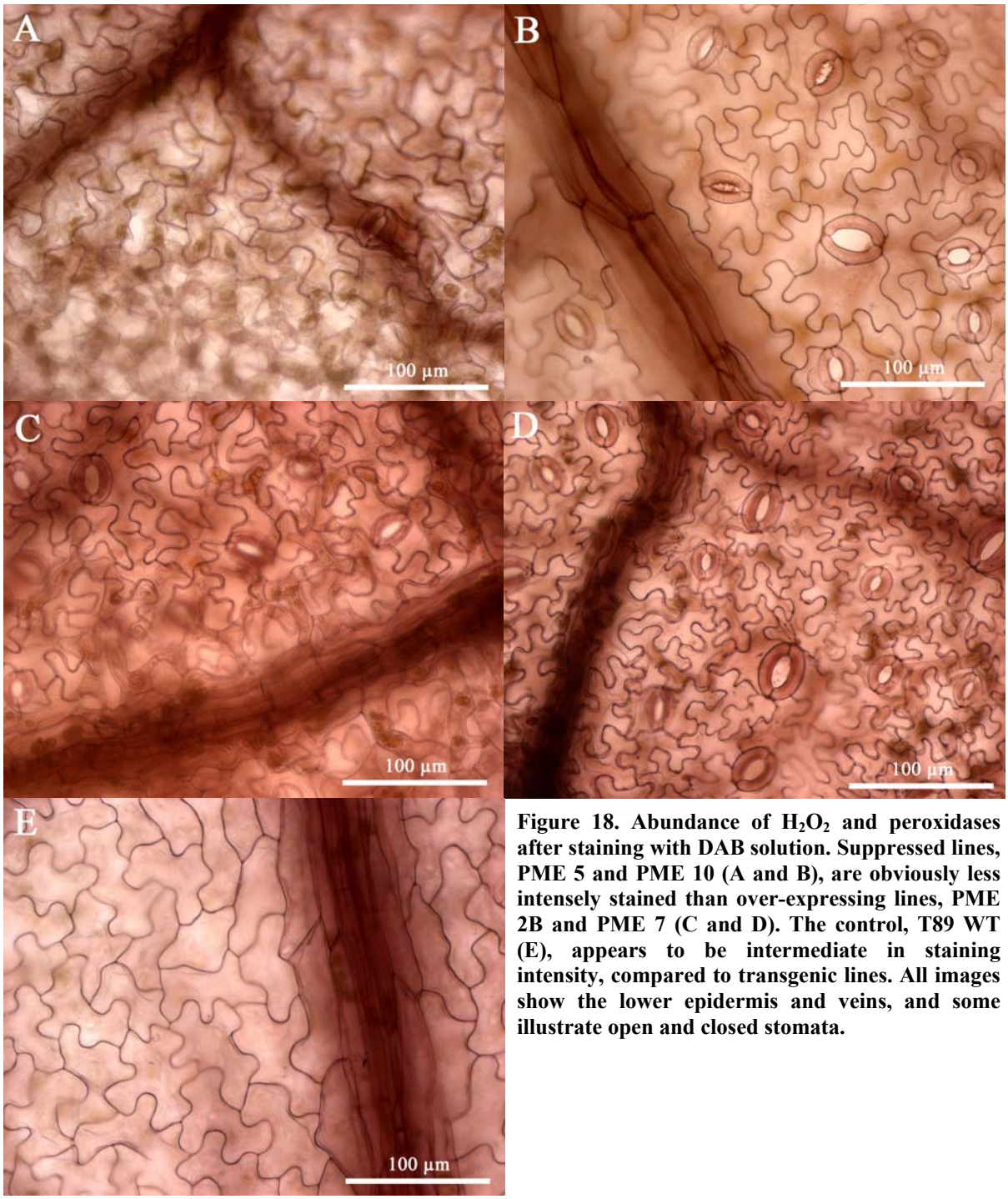

Figure 18. Abundance of H_2O_2 and peroxidases after staining with DAB solution. Suppressed lines, PME 5 and PME 10 (A and B), are obviously less intensely stained than over-expressing lines, PME 2B and PME 7 (C and D). The control, T89 WT (E), appears to be intermediate in staining intensity, compared to transgenic lines. All images show the lower epidermis and veins, and some illustrate open and closed stomata.

Intense Activity of Plant Peroxidases Added Further Confidence to the Theory That Modified Levels of PME1 Activate Stress Signaling Pathways

Higher plant peroxidases play essential roles in the construction of cell walls and regulation of cell wall plasticity, and are also involved in oxidative cross-linking of many aromatic molecules in cell wall, simultaneously catalyzing the reduction of H_2O_2 (Carpin et al., 2001). These reactions results in the formation of lignin, suberin, and the establishment of covalent bonds between hydroxycinnamate ester moieties or flavonoids associated with pectins or hemicellulose. Carpin et al. (2001) reported that some peroxidases, residing in the apoplast, are capable of binding to HG domains of pectin chains, cross-linked by Ca^{2+}; i.e. Ca^{2+}-pectate. This particular conformation of pectins occurs mainly in the middle lamella and cell corners (but also in other sites of the cell wall). Since the PME-modified lines had more or less methylesterified HGs compared to WT when *PME1* was down- or up-regulated, respectively (Mellerowicz et al. 2004), the Ca^{2+}-pectate levels would differ and, therefore, changes in abundance of pectate-bound peroxidases can be predicted. To test this hypothesis, sections of developing wood were stained with the 'Syringaldazine mehod', described in Krishnamurthy (1999) to detect peroxidase. This test revealed that peroxidases were less abundant in wild-type line in comparison with transgenic lines, regardless whether they were over- or under-expressing (Fig.19). As a consequence, the presence of higher or lower abundance of pectate apparently did not correlate with the abundance of wall-bound peroxidases. It is possible that peroxidases were induced by different mechanisms in the under- and over-expressing lines.

Accumulation of H_2O_2, demonstrated for the over-expressing lines (Fig. 18), should, in theory, promote gene expression of ROS-scavenging enzymes in these lines, such as peroxidases, that utilizes H_2O_2 as a substrate to restore the redox homeostasis in the stressed cell. In the MA-data, however, genes encoding for some peroxidase enzymes were differentially regulated in a highly conflicted way; i.e. represented by comparatively equal numbers of up- and down-regulated genes in all six experimental conditions (data not shown). Could this imply that an, yet to be determined, induced negative feedback loop regulates these genes on a transcriptional level? Nevertheless, the intensely stained sections of the over-expressing lines, reflecting a high peroxidase activity, together with demonstrated accumulation of H_2O_2 (Fig. 18-19), could explain the higher lignin contents in these lines (Mellerowicz et al., 2004). Moreover, considering that demethylated pectins are more susceptible to cleavage by PGs (Limberg et al., 2000; Van Alebeek et al., 2002), resulting in an increase of OGA fragments, it is likely that the observed accumulation of H_2O_2 could be explained by the build up of a pool of OGAs, thus triggering a down-stream signaling event in the over-expressing lines.

The increased cellulose content of line 5 has been reported previously (Mellerowicz et al., 2004), as well as reduced lignin and Ca^{2+}-pectate content. These features could result in reduced stiffness of the cell wall, which might be perceived and responded by the plant cell. In fact, Ellis et al. (2002) reported an impaired cellulose synthesis pattern in the *cev1* mutant (knock-out mutation of *CesA3*), giving rise to a phenotype displaying overproduction of JA and ET, which they hypothesize is due to alterations of cell wall properties. Likewise, Decreux and Messiaen (2005) postulate a role for wall-associated kinase 1 (WAK1) in pectin interactions; i.e. WAK1 might constitute a perception mechanism that allows the protoplast to recognize deposition of pectins and to respond when pectin content/structure is changed. Therefore, even though no *WAK1* genes were observed as differentially regulated in this study, it is still tempting to speculate that high abundance of methylesterified pectins (*in muro* disturbances of the pectin network), in addition to weakening of the cell wall (due to less formation of calcium bridges and less cross-linking of pectin polymers), activate and

mediate JA- and ET-dependent stress/defense responses. Another striking feature of line 5 is the reduced content of the pectin polymer itself. Interestingly, Vogel et al. (2002) described a pectate lyase-like gene, *PMR6*, which confers susceptibility to powdery mildew. Indeed, two genes encoding pectin/pectate lyase proteins (*PL1_26* and *PL1_27*) were apparently up-regulated (data not shown) in PME 5 Xylem in the present study, suggesting interference of an additional factor that might contribute to the altered cell wall composition in this line. Altogether, the high abundance of peroxidases (Fig. 19) in line 5 is concurrent with the hypothesized stress/defense response, even though the H_2O_2 content was slightly less than wild-type (Fig. 18); i.e. the signal transduction, *per se*, originates from triggering factors other than H_2O_2. In fact, polymerization of lignin monomers, which gives rise to a tough, water-repellent plant polymer, is thought to be stimulated by accumulation of H_2O_2, in addition to giving structural strength and protection to the plant cell wall and conferring resistance towards biodegradation (Yang et al., 1997). The less lignin content (possibly reflected by less Ca^{2+}-pectate and, as a consequence, less lignin polymerization), though, would explained the lower abundance of H_2O_2 (compared to wild-type) in line 5.

Contrary, in the over-expressing lines, a high abundance of H_2O_2 (compared to wild-type) was observed (Fig. 18). Likewise, with line 5, a high abundance of peroxidases was detected (Fig. 19), implicated in activation of stress/defense responses. Considering that the over-expressing lines displayed phenotype characteristics opposite to those in line 5, reported previously by Mellerowicz et al. (2004) and results obtained from the present study, it is more likely that activation of stress signal pathways in the two PME-overproducing lines are triggered by H_2O_2. In other words, over-expressing lines and suppressed line might exhibit signal transductions that flows down-stream through the same defense pathways, although the origin of the triggering mechanism could be derived from elicitors, different in nature.

Important to bear in mind is that the staining assay itself revealed occurrence of many different classes of peroxidases and, considering the vital roles they all play in plant metabolism, a high abundance might imply additional effects other than the attempt to restore the redox balance of the stressed cell. Altogether, considering this experiment was performed once only, repetitions are required for a correct verification of obtained results.

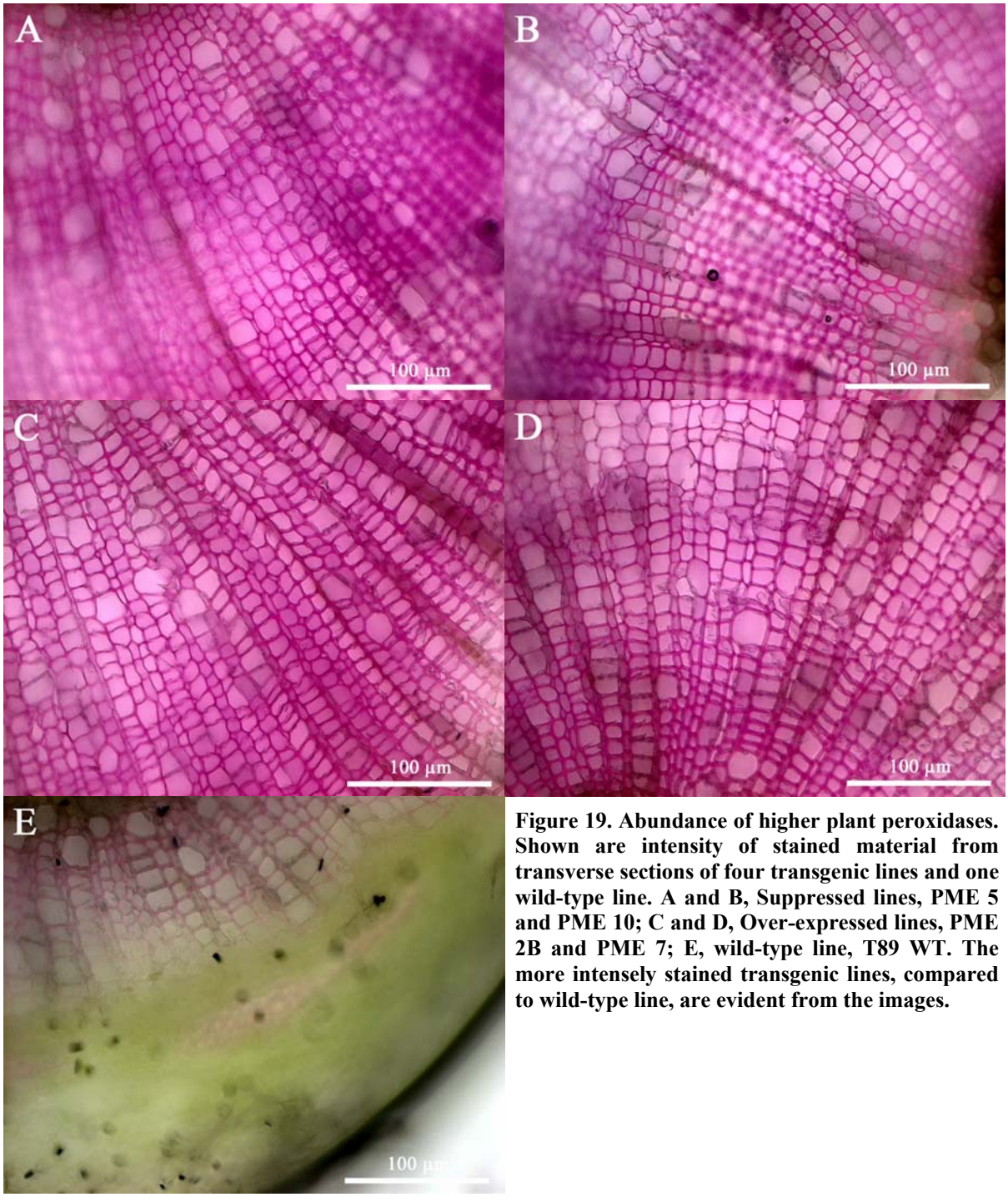

Figure 19. Abundance of higher plant peroxidases. Shown are intensity of stained material from transverse sections of four transgenic lines and one wild-type line. A and B, Suppressed lines, PME 5 and PME 10; C and D, Over-expressed lines, PME 2B and PME 7; E, wild-type line, T89 WT. The more intensely stained transgenic lines, compared to wild-type line, are evident from the images.

Short Metabolomic Study

Global Analysis of Metabolites Verified the Separation of Suppressed Lines from Over-Expressing Lines, Analogous with the Transcriptome Analysis

Utilizing the same lines and tissues as those that were used in the microarray experiment, a global analysis of metabolites was implemented, by subjecting samples to mass spectrometry by GC/TOF-MS. Differences between lines were detected by partial least squares to latent structures discriminate analysis (PLS-DA) and PCA analysis. In the PCA plot for all samples, generally, the two tissues xylem and phloem separated in a satisfactory way, contrary to what

was observed in the PCA plots of the microarray data. Further, when the tissues were treated separately, however, PME 6N Phloem and Xylem in each tissue plot, respectively, constituted two unique groups that were set apart from all other lines. Similarly, in the PLS-DA plots, where both tissues are treated separately as well, the same grouping of PME 6N Phloem and Xylem was observed clearly set apart from the remaining lines. Finally, all 10 experimental conditions (four samples in each) were combined into classes, based on correlation of *PME1* expression, to obtain more replicates. This resulted in three classes for each tissue: PME 2B and PME 7, PME 5 and PME 6N, and T89 WT. The general appearance of the two PLS-DA combined plots for each tissue had a striking resemblance with the outcome of the microarray experiment, concerning transcription patterns used for establishing relationships between transcriptome profiles of each line and tissue. The metabolite profiling pattern, evidently, set PME 6N apart from the remaining lines, as well as T89 WT (although not at the same distance as with PME 6N), grouped PME 2B and PME 7 together, and placed PME 5 somewhat between in the middle. Despite a highly possible confirmation of the MA-data, there are drawbacks in the metabolome study that have to be considered. Most importantly, there were too few biological replicates to process, which is a vast limiting factor in order to retrieve reliable results. For instance, two dots, positioned at the same distance from a central point, would cancel each other out, thus an adequate number of biological replicates are required to observe any variation in the data. Altogether, a repetition of this experiment in the future should involve at least 10 biological samples/replicates (trees) for each experimental condition.

Quantification of Salicylic Acid Yielded Inconclusive Results

An advantage with the metabolome study was the possibility to retrieve retention indexes for SA in all samples, hence, allowing for quantification of this compound. This provided insights into other level than transcription, *per se*, a necessity to confirm obtained MA-data. Despite the fact that differences in the concentration of SA (ng of SA/mg of sample) between transgenic lines and wild-type line were not immense, and perhaps not even significant, variations were still evident. For instance, the suppressed lines PME 5 and PME 6N experienced concentrations of: 89.36% (87.53% in pool 1 and 91.19% in pool 2) and 134.20% (119.53% in pool 1 and 148.87% in pool 2), that of T89 WT, concerning phloem tissues, respectively, while concentrations of: 94.76% (91.08% in pool 1 and 98.44% in pool 2) and 110.26% (110% in pool 1 and 110.42% in pool 2) were true for the xylem tissues, respectively. On the other hand, when inspecting the over-expressing lines PME 2B and PME 7, an unexpected result was discovered. Apparently, the concentrations of SA in phloem tissues of line 2B and 7 were: 89.14% (89.08% in pool 1 and 89.20% in pool 2) and 102.81% (114.54% in pool 1 and 91.09% in pool 2), respectively, while the values in the xylem tissues were: 98.22% (93.45% in pool 1 and 102.99% in pool 2) and 87.13% (84.83% in pool 1 and 89.44% in pool 2), respectively. Obviously, there are discrepancies in the data, possibly explained by biological variation between samples, and this was evident in PME 7 Phloem and PME 2B Xylem; i.e. noteworthy epigenetic variability between sample pools of the same line. Nevertheless, the SA concentrations recovered for PME 6N displayed values highly dissimilar from the other lines, in accordance with previous analysis in this study. This might reflect an active expression of defense proteins through SA-dependent pathway, thus strengthening the hypothesis of infections influencing the growth of this line. On average, the obtained values for lines 5, 2B, and 7 might verify the transcriptome analysis, preceding this, suggesting that the pools of key stress-related genes, in terms of both transcription and expression, are negatively regulated; i.e. deactivation of stress-related pathways.

Concluding Remarks and Future Prospects

The main theme with this study was to unravel the gene expression profiles of transgenic poplar lines, exhibiting an altered expression level of *PME1* in two opposite directions/conditions: over-expression and suppression. This entailed a transcriptomic approach, where implementation of spotted cDNA microarray technology comprised the most suitable method of choice. Although the sensitivity and reliability of hybridized arrays remains largely indisputable, some limitations of the information obtained have to be taken into account, when drawing conclusions on affected metabolism. For example, interfering cross-hybridization events, due to sequence similarities of transcripts, constitute major problems. Furthermore, there are numerous modes of posttranscriptional and posttranslational modifications, which remain to be elucidated by further research. An array experiment alone allows for a study only on a transcriptional level, relying heavily on intelligent guesswork to deduce effects in phenotype on other levels.

Nevertheless, the results of the present microarray study provided new insights into how xylogenesis, especially lignification, is regulated in a woody perennial species like *Populus*. The main conclusion to be drawn is that when the chemical composition of the cell wall is modified, due to the action of *PME1*, down-stream stress signaling events are triggered by accumulation of H_2O_2. This was revealed by analysis of differentially regulated transcript levels of genes involved in stress signaling cascades, and by cyto and histochemistry of the wood-forming tissues. In the PME over-expressing lines in common, this observation might originate from accumulation of the elicitor OGA, which is a well-known stress signal molecule, derived from action of PGs in the cell wall. Although the same stress response is observed in the PME suppressed line as well, the chemical properties of the cell wall and the plant phenotype as a whole, showed mainly the opposite compositions and characteristics. The decreased lignin content of this line, reflecting a possible weakening of the cell wall due to reduced levels of Ca^{2+}-pectate, could have triggered the same stress signaling cascades as observed in PME over-expressing lines via ROS (e.g. H_2O_2). Strong correlations to this argument are, first, the activation of peroxidases (as demonstrated by cyto and histochemical staining) in all lines; and, secondly, triggering/activation of the same stress response genes as observed in the PME over-expressing lines. It is likely that all three lines posses the ability to tolerate stress better than wild-type line; i.e. they exhibit stress-resistance and *not* stress-susceptibility, and this could be indirectly linked to modifications of the plant cell wall biochemistry. Moreover, what impact the activation of oxidative stress signaling pathways might have on wood-formation in PME modified lines, constitutes an important issue to be resolved by further research. However, considering that stress signal transduction flows downstream through three main pathways, involving the three renowned key regulating signal molecules, namely SA, JA, and ET, which are all known to influence plant developmental processes, the possibility of affects in metabolism *not* caused by modified levels of PME alone cannot be ruled out.

This investigation revealed novel bio-information, stating that the lignin biosynthesis genes were not significantly affected at the transcript level, which is supported by the microarray experiment analysis, even though the lignin content was altered (as reported from a previous study). This illustrates the complexity in understanding how plants regulate their metabolism, in order to cope with different sets of conditions (i.e. mutations). Verification of disrupted or compromised cellular processes requires an expansion of the present study, and this entails application of different approaches, such as RT-PCR and Northern blotting of key significant genes; and proteomics/metabolomics (MS). HPLC-ESI-MS holds great promises in detecting and quantifying OGA, in addition to other, state of the art, applications, such as NMR and FT-IR spectroscopy on relevant plant tissues, in the quest for knowledge.

References

Anderson, J.P., Badruzsaufari, E., Schenk, P.M., Manners, J.M., Desmond, O.J., Ehlert, C., Maclean, D.J., Ebert, P.R., and Kazan, K. (2004). Antagonistic interaction between abscisic acid and jasmonate-ethylene signaling pathways modulates defense gene expression and disease resistance in *Arabidopsis*. Plant Cell. **16:** 3460-3479.

Anderson, J.P., Thatcher, L.F., and Singh, K.B. (2005). Plant defence responses: conservation between models and crops. Func. Plant Biol. **32:** 21-34.

Antosiewicz, D.M., Purugganan, M.M., Polisensky, D.H., and Braam, J. (1997). Cellular localization of Arabidopsis xyloglucan endotransglycosylase-related proteins during development and after wind stimulation. Plant Physiol. **115:**1319-1328.

Baier, M., Kandlbinder, A., Golldack, D., and Dietz, K-J. (2005). Oxidative stress and ozone: perception, signalling and response. Plant Cell Environ. **28:** 1012-1020.

Boerjan, W., Ralph, J., and Baucher, M. (2003). Lignin biosynthesis. Annu. Rev. Plant Biol. **54:** 519-546.

Bosch, M., Cheung, A.Y., and Hepler, P.K. (2005). Pectin methylesterase, a regulator of pollen tube growth. Plant Physiol. **138:** 1334-1346.

Bretschneider, K.E., Gonella, M.P., and Robeson, D.J. (1989). A comparative light and electron microscopical study of compatible and incompatible interactions between *Xanthomonas campestris* pv. *campestris* and cabbage (*Brassica oleracea*). Physiol. Mol. Plant Pathol. **34:** 285-297.

Camardella, L., Carratore, V., Ciardiello, M.A., Servillo, L., Balestrieri, C., and Giovane, A. (2000). Kiwi protein inhibitor of pectin methylesterase: amino-acid sequence and structural importance of two disulfide bridges. Eur. J. Biochem. **267:** 4561-4565.

Canny, M.J. (1997). Tyloses and the maintenance of transpiration. Ann. Bot. **80:** 565-570.

Cao, H., Glazebrook, J., Clarke, J.D., Volko, S., and Dong, X. (1997). The *Arabidopsis NPR1* gene that controls systemic acquired resistance encodes a novel protein containing ankyrin repeats. Cell. **88:** 57-63.

Carpin, S., Crèvecoeur, M., De Meyer, M., Simon, P., Greppin, H., and Penel, C. (2001). Identification of a Ca^{2+}-pectate binding site on an apoplastic peroxidase. Plant Cell. **13:** 511-520.

Catoire, L., Pierron, M., Morvan, C., Du Penhoati, C.H., and Goldberg, R. (1998). Investigation of the action patterns of pectinmethylesterase isoforms through kinetic analyses and NMR spectroscopy. Implications in cell wall expansion. J. Biol. Chem. **273:** 33150-33156.

Dangl, J.L., and Jones, J.D. (2001). Plant pathogens and integrated defence responses to infection. Nature. **411:** 826-833.

Decreux, A., and Messian, J. (2005). Wall-associated kinase WAK1 interacts with cell wall pectins in a calcium-induced conformation. Plant Cell Physiol. **46:** 268-278.

Desikan, R., A.-H.-Mackerness, S., Hancock, J.T., and Neill, S.J. (2001). Regulation of the arabidopsis transcriptome by oxidative stress. Plant Physiol. **127:** 159-172.

Devoto, A. and Turner, J.G. (2005). Jasmonate-regulated Arabidopsis stress signalling network. Physiol. Plant. **123:** 161–172.

Di Matteo, A., Giovane, A., Raiola, A., Camardella, L., Bonivento, D., De Lorenzo, G., Cervone, F., Bellincampi, D., and Tsernoglou, D. (2005). Structural basis for the interaction between pectin methylesterase and a specific inhibitor protein. Plant Cell. **17:** 849-858.

Djerbi, S., Lindskog, M., Arvestad, L., Sterky, S., and Teeri, T.T. (2005). The genome sequence of black cottonwood (*Populus trichocarpa*) reveals 18 conserved cellulose synthase (*CesA*) genes. Planta. **221:** 739-746.

Ellis, C., Karafyllidis, I., Wasternack, C., and Turner, J.G. (2002). The *Arabidopsis* mutant *cev1* links cell wall signaling to jasmonate and ethylene responses. Plant Cell. **14:** 1557-1566.

Eriksson, E.M., Bovy, A., Manning, K., Harrison, L., Andrews, J., De Silva, J., Tucker, G.A., and Seymour, G.B. (2004). Effect of the *Colorless non-ripening* mutation on cell wall biochemistry and gene expression during tomato fruit development and ripening. Plant Physiol. **136:** 4184-4197.

Eulgem, T., Rushton, P.J., Robatzek, S., and Sommssich, I.E. (2000). The WRKY superfamily of plant transcription factors. Trends Plant Sci. **5:** 199-206.

Foyer, C.H., and Noctor, G. (2005). Oxidant and antioxidant signalling in plants: a re-evaluation of the concept of oxidative stress in a physiological context. Plant Cell Environ. **28:** 1056-1071.

Frye, C.A. and Innes, R.W. (1998). An *Arabidopsis* mutant with enhanced resistance to powdery mildew. Plant Cell. **10:** 947-956.

Geisler-Lee, J., Geisler, M., Coutinho, P.M., Segerman, B., Nishikubo, N., Takahashi, J., Aspeborg, H., Djerbi, S., Master, E., Andersson-Gunnerås, S., Sundberg, B., Karpinski, S., Teeri, T.T., Kleczkowski, L.A., Henrissat, B., and Mellerowicz, E.J. (2006). Poplar carbohydrate-active enzymes (CAZymes). Gene identification and expression analyses. Plant Physiol. **140:** 946-962.

Giovane, A., Servillo, L., Balestrieri, C., Raiola, A., D'Avino, R., Tamburrini, M., Ciardiello, M.A., and Camardella, L. (2004). Pectin methylesterase inhibitor. Biochimica et Biophysica Acta. **1696:** 245– 252.

Gray-Mitsumune, M., Mellerowicz, E.J., Abe, H., McQueen-Mason, S., Winzéll, A., Sterky, F., Blomqvist, K., Schrader, J., Teeri, T.T., and Sundberg, B. (2004). Expansins abundant in secondary xylem belong to subgroup a of the α-expansin gene family. Plant Physiol. **135:** 1552-1564.

Guglielmino, N., Liberman, M., Catesson, A.M., Mareck, A., Prat, R., Mutaftschiev, S., and Goldberg, R. (1997). Pectin methylesterases from poplar cambium and inner bark: localization, properties and seasonal changes. Planta **202:** 70-75.

Hasunuma, T., Fukusaki, E., and Kobayashi, A. (2004). Expression of fungal pectin methylesterase in transgenic tobacco leads to alteration in cell wall metabolism and a dwarf phenotype. J. Biotechnol. **111:** 241-251.

Henrissat, B., Coutinho, P.M., and Davies, G.J. (2001). A census of carbohydrate-active enzymes in the genome of *Arabidopsis thaliana*. Plant. Mol. Biol. **47:** 55-72.

Hothorn, M., Wolf, S., Aloy, P., Greiner, S., and Scheffzek, K. (2004). Structural insights into the target specificity of plant invertase and pectin methylesterase inhibitory proteins. Plant Cell. **16:** 3437-3447.

Hu, X.Y., Neill, S.J., Cai, W.M., and Tang, Z.C. (2004). Induction of defence gene expression by oligogalacturonic acid requires increases in both cytosolic calcium and hydrogen peroxide in *Arabidopsis thaliana*. Cell Research. **14:** 234-240.

Hung, S-H., Yu, C-W., Lin, C.H. (2005). Hydrogen peroxide functions as a stress signal in plants. Bot. Bull. Acad. Sin. **46:** 1-10.

Jiang, L., Yang, S-L., Xie, L-F., Puah, C.S., Zhang, X-Q., Yang, W-C., Sundaresan, V., and Yea, D. (2005). *VANGUARD1* encodes a pectin methylesterase that enhances pollen tube growth in the arabidopsis style and transmitting tract. Plant Cell. **17:** 584–596.

Kim, H.S., and Delaney, T.P. (2002). *Arabidopsis* SON1 is an F-box protein that regulates a novel induced defense response independent of both salicylic acid and systemic acquired resistance. Plant Cell. **14:** 1469-1482.

Kpémoua, K., Boher, B., Nicole, M., Calatayud, P., and Geiger, J.P. (1996). Cytochemistry of defense responses in cassava infected by *Xanthomonas campestris* pv. *manihotis*. Can. J. Microbiol. **42:** 1131-1143.

Krishnamurthy, K.V. (1999). Methods in cell wall cytochemistry. CRC Press, Boca Raton, London, New York, Washington, D.C.

Limberg, G., Körner, R., Buchholt, H.C., Christensen, T.M.I.E., Roepstorff, P., and Mikkelsen, J.D. (2000). Analysis of different de-esterification mechanisms for pectin by enzymatic fingerprinting using endopectin lyase and endopolygalacturonase II from *A. niger*. Carbohydr. Res. 327: 293-307.

Martin, G.B., Bogdanove, A.J., and Sessa, G. (2003). Understanding the functions of plant disease resistance proteins. Annu. Rev. Plant. Biol. **54:** 23-61.

Matsunaga, T., Ishii, T., Matsumoto, S., Higuchi, M., Darvill, A., Albersheim, P., and O'Neill, M.A. Occurrence of the primary cell wall polysaccharide rhamnogalacturonan II in pteridophytes, lycophytes, and bryophytes. Implications for the evolution of vascular plants. Plant Physiol. **134:** 339-351.

Mellerowicz, E.J., Baucher, M., Sundberg, B., and Boerjan, W. (2001). Unravelling cell wall formation in the woody dicot stem. Plant Mol. Biol. **47:** 239-274.

Mellerowicz, E.J., Sundberg, B., and Berthold, F. (2004). New transgenic plants and method of their production. Filed in Sweden by SweTree Technologies AB under No. SE 0403132-4, December 21, 2004.

Micheli, F., Sundberg, B., Goldberg, R., and Richard, L. (2000). Radial distribution pattern of pectin methylesterases across the cambial region of hybrid aspen at activity and dormancy. Plant Physiol. **124:** 191-199.

Micheli, F. (2001). Pectin methylesterases: cell wall enzymes with important roles in plant physiology. Trends Plant Sci. **6:** 414-419.

Mittler, R., Vanderauwera, S., Gollery, M., and Van Breusegem, F. (2004). Reactive oxygen gene network of plants. Trends Plant Sci. **9:** 490-498.

Nanjo, T., Futamura, N., Nishiguchi, M. Igasaki, T., Shinozaki, K., and Shinohara, K. (2004). Characterization of full-length enriched expressed sequence tags of stress-treated poplar leaves. Plant Cell Physiol. **45:** 1738-1748.

Neill, S.J., Desikan, R., Clarke, A., Hurst, R.D., and Hancock, J.T. (2002). Hydrogen peroxide and nitric oxide as signalling molecules in plants. J. Exp. Botany. **53:** 1237-1247.

Orozco-Cárdenas, M.L., Narváez-Vásquez, J., and Ryan, C.A. (2001) Hydrogen peroxide acts as a second messenger for the induction of defense genes in tomato plants in response to wounding, systemin, and methyl jasmonate. Plant Cell. **13:** 179-191.

Parre, E., and Geitmann, A. (2005). More than a leak sealant. The mechanical properties of callose in pollen tubes. Plant Physiol. **137:** 274–286.

Petersen, M., Brodersen, P., Naested, H., Andreasson, E., Lindhart, U., Johansen, B., Nielsen, H.B., Lacy, M., Austin, M.J., Parker, J.E., Sharma, S.B., Klessig, D.F., Martienssen, R., Mattsson, O., Jensen, A.B., and Mundy, J. (2000). *Arabidopsis* MAP kinase 4 negatively regulates systemic acquired resistance. Cell. **103:** 1111-1120.

Plomion, C., Leprovost, G., and Stokes, A. (2001). Wood formation in trees. Plant Physiol. **127:** 1513-1523.

Ren, C., and Kermode, A.R. (2000). An increase in pectin methyl esterase activity accompanies dormancy breakage and germination of yellow cedar seeds. Plant Physiol. **124:** 231-242.

Ridley, B.L., O'Neill, M.A., and Mohnen, D. (2001). Pectins: structure, biosynthesis, and oligogalacturonide-related signaling. Phytochem. **57:** 929–967.

Rioux, D., Nicole, M., Simard, M., and Ouellette, G.B. (1998). Immunocytochemical evidence that secretion of pectin occurs during gel (gum) and tylosis formation in trees. Phytopathol. **88:** 494-505.

Ruan, Y-L., Xu, S-M., White, R., and Furbank, R.T. (2004). Genotypic and developmental evidence for the role of plasmodesmatal regulation in cotton fiber elongation mediated by callose turnover. Plant Physiol. **136:** 4104–4113.

Scheckler, S.E., and Galtier, J. (2003). Tyloses and ecophysiology of the early carboniferous progymnosperm tree *Protopitys buchiana*. Ann. Bot. **91:** 739-747.

Schmohl, N., and Horst, W.J. (2000). Cell wall pectin content modulates aluminium sensitivity of *Zea mays* (L.) cells grown in suspension culture. Plant Cell Environ. **23:** 735-742.

Segerman, B., Jansson, S., and Karlsson, J. (2006). Characterization of genes with narrow expression patterns in *Populus*. (Submitted).

Stennis, M.J., Chandra, S., Ryan, C.A., and Low, P.S. (1998). Systemin potentiates the oxidative burst in cultured tomato cells. Plant Physiol. **117:** 1031–1036.

Sterky, F., Regan, S., Karlsson, J., Hertzberg, M., Rohde, A., Holmberg, A., Amini, B., Bhalerao, R., Larsson, M., Villarroel, R., Van Montagu, M., Sandberg, G., Olsson, O., Teeri, T.T., Boerjan, W., Gustafsson, P., Uhlén, M., Sundberg, B., and Lundeberg, J. (1998). Gene discovery in the wood-forming tissues of poplar: Analysis of 5,692 expressed sequence tags. Proc. Natl. Acad. Sci. USA. **95:** 13330-13335.

Sterky, F., Bhalerao, R.R., Unneberg, P., Segerman, B., Nilsson, P., Brunner, A.M., Charbonnel-Campaa, L., Lindvall, J.J., Tandre, K., Strauss, S.H., Sundberg, B., Gustafsson, P., Uhlén, M., Bhalerao, R.P., Nilsson, O., Sandberg, G., Karlsson, J., Lundeberg, J., and Jansson, S. (2004). A *Populus* EST resource for plant functional genomics. Proc. Natl. Acad. Sci. USA. **101:** 13951-13956.

Tieman, D.M., and Handa, A.K. (1994). Reduction in pectin methylesterase activity modifies tissue integrity and cation levels in ripening tomato *(Lycopersicon esculentum* Mill.) fruits. Plant Physiol. **106:** 429-436.

Thatcher, L.F., Anderson, J.P., and Singh, K.B. (2005). Plant defence responses: what have we learnt from *Arabidopsis*? Func. Plant Biol. **32:** 1-19.

Thordal-Christensen, H., Zhang, Z., Wei, Y., and Collinge, D.B. (1997). Subcellular localization of H_2O_2 in plants. H_2O_2 accumulation in papillae and hypersensitive response during the barley - powdery mildew interaction. Plant J. **11:** 1187-1194.

Yang, Y., Shah, J., and Klessig, D.F. (1997). Signal perception and transduction in plant defense responses. Genes Dev. **11:** 1621-1639.

Van Alebeek, G-J.W.M., Christensen, T.M.I.E., Schols, H.A., Mikkelsen, J.D., and Voragen, A.G.J. (2002). Mode of action of pectin lyase A of *Aspergillus niger* on differently C_6-substituted oligogalacturonides. J. Biol. Chem. **277:** 25929-25936.

Vogel, J., and Somerville, S. (2000). Isolation and characterization of powdery mildew-resistant *Arabidopsis* mutants. Proc. Natl. Acad. Sci. **97:** 1897-1902.

Vogel, J.P., Raab, T.K., Schiff, C., and Somerville, S.C. (2002). *PMR6*, a pectate lyase-like gene required for powdery mildew susceptibility in *Arabidopsis*. Plant Cell. **14:** 2095-2106.

Wang, K.L.C., Li, H., and Ecker, J.R. (2002). Ethylene biosynthesis and signalling networks. Plant Cell. **14:** 131-151.

Wen, F., Zhu, Y., and Hawes, M.C. (1999). Effect of pectin methylesterase gene expression on pea root development. Plant Cell. **11:** 1129–1140.

Zhou, J.M., Trifa, Y., Silva, H., Pontier, D., Lam, E., Shah, J., and Klessig, D.F. (2000). NPR1 differentially interacts with members of the TGA/OBF family of transcription

factors that bind an element of the *PR-1* gene required for induction by salicylic acid. Mol. Plant-Mic. Inter. **13:** 191-202.

Acknowledgements

My deepest gratitude goes to my supervisor, Dr. Ewa Mellerowicz, for having so great patience with me, supporting me from start to finish of writing this master thesis. Your vast experience as an active researcher regarding the topic of this study has proved important, especially during the writing process. Without your endless support, I doubt this assay would have been finished within a reasonable time course. I have to admit it has been really fun working with this project and with you as well, which is one of the main reasons why I choose to continue with PhD studies at UPSC graduate school.

I would also like to thank Prof. Björn Sundberg and Drs. Sara Andersson Gunnerås and Jan Karlsson for sharing general opinions and providing me with important guidelines how to set up and interpret everything that is related to microarray experiments. Thanks also to Simon Björklund for the valuable demonstration of lab practice when processing microarrays manually. This also concerns other people working actively in the MA-lab, just to mention a few: Oskar Skogström, Andreas Sjödin, Natalie Druart, Charleen Moreau, and Ingela Sandström. Finally, there are administrators and research engineers, such as Max Bylesjö, and Bo Segerman that, without their help, the obtained microarray data would have been incorrectly analyzed, rest assure!

Thanks to Kjell Olofsson for his assistance with cryo sectioning, preparation of staining solutions, microscopy, and also sharing advises how to work in a proper manner in the anatomy lab. Your valuable help has been and will always be appreciated. Many thanks go to Dr. Joanna Leśniewska, as well, for providing me with those beautiful images of cross and longitudinal sections visualizing tyloses, which served as a good complement to my thesis.

Many thanks also for all these friday afternoon-sessions; that is: group meetings and Journal Clubs, involving and coordinated by Björn Sundberg's, Ewa Mellerowicz's, and Hannele Tuominen's research groups, respectively. It has been really fun and interesting, expanding each and every ones range of knowledge, when it comes to understanding the mysterious and complex world of plant science. Still, I have to admit, very difficult to grasp, occasionally.

Lastly, I would like to express my gratitude to Junko Takahashi for spending her valuable time on showing me around and teaching me common lab practice, and always sharing her experience when I required help. This was especially important in the initiating phase of the project, for both the theoretical and the practical parts. It's a privilege to work with such generous people that always keep their doors open, no matter how many questions you bombard them with. I'm also very grateful to Jonathan Love, for showing positive interest in my work and putting some effort into commenting it during thesis defense/presentation.

And, of course, thanks to everyone else, both old and new people at the two departments that, more or less, contributed to completing this exam work. I'm looking forward to continue working with a new project set up by Prof. Björn Sundberg and also for collaboration with all the kind and accommodating people presently working at UPSC.

Appendix

List of Chief Protocols Employed for This Study

A prominent number of protocols were applied for the practical and analytical part of this thesis, which is the reason why only the three major ones (with great impact on the outcome) are presented in the Appendix-section. The remaining protocols, however, are referred to their respective author(s)/papers and URLs throughout the thesis, and can be located mainly in the Materials and Method-section. The author would like to declare the fact that the following attached protocols, which in the thesis are referred to by their roman numerals, are modified from the previous and/or original author(s), and try to follow general guidelines set up according to the manufacturer's/author's recommendations:

I. Total RNA Preparation for cDNA Microarray Applications

II. Application of RT-PCR

III. Application of cDNA Microarray

Total RNA Preparation for cDNA Microarray Applications

Based on protocols provided by: RNeasy Plant Mini Kit (Qiagen, Catalog No. 74903 (20) or 74904 (50))
Modified by: David Öhman, MSc, April 2005 (Swedish University of Agricultural Sciences)

NB: This protocol is intended to increase the yield of total RNA from pulp of scraped poplar xylem and is *not* relevant for scraped poplar phloem since the total RNA yield from that kind of pulp often can be regarded as sufficient. For total RNA extraction of scraped poplar phloem pulp, please consult the manufacturer's (Qiagen) manual under the section "Protocol - Plant + Fungi" and follow it step by step (page 75-78). Some advices: making a routine of working in a rapid fashion and in an as clean, sterile, and RNase-free environment as possible will vastly improve the chances of obtaining high-quality total RNA ready for cDNA Microarrays.

1. Transfer ≈ 4 ml of the frozen tissue (do not allow it to thaw at any time) quickly into an RNase-free, liquid-nitrogen-cooled, falcon tube (15 ml). No weighing is required; the sample volume is roughly estimated by using the scale of the falcon tube.
2. Add 3.6 ml **Buffer RLT** (1st of choice) or **Buffer RLC** (2nd of choice, if the **Buffer RLT** runs out). Vortex vigorously and invert the falcon tube several times.
3. Pour the lysate gently (pipetting it is usually challenging, but might be feasible if the end of the pipet tip is cut off) directly onto as many QIAshredder spin columns (lilac) as necessary (8-10 will usually suffice). Be careful not to overload them (>700 µl = overloading). Centrifuge them for 2 min at 14,000 rpm. This will result in flow-through fractions that will be contained within each and every 2 ml collection tube, which have been attached to the spin columns previously. Carefully transfer the supernatant of all collection tubes (do not disturb the pellets) into a new falcon tube.
4. Add 0.5 volume **ethanol (99.5%)** and mix by inverting the tube carefully twice.
5. Apply sample (≈ 650 µl) to an RNeasy mini column (pink) placed in a 2 ml collection tube. Centrifuge for 15 s at 10,000 rpm. Discard the flow-through and reuse the collection tube. Repeat this step until the entire falcon tube is empty. Note: this implies *using the same mini column for this step and for all subsequent steps*. This will result in an amplification of total RNA on the RNeasy silica-gel membrane.
6. Add 700 µl **Buffer RW1** to the mini column. Centrifuge for 15 s at 10,000 rpm. Discard flow-through and reuse collection tube. Proceed to the next step.
7. Add 500 µl **Buffer RPE** to the mini column. Centrifuge for 15 s at 10,000 rpm. Discard flow-through and reuse collection tube. Proceed to the next step.
8. Add another 500 µl **Buffer RPE** to the mini column. Centrifuge for 2 min at 14,000 rpm. Discard flow-through *and* collection tube. Proceed to the next step.
9. Place the mini column in a new collection tube and centrifuge for 1 min at 14,000 rpm (in order to eliminate any chance of possible **Buffer RPE** carryover). Transfer the mini column into an RNase-free 1.5 ml eppendorf tube. Proceed to the next step.
10. To elute, add 20 µl of **RNase-free water** directly onto the membrane and leave to incubate for 5 min. Centrifuge for 1 min at 10,000 rpm. Repeat this step (step 10) once (in order to obtain maximum yield of RNA), and elute into the same eppendorf tube.

Concluding remarks: By implementing this method, the average yield will correspond to ≥ 100 µg total RNA for *one* mini column. This amount is fairly adequate for 2-4 Microarray hybridizations (2-4 slides), depending on the amount of sample submitted for the cDNA synthesis subsequently (recommendations: 25-50 µg total RNA per sample). Due to the possibilities of contaminations and also in order to check the integrity of the total RNA, it is highly recommended to run a quality check on a denaturing agarose gel electrophoresis and ethidium bromide staining. Pure samples will give rise to 2 sharp bands (corresponding to the 18S and 26S rRNA), while a smear indicates degradation. In addition, quality can be checked by applying a NanoDrop that measures the absorbance at 260 nm (nucleic acids) and 280 nm (proteins). A ratio (A_{260}/A_{280}) of ≈ 2, indicates high purity. The NanoDrop is also capable of giving an estimation of the quantity of the sample with fairly reliable outcome.

Application of RT-PCR

Based on the following protocols:
DNA-*free* kit (Ambion, Cat #1906) & RETROscript kit (Ambion, Cat #1710).
Optimalisation of RT-PCR, Created by: Dr. Anna Siedlecka, PhD, 2003-07-21.
Modified by: David Öhman, MSc, July 2005 (Swedish University of Agricultural Sciences).
NB: All steps are scaled down for utilization of 10 µl in each PCR-reaction. This allows for a more cost-efficient utilization of Ambion's RETROscript kit (e.g. 200 PCR reactions can be processed, instead of 40 previously).

Removal of Contaminating DNA from RNA Preparations

1. Dilute sample to 250 µg RNA/ml – assemble 50 µl/tube (12.5 µg) for each reaction.
2. Add 5 µl 10X DNase I Buffer and 1.5 µl rDNase I (3 U), and mix gently.
3. Incubate at 37°C for 20-30 min (maximum: 1 h).
4. Resuspend (always) the DNase Inactivation Reagent by vortexing, prior to usage. Add 10 µl/reaction (ensure that white colored volume is pipetted, not clear fluid), mix well.
5. Incubate 2 min (optional: 3 min) at room temperature, flicking the tube occasionally (typically 2-3 times during the incubation period in order to redisperse the reagent).
6. Centrifuge at 9,700 rpm for 1.5 min (optional: 1 min) and transfer the supernatant (containing RNA) *carefully* to a fresh tube. This step pellets the DNase Inactivation Reagent and if the pellet is disturbed, recentrifuge to repack the reagent.
7. Repeat step 6 once by recentrifuging the supernatant *collected in step 6*. **NB:** When transferring the supernatant in step 6 & 7, avoid at all times any contact with the pellet (containing the reagent), which could otherwise, if it is introduced into the fresh RNA solution, impede downstream applications (i.e. RT-PCR). It is recommended that a small amount of supernatant be left behind, in order to accomplish a safer transfer.

Optimization of RT-PCR

Determining the Linear Range for RT-PCR

1. On ice, assemble RT reaction in a thin wall PCR tube (1 PCR tube/reaction):
   - 10 µl total RNA (1.25 µg DNA-free RNA from step above).
   - 4 µl dNTP mix (2.5 mM each dNTP).
   - 2 µl Random Decamers (random sequence oligonucleotides) (50 µM).

   Final volume: 16 µl/reaction.
   NB: Include a negative control, which lacks Reverse Transcriptase (minus-RT control), to ensure that RNA samples are not contaminated with genomic DNA.
2. Denature RNA:
   a. Mix, spin briefly, and run the following program on the PCR machine:
   b. 80°C – 3 min.
   c. 4°C – 1 min.
   d. Remove tube(s) to ice, spin briefly, and replace on ice.
3. Add the remaining RT components (1 PCR tube/reaction):
   - 2 µl 10X RT Buffer.
   - 1 µl Placental RNase Inhibitor (10 U) (optional).
   - 1 µl MMLV-RT (100 U) (Reverse Transcriptase).

   Final volume: 20 µl/reaction.
   Mix gently, and spin briefly.
4. Run the RT reaction with the following program on the PCR machine:

a. 42°C – 1 h (incubation period).
b. 95°C – 5 min (in order to inactivate the Reverse Transcriptase).
c. 4°C – 2 min (cooling).
d. Store reaction at -20°C (long-term storage) or proceed to the next step (PCR step).

5. Check the RT efficiency by 18S-PCR (optional) by preparing the following mixture:
   - 2 µl RT reaction from step above.
   - 1 µl 10X PCR Buffer.
   - 0.8 µl dNTP mix (2.5 mM each dNTP).
   - 0.4 µl 18S Primer pair (mixture with 0.2 µl of each primer).
   - 0.1 µl Taq polymerase (Thermostable DNA Polymerase) (5 U).
   - 5.7 µl Nuclease-free Water.

   Final volume: 10 µl/reaction.
6. Subject samples to PCR, by running the following program on the PCR machine:
   a. 94°C – 5 min (denaturing).
   b. 20 cycles of: 94°C – 30 sec (denaturing).
      58°C – 30 sec (NB: Optimal annealing temperature may vary).
      72°C – 30 sec (polymerization).
   c. 72°C – 5 min (final extension).
   d. 4°C – 5 min (cooling).
   e. Check results on a 1.5% agarose gel stained with EtBr.
7. On ice, assemble the following master mixture (10 µl/reaction):
   - 2 µl RT reaction (from steps above).
   - 1 µl 10X PCR Buffer.
   - 0.8 µl dNTP mix (2.5 mM each dNTP).
   - 0.8 µl Gene specific primer pair (10 µM each; final concentration: 0.4 µM each).
   - 0.1 µl Taq Polymerase (Thermostable DNA Polymerase) (5 U).
   - 5.3 µl Nuclease-free Water.

   Final volume: 10 µl/reaction.
   NB: Include a negative control, where the template is replaced by water (minus-template PCR), to verify that none of the PCR reagents are contaminated with DNA.
8. Run the following program profile on the PCR machine:
   a. Denaturing: 94°C – 5 min.
   b. 33 cycles of: 94°C – 30 sec (denaturing).
      62°C – 30 sec (annealing temperature) (**NB:** Annealing temperature varies depending on gene of interest, i.e. gene specific primer pair, reasonable temperature lies between 55-68°C).
      72°C – 30 sec (polymerization).
   c. Final extension: 72°C – 5 min.
   d. Cooling: 4°C – 5 min (optional: forever mode).
9. During the PCR run, remove samples after each odd numbered cycle, and place them on ice, starting with cycle 15 and ending with cycle 33 (for a total of 10 withdrawals).
   NB: The PCR machine is counting the first denaturing step as cycle 1, which implies that when cycle 15 is reached, the PCR machine displays it as cycle number 16.
10. Analyze the results:
    a. Run the RT-PCR reaction (10 µl) on a native agarose gel, stained with EtBr.
    b. Visualize the product under UV-light by application of the Typhoon 9400 scanner.
    c. Quantify the product by implementing the ImageQuant software program.
    d. Plot results in a diagram (Excel), and select the most appropriate cycle number.

Determining the Optimal Ratio of 18S Primers:Competimers

1. Prepare the following Primer:Competimer mixtures:

Ratio:	1:9	2:8	3:7
18S Competimers	9 µl	8 µl	7 µl
18S Primer pair	1 µl	2 µl	3 µl

2. On ice, make a PCR master mixture (5 samples) and use aliquots from RT:
   - 6 µl 10X PCR Buffer.
   - 4.8 µl dNTP mix (2.5 mM each dNTP).
   - 0.6 µl Taq Polymerase (Thermostable DNA Polymerase) (30 U).
   - 36.6 µl Nuclease-free Water.

   Final volume: 48 µl.
3. Mix well and aliquot 8 µl of the master mixture from step 2 to 5 sample tubes. Proceed to step 4, which encompasses: addition of gene specific primers (if gene specific primer volume is less than 1 µl; add Nuclease-free Water up to 1 µl) and aliquots of 18S PCR Primer:Competimer mixtures (according to tables in step 1 and step 4).
4. Assemble the following combination of reactions to each tube already containing 8 µl:

Tube	Amount	Components
1	x µl	Gene specific primer pair mixture (typically 0.4 µl of each primer)
	1 µl	Nuclease-free Water (negative control for the 18S primer pair)
2	x µl	Gene specific primer pair mixture (typically 0.4 µl of each primer)
	1 µl	1:9 18S PCR Primer:Competimer mixture (from table in step 1)
3	x µl	Gene specific primer pair mixture (typically 0.4 µl of each primer)
	1 µl	2:8 18S PCR Primer:Competimer mixture (from table in step 1)
4	x µl	Gene specific primer pair mixture (typically 0.4 µl of each primer)
	1 µl	3:7 18S PCR Primer:Competimer mixture (from table in step 1)
5	1 µl	Nuclease-free Water (negative control for gene specific primers)
	1 µl	1:9 18S PCR Primer:Competimer mixture (from table in step 1)

5. Subject the 5 reaction mixtures to the following steps:
   a. Run PCR with selected number of cycles, which were optimized previously.
   b. Run product (10 µl) on a 1.5% agarose gel stained with EtBr.
   c. Visualize the product under UV-light by application of the Typhoon 9400 scanner.
   d. Quantify the product by implementing the ImageQuant software program.
   e. Select conditions in which both 18S and gene of interest are amplified at a similar level. RT-PCR is now optimized. Run optimized PCR on experimental samples.

NB: When PCR is run on experimental samples with optimized conditions, 1 µl of 18S primers:competimers (optimized in step 5) mixture have to be added to the PCR master mixture. Hence, addition of Nuclease-free Water will correspond to 4.3 µl, *not* 5.3 µl. The 18S product serves as an internal standard, i.e. it is exploited in order to quantify the PCR products (ratio of: specific gene/18S) and compare them relative to each other. In addition, when multiple reactions are done at the same time (e.g. RT reaction and PCR), prepare master mixtures of appropriate components (in order to maintain uniform conditions) and aliquot the correct amount to each sample tube. *Recommended:* AVOID adding the enzyme Reverse Transcriptase to a master mixture; add this enzyme to each sample tube separately instead, before the RT reaction. This usually yields more consistent and reliable results at the end.

cDNA-synthesis of Poplar Total RNA for Microarrays

Modified by: Dr. Oskar Skogström, PhD, 2002-12-04 (Umeå University)
Modified by: David Öhman, MSc, June 2005 (Swedish University of Agricultural Sciences)

To denature the sample, prepare the following mixture in each tube (17.5 µl/reaction):

- 25-50 µg total RNA in 16 µl RNase-free H_2O.
- 1.5 µl Oligo(dT)-anchor (5 µg/µl).

Incubate on heating block at 70°C for 5 min, and then chill each sample tube on ice.

For reverse transcription, prepare the following master mixture (12.5 µl/reaction):

- 6 µl 5X RT-buffer (final concentration: 1X).
- 3 µl DTT (0.1 M), which must be added *before* addition of the RNase inhibitor.
- 1 µl 50X aa-dUTP/dNTP.
- 1 µl RNase inhibitor (30-40 U).
- 1.5 µl Superscript II (300 U).

Add 12.5 µl to each sample tube, which already contains 17.5 µl (for a final volume of 30 µl).
Incubate on heating block at 42°C for 2-3 h (recommended time period).

RNA degradation:

1. 10 µl 0.5 M EDTA – Stop reaction.
2. 10 µl 1 N NaOH – Degrade RNA.
3. Incubate on heating block at 65°C for 15 min.
4. 50 µl 1 M Hepes, pH 7.0 – Neutralize reaction.

Purification and Desalting of cDNA by Microcon 30 Concentrator

1. 400 µl dH_2O to 100 µl sample + Spin at 9500 rpm for 8 min + Remove flow-through.
2. 500 µl dH_2O + Spin at 9500 rpm for 8 min (1^{st} wash) + Remove flow-through.
3. 500 µl dH_2O + Spin at 9500 rpm for 8 min (2^{nd} wash) + Remove flow-through.
4. 500 µl dH_2O + Spin at 9500 rpm for 6 min (3^{rd} wash).
5. Change tube + Spin at 9500 rpm for 3 min into the new tube (invert the membrane).
6. Measure concentration on the NanoDrop (and confirm that cDNA has been obtained).
7. Speedvac down (evaporate) to dry tube (to evaporate 60 µl: 60 min at 40°C).

Indirect CyDye (Cy5+Cy3) Coupling of Poplar cDNA for Microarrays

Post-labeling Coupling Reaction:

1. Resuspend the CyDye (Cy5 & Cy3) concentrates, for utilization of 6-8 reactions, in 120 µl of 0.1 M $NaHCO_3$, pH 9.0 (8 x 15 µl = 120 µl, for each CyDye).
2. Add 15 µl of dye to the correct *dry* cDNA sample tube (try to avoid exposure to light).
3. Incubate at room temperature in the dark for 2 h (maximum: 3 h).

Purification of CyDye-labeled cDNA by GFX Spin Columns:

1. Apply 500 µl Capture buffer onto the membrane inside every column.
2. Transfer the CyDye-labeled cDNA to the columns and mix 5 times with the buffer.
3. Quickly centrifuge at 13,800 g for 30 s + Discard flow-through.
4. Apply 600 µl 80% ethanol and spin at 13,800 g for 30 s + Discard flow-through.

5. Repeat step 4 once (for a total of 2 washes).
6. Transfer column to a new tube (subsequently referred to as *sample tube*).
7. Apply 50 µl of preheated (65°C) Elution buffer + Incubate the membrane for 1-5 min.
8. Centrifuge at 13,800 g for 1 min.
9. Repeat step 7 and 8 once (for a total eluted volume of 100 µl in each *sample tube*).
10. Close each *sample tube* + Measure incorporation of each CyDye on the NanoDrop.
11. Mix the correct dye *sample tubes* into one *sample tube* + Speedvac down to ≈ 40 µl.

Manual Hybridization (Work in a Dark Environment)

For prehybridization, prepare the following prehybridization master mixture (1 ml):

- 100 µl 50X Denhardts (final concentration: 5X).
- 250 µl 20X SSC (final concentration: 5X).
- 500 µl 100% dFA (deionized formamide) (final concentration: 50%).
- 11 µl CT (Calf Thymus)-DNA (10 mg/ml) (final concentration: 100 µg/ml).
- 139 µl dH_2O (or add dH_2O up to 1 ml).

1. Apply 8 µl 25% dFA in the small wells of the hybridization chamber.
2. Wash the cover slip (LifterSlip) before utilization, in the following order (abc):
   a. Twice with dH_2O.
   b. Once with 95-100% ethanol.
   c. Dry with $N_{2(g)}$ (check that the surface is clean; repeat the washing if required).
3. Place the cover slip on the slide correctly and gently apply the prehybridization mixture (65-70 µl), drop by drop in opposite corners, until the entire slide is covered.
4. Directly place in chamber, close, and incubate in water bath at 42°C for 30-50 min.
5. Open chamber and wash the slide with tap water until the cover slip detaches.
6. Directly place the slide in 2-propanol (isopropanol), followed by drying it with $N_{2(g)}$.

For hybridization, prepare the following hybridization mixture (80 µl/slide):

- 39.4 µl Target (CyDye-labeled cDNA in *one sample tube*)
- 0.5 µl tRNA (25 mg/ml) (blocker)
- 1.5 µl Oligo-dA(80mer) (10 mg/ml) (blocker)
- 16 µl 20X SSC
- 20 µl 100% dFA
- 2.6 µl 10% SDS

1. Wash the cover slip prior to usage, as described previously (see above).
2. Denature hybridization mixture on heating block at 95°C for 2 min.
3. Immediately place on ice for 15-20 s.
4. Vortex and spin down.
5. Apply hybridization mixture (70 µl), as described previously (see above).
6. Incubate in water bath over night or ca 18 hours.

Washing Process (Wash at Room Temperature):

1. 5 min with shaking in each washing buffer, in the following order (abc):
   a. WB#I (50 ml 20X SSC, 3 ml 10% SDS, and dH_2O up to 1 l).
   b. WB#II (10 ml 20X SSC, and dH_2O up to 1 l).
   c. WB#III (2.5 ml 20X SSC, and dH_2O up to 1 l).
2. Dry with $N_{2(g)}$ (check that the surface is clean; repeat the washing if required).